International Journal of
Young Scientist Research

Vol 7, No1, Feb 2023
ISSN: 2588- 5111

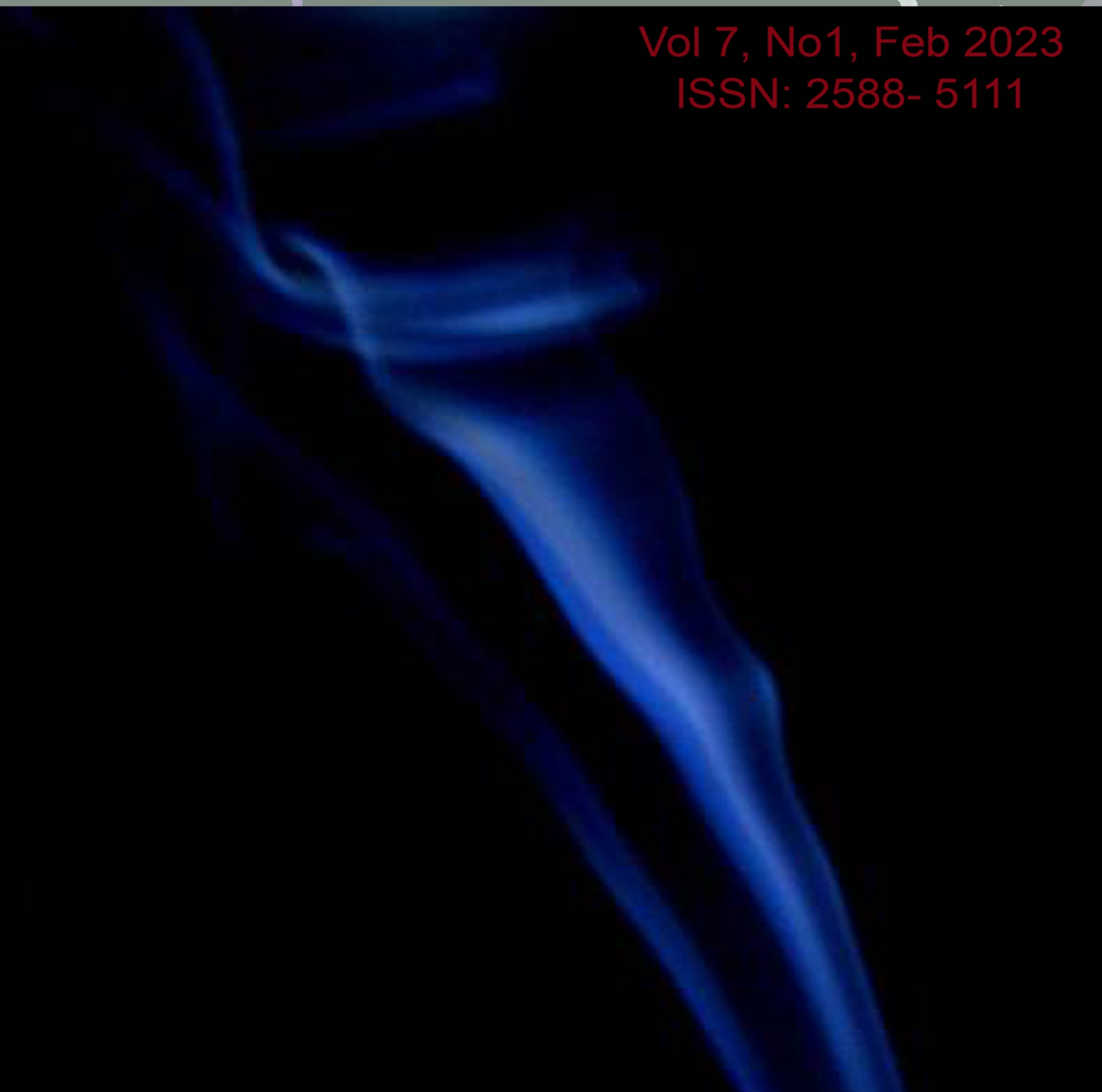

Contents

Young Scientist Research

Title proper: Young scientist research

Subject: NATURAL SCIENCES, ART, ENGINEERING AND TECHNOLOGY

Corporate contributor: Ariaian Young Innovative Minds Institute

Publisher: Tehran: Ariaian Young Innovative Minds Institute

Dates of publication: 2017- Present

Frequency: Annual

Type of resource: Periodical

Language: English

Country: Iran

Medium: Online

Indexed by: ROAD (The Directory of Open Access Resources)

ISSN- 2588-5111
ISSN International Centre
45 rue de Turbigo
75003 Paris
France

Address:

Unit 14, No.32, Malek Ave., Shariati St.

Post Code: 1565843537

Tel:+9821-77507013, 77522395

WELCOME TO THE INTERNATIONAL JOURNAL of YOUNG SCIENTIST RESEARCH

Young Scientist Research is a research journal based on scientific projects and we are pleased to present our students' work in scientific activities. This open-access journal includes young students' research in any field of science which publishes full-length and abstract research on any aspects of applied sciences in relation to work presented in both national and international conferences, competitions and tournaments of all types.

Programs that have educational opportunities for high school students to present their distinguished projects from regional, national and international events such as International Conference of Young Scientists (ICYS), International / Persian Young Physicists' Tournament (IYPT/ PYPT), International / Iran Physics' Tournament (IPT/ IRPT), International Music , Science , Engineering Fair (IMSEF).

New manuscripts sent to the Journal will be handled by the Editorial Office who checks compliance with the guidelines to authors. Then a rapid screening process at which stage a decision to reject or to go to full review is made.

By submission of a manuscript to the Journal, all authors warrant that they have the authority to publish the material and that the paper, or one substantially the same, has neither been published previously, nor is being considered for publication elsewhere.

This journal belongs to Ariaian Young Innovative Minds Institute, AYIMI, and one to two issues are published in a year. All details are on the YOUNG SCIENTIST RESEARCH Journal website (http://journal.ayimi.org)

Editor in Chief
Dr. Dina Izadi
Researcher & President of
AYIMI , International Research Institute
ADIB, Cultural and Artistic Institute
http://www.ayimi.org
http://adib.ayimi.org
http://journal.ayimi.org
Email: info@ayimi.org
Unit 14, No. 32, Malek Ave., Shariati St.,
Post Code: 1565843537
Young Scientist Research Journal, ISSN: 2588-5111
Tehran/ Iran

CURRENT ISSUE
Vol 7 NO 1 FEB. 2023

A COMPARISON BETWEEN THE INFLUENCE OF THREE DIFFERENT SIZES OF EXFOLIATED VERMICULITE ON THE THERMAL AND MECHANICAL PROPERTIES OF CEMENT CONSTRUCTION BRICKS

Pieter Adrian Huysamen,Western CAPE / STELLENBOSCH,Jan Van Riebeeck High School, adrian.huysamen@janvanriebeeck.org

ARTICLE INFO

Gold medalist in BUCA IMSEF 2022

Mrs Milandré Bezuidenthout(Advisor)

Awarded by Ariaian Young Innovative

Minds Institute , AYIMI

http://www.ayimi.org ,info@ayimi.org

ABSTRACT

A study was embarked on to determine what influence replacing increasing proportions of sand with exfoliated vermiculite will have on a cement brick's strength and insulation properties. These bricks, with various ratios of sand and exfoliated vermiculite, were compared to control sample bricks, made according to the industry standard formula of a ratio of 8:1 by volume of sand and cement. The study also investigated if the size of exfoliated vermiculite would influence the results. The study conclusively proved that exfoliated vermiculite is a viable filler in cement brick making.

Keywords : *Bricks,Cement , Exfoliated Vermiculite*

1. Introduction

South Africa has a backlog of affordable housing for its growing population. An in-depth review of all the alternative building materials currently available on the market and available skilled labour needs to be undertaken.

Due to the lack of skills to build with alternative materials such as wood or panel boards, a high demand remains for houses built with conventional bricks and mortar. Such buildings are perceived to be reliable and strong, but costly and take more time to construct. Building with bricks and mortar requires a strong, skilled labourer as it is strenuous work laying on average 500 - 600 bricks per day. This together with the declining artisanship in the building industry is worrying as shown by Doku (2009).

According to the quarterly report published by The Construction Industry Development Board in October 2018, there are around 89% males and 11% females in the construction industry. This problem can substantially be addressed by introducing lightweight construction bricks to this industry.

Buildings are considered to be an open system, and therefore interact with the environment. Thermal energy transfer take place between a building and its immediate environment. 25% - 30% of all the energy consumed in the world. 80% of the energy used by a building is due to heating or cooling(How is heat transferred? Conduction -- Convection -- Radiation, 2022), Hence, by ensuring these lightweight bricks have superior insulation properties it will assist in reducing the energy consumption of homeowners across the country. This will in turn reduce the threat to climate change, environmental pollution and human health by reducing emissions from coal-fired power stations which are South Africa's main source of electrical energy.

There are also other disadvantages of the common cement construction brick. Firstly, it is very heavy and some configurations cumbersome thus extending construction time and increasing construction cost. The accumulative mass of dwellings or residential property structures constructed with cement bricks requires substantial foundations. Secondly, the common cement brick is not very fire resistant meaning it loses much of its structural strength during a fire. Finally, these bricks have poor insulation properties and as mentioned, do little to reduce the electrical energy demand on the power grid in South Africa.

Drawing on the excellent thermal properties of exfoliated vermiculite and its resilience to fire, such an addition to cement brick making could revolutionize the building industry. Lighter bricks would require lesser foundations and the improvement of insulation properties would reduce residential energy consumption used for heating and cool dramatically. This would reduce the demand on the electricity grid as well as reduce the volume of harmful greenhouse gasses released by conventional coal-fired power stations.

Vermiculite is a naturally occurring mineral that takes the form of glossy flakes, varying in colour from dark grey to sandy brown. These flakes, a hydrated magnesium iron aluminium silicate mineral, are easily exfoliated by a heat source or microwaves and in so doing expand on average ten times in volume forming wormlike particles.

Exfoliated vermiculite is a light, non-toxic, sterile material and is pH neutral. It is commonly used in passive fire protection plaster mixtures, as loose media in insulation applications, as conveyors of minerals in animal feed and as a growing medium in the agriculture industry. Its name comes from the Latin word "vermiculare," which means "to breed worms," and the English suffix "ite," which means "mineral" or "rock".

To be noted is that this study was embarked on not to redesign a building brick, but to rather investigate if exfoliated vermiculite could be a suitable additive to common cement bricks. All sample bricks were produced following a set procedure to ensure batch conformity. By replacing part of the sand in the cement brick with exfoliated vermiculite it is believed that such bricks would retain enough strength rendering them suitable for the construction industry. To form a definitive view, three size ratios of exfoliated vermiculite were used in the study to determine if one is more suitable than the other.

Two more variables were introduced as both were deemed relevant. The first variable was fire, whereby influence of fire on the strength of bricks was investigated, and secondly the insulation properties of the bricks. The purpose of the study was to find the perfect size of exfoliated vermiculite and the ratio of an aggregate mix

mix (building sand to exfoliated vermiculite) that would render a strong yet lightweight brick with improved insulation properties.

2. Literature Review

Developing lighter building material with better insulation properties has been a topic of many research papers, such as, Köksal, DiazGencel and Rabanal (2013), Georgiev, Yoleva, Djambazov, Dimitrov, Ivanova (2017) and Beal, Selby, Atwater, James, Viens, Almquist (2019). The benefit of such materials ranges from energy savings due to reduced heating and/or cooling required to cost savings as less structural materials are required e.g. lesser foundations. Lightweight houses are specifically beneficial in parts of the world where ground subsidence is common as these types of dwelling place less pressure on the ground beneath the house or structure.

Much research has been done on lightweight building bricks such as, Dimitrov, Ivanova (2017) and Beal, Selby, Atwater, James, Viens, Almquist (2019). These studies reviewed the relationship between lightweight fillers to normal aggregate in construction bricks. In these studies, mixtures were varied to create an optimal recipe that not only reduces the mass of the brick but also ensured that sufficient strength or structural integrity was retained.

Köksal, DiazGencel and Rabanal (2013), investigated the properties of the cement mortar modified with styrene-acrylic ester copolymer. were investigated. Exfoliated vermiculite as a lightweight aggregate was used for making the polymer-modified mortar test specimens. Tests showed that the bulk density and thermal conductivity of the specimens decreased, whereas the water absorption and porosity increased. Conversely, flexural and compressive strengths decreased with increases in the percentage of exfoliated vermiculite in the mortar mixture. The study also found that the thermal conductivity measured in W/mK of cement bricks reduced as the volume of exfoliated vermiculite increased.

The research was also done on how to improve the thermal insulation properties of cement brick. Better thermal insulation properties were achieved by increasing the porosity of the cement bricks by introducing pore-forming additives to the cement. Georgiev, Yoleva, Djambazov, Dimitrov, Ivanova (2017), used exfoliated vermiculite and exfoliated perlite was selected as pore formers. Both materials have very low density and good thermal insulation properties. The results showed an increase in water absorption and apparent porosity compared to fired pure clay bricks, but more importantly lower thermal conductivity.

In an additional paper Beal, Selby, Atwater, James, Viens, Almquist (2019), studied the thermal and mechanical properties of fired clay bricks were. Clay bricks containing three different pore-forming additives were investigated. The additives included three types: inorganic (vermiculite), organic (sawdust), and ash (wood ash). In this study, the trends in bulk density, porosity, water absorption, compressive strength, and thermal conductivity were investigated. The study found that vermiculite as an additive decreased thermal conductivity.

All of the research conducted on porous additives in brick making came to the same conclusion, namley that the use of exfoliated vermiculite in building bricks reduced the bulk density, reduced the thermal conductivity and decreased the compressive strength of the building brick. In the literature review, no published research on the various commercially available sizes of exfoliated vermiculite nor the structural integrity of such brick when exposed to fire could be found indicating a gap in the research.

This report will draw from some of the methods used in the studies cited to conduct tests on bricks with different ratios of exfoliated vermiculite to sand. As a variation, batches of cement bricks will also contain three different sizes of exfoliated vermiculite: micron, super fine and fine. The particle size distribution (PSD) of micron grade range between 0.18 to 1mm, super fine between 0.355 and 2mm and a fine between 0.355 and 2.8mm.

3. Problem Statement

Due to the mass of the common cement bricks used in the building industry, there are many more male than female brick-layers. To create equal opportunities for women one of the main hurdles to overcome is the mass of the cement brick. A bricklayer lays up to 500 bricks a day each weighing 2.3 kg. In other words, a bricklayer will pick up and place 1.15t bricks per day.

Once a dwelling (house) is completed, the brick gives structural integrity, but limited insulation to the outside environment as interior spaces require either heating in winter and/or cooling in summer.

Home fires are therefore common in winter months as open flame heaters such as paraffin heaters or fireplaces are used to warm the interiors of such dwellings. These heating methods frequently lead to home fires and the subsequent structural damage to building bricks in such fires requires that most fire-damaged walls be demolished and rebuilt with new bricks.

To find the perfect ratio of an aggregate made up of a mixture of exfoliated vermiculite and building sand that will render a strong yet lightweight brick even after fire damage. In addition, three different sizes of exfoliated vermiculite will be used to see if this influences the result.

Research Question and Hypothesis:What is the perfect ratio of three common sizes of exfoliated vermiculite each to sand, to make a lightweight brick that is still suitable for the construction industry? To be suitable the mixture must render a brick that retains sufficient strength, retains its structural integrity after exposure to an open flame, has good insulating properties and must weigh less than a standard cement brick (Fig. 1) .

Fig. 1: (Left to Right) Grades of exfoliated vermiculite fine, super fine and micron (Picture: P.A. Huysamen)

The perfect ratio for a suitable lightweight brick is such that exfoliated vermiculite will replace 50% of the volume of coarse sand used in a standard 8:1 (sand to cement) ratio cement brick. The compression strength-to-mass value of this lightweight brick will be as good as that of normal cement brick, but its mass will be significantly less, have better insulation properties, and its compression strength-to-mass value will be greater than that of a standard cement brick after both have been exposed to a simulated fire (Figs. 2 and 3).

Fig.2: Sample brick M5/3 -1: five volume portions exfoliated micron grade vermiculite, three-volume portions sand and one volume portion cement (Picture: P.A. Huysamen)

Fig. 3: Control sample brick C -1: eight volume portions sand and one volume portion cement (Picture: P.A. Huysamen)

4. Materials and Method

4.1. Mass

Variables:

- Independent variable: Sample bricks with various sizes and volume ratios of exfoliated vermiculite.
- Dependent variable: The mass of the sample bricks.
- Constant variable: The dimensions of the sample bricks.

Materials

- Digital scale with a measurement scale in milligrams
- A sheet of paper
- Pencil

Procedure :

1. Place a sample brick on a scale that has been set to zero.
2. Allow the digital display to stabilise.
3. Record the mass of the sample brick on a tabled sheet.
4. Repeat the proses until all 30 sample bricks are weighed.

4.2. Strength

Variables:

- Independent variable: The downward pressure applied to the sample brick.
- Dependent variable: The downward pressure at which the brick falls.
- Constant variable: The dimensions of the sample bricks and placement position on the hydraulic press. The rate at which the force on the press plate is increased.

4.3. Materials

- A workshop hydraulic press with gauge
- Flat steel press plate
- Flat base plate with markings
- Cellular phone with video capability
- A sheet of paper
- Pencil

Procedure:

1. Place the sample brick on the base plate with the top face facing upwards.
2. Ensure the sample brick is placed within the predetermined markers on the fixed base plate.
3. Place a steel press plate on top of the sample brick to ensure the applied pressure is evenly spread across the top face of the sample brick.
4. Start a recording of the pressure gauge.
5. Apply an increasing load onto the press plate increasing it at a steady rate until the sample brick fails.
6. Stop the recording.
7. Review the video footage in slow motion and record the pressure at which the pressure suddenly reduced (this is the point where the brick failed).
8. Repeat the proses until all 20 sample bricks are tested (Figs. 4 and 5).

4.4. Open Flame Structural Integrity Test

Variables:

- Independent variable: The downward force applied to the flame exposed sample brick.
- Dependent variable: The downward force at which the brick fails.
- Constant variable: Exposure time of the sample brick to the flame of a butane torch. Position at which the flame makes contact with the sample brick surface.

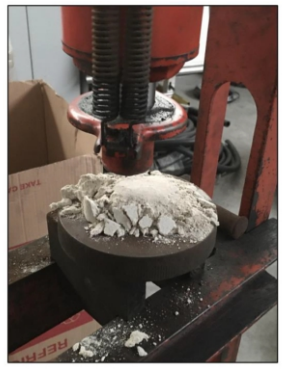

Fig. 4: An example of a crushed sample brick (Picture: P.A. Huysamen)

Fig. 5: A typical workshop hydraulic press Picture: (RP-20T, n.d)

4.4.1 Materials

- Non-flammable tile or paver
- Butane torch
- Ruler
- Stopwatch
- A workshop hydraulic press
- Flat base plate
- Press plate
- Cellular phone with video capability
- A sheet of paper
- Pencil

Procedure :

1. Place a sample brick onto the non-flammable surface i.e. tile or paver.
2. Ignite the butane torch.
3. Place the butane torch a set distance away from the sample brick at which the open flame contacts the sample brick at a predetermined position.
4. Allow the flame to stay in contact with the brick for 2 minutes.
5. Remove the flame from the brick and extinguish the flame.
6. Allow the brick to cool for 20 minutes.
7. Place the sample brick on the base plate with the top face facing upwards.
8. Ensure the sample brick is placed within the predetermined markers on the fixed base plate.
9. Place a steel press plate on top of the sample brick to ensure the applied pressure is evenly spread across the top face of the sample brick.
10. Start a recording of the pressure gauge.

11.Apply an increasing load onto the press plate increasing it at a steady rate until the sample brick fails.
12.Stop the recording.
13.Review the video footage in slow motion and record the pressure at which the pressure suddenly reduced (this is the point where the brick failed).
14.Repeat the proses until all 10 sample bricks are tested (Fig. 6).

Fig. 6: Sample brick after being exposed to a butane torch flame for 2 minutes (Picture: P.A. Huysamen)

4.5. Insulation

Variables:
-Independent variable: Sample bricks with various sizes and volume ratios of Vermiculite.
-Dependent variable: The temperature of the exposed side of the sample brick.
-Constant variable: Exposure temperature, time and sample brick dimensions.
Materials
-Non-flammable tile or paver
-Butane torch
-Ruler
-Carpenters Pencil
-Stopwatch
-A sheet of paper
-Infrared electronic temperature gauge
-Pencil
Procedure:
1.Using a pencil draw two well-defined crosses on the bottom face of the sample brick 3cm apart.
2.Place a sample brick onto the non-flammable surface i.e. tile or paver.
3.Turn the sample brick on its side with the crosses facing the side of the butane torch.
4.Ignite the butane torch.
5.Place the butane torch a set distance away from the sample brick ensuring the flame strikes one of the marked crosses.
6.Allow the flame to heat the brick until the temperature at the unheated cross reaches 400 ºC as measured with an infrared temperature gauge.
7.Remove the flame from the brick and extinguish the flame.
8.Continue to take surface temperature readings at the second cross position at 10-seconds intervals for 60 seconds.
9.Record the temperature readings in a set table format.
10.Repeat the process until all 10 sample bricks are tested (Figs. 7 and 8).

Fig. 7: Picture 7: Two crosses 3cm apart in the centre of the bottom brick face (Picture: P.A. Huysamen)

Fig. 8: Surface temperature readings were taken 3cm from the flame impact point (Picture: P.A. Huysamen)

5. Results

All the sample bricks were weighed, and the average mass of each mixture was calculated. This was done to determine the mass of each mixing ratio required to calculate the average compression strength-to-mass ratio of each mixing ratio and for the mass, comparison stated in the hypothesis. The volume of exfoliated vermiculite in the different sample bricks was found to be directly correlated to the mass of the brick. The mass of the sample bricks containing exfoliated vermiculite was found to be on average 31.3% lower than the control cement brick (C) made from sand and cement at a volume ratio of 8:1. The relationship of all the specimens to the control brick can be seen in table (1), figures (9 and 10). Even the mass of the heaviest brick was 26.6% lower than the control. This is in accordance with the hypothesis.It is clear that the control sample bricks C (1-3) were on average the heaviest. Sample bricks M 6/2 (1-3) were on average the lightest. Also apparent is that sample bricks containing exfoliated vermiculite were all lighter than the batch average of control sample bricks C.

Table 1: Individual and batch average mass in kg of the different sample bricks

Different Sample Bricks	Mass (kg)	Sample Brick Batches	Batch Average Mass (kg)
C-1	0.196	C	0.195
C-2	0.197		
C-3	0.191		
M 4/4-1	0.140	M 4/4	0.140
M 4/4-2	0.137		
M 4/4-3	0.143		
M 5/3-1	0.126	M 5/3	0.126
M 5/3-2	0.123		
M 5/3-3	0.128		
M 6/2-1	0.104	M 6/2	0.106
M 6/2-2	0.108		
M 6/2-3	0.105		
SF 4/4-1	0.140	SF 4/4	0.141
SF 4/4-2	0.140		
SF 4/4-3	0.144		
SF 5/3-1	0.124	SF 5/3	0.125
SF 5/3-2	0.127		
SF 5/3-3	0.123		
SF 6/2-1	0.110	SF 6/2	0.108
SF 6/2-2	0.106		
SF 6/2-3	0.109		
F 4/4-1	0.141	F 4/4	0.143
F 4/4-2	0.143		
F 4/4-3	0.145		
F 5/3-1	0.134	F 5/3	0.135
F 5/3-2	0.132		
F 5/3-3	0.138		
F 6/2-1	0.120	F 6/2	0.119
F 6/2-2	0.122		
F 6/2-3	0.116		

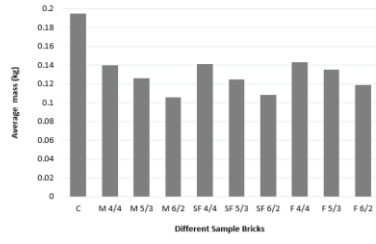

Fig. 9: Average mass in kg of the different sample bricks

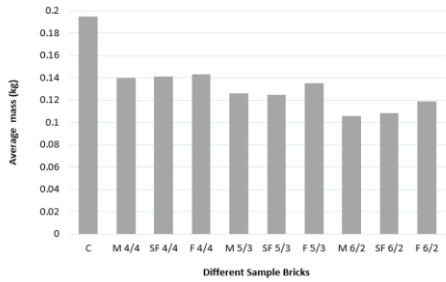

Fig.10: The average mass of the similar mix ratio sample bricks in kg

To determine the compression strength-to-mass value of the sample bricks each sample was crushed in a hydraulic press. This test was performed to assess the hypothesis that the compression strength-to-mass value of bricks will not be significant compromised by replacing a volume portion of the sand in a cement brick with exfoliated vermiculite.
The volume ratio of exfoliated vermiculite to sand in the different sample bricks was found to have a direct correlation to the compression strength-to-mass value of the bricks. The compression strength of bricks containing vermiculite was on average 35.7% lower than the control brick made from sand and cement. The impact different volume ratio mixtures had on the compression strength of the sample brick can be seen in Table (2) and Figure (11). Dividing the batch average maximum compression strength of the sample bricks by the same batch average mass presented a different outcome (Table 3 and Fig. 12).

Table 2: The pressure at which the sample bricks failed

Individual Sample Bricks	Press Gauge Readings (kPa) at Failure	Press Force (N) at failure	Pressure on Brick (Pa) at failure	Sample Brick Batches	Ave Batch Pressure (Pa) at failure
C-1	970	1,627	4,089,692	C	4,026,450
C-2	940	1,576	3,963,207		
M 4/4-1	700	1,174	2,951,324	M 4/4	2,909,163
M 4/4-2	680	1,140	2,867,001		
M 5/3-1	700	1,174	2,951,324	M 5/3	3,035,648
M 5/3-2	740	1,241	3,119,972		
M 6/2-1	560	939	2,361,060	M 6/2	2,403,221
M 6/2-2	580	973	2,445,383		
SF 4/4-1	580	973	2,445,383	SF 4/4	2,656,192
SF 4/4-2	680	1,140	2,867,001		
SF 5/3-1	680	1,140	2,867,001	SF 5/3	2,909,163
SF 5/3-2	700	1,174	2,951,324		
SF 6/2-1	600	1,006	2,529,707	SF 6/2	2,487,545
SF 6/2-2	580	973	2,445,383		
F 4/4-1	460	771	1,939,442	F 4/4	1,981,604
F 4/4-2	480	805	2,023,765		
F 5/3-1	640	1,073	2,698,354	F 5/3	2,677,273
F 5/3-2	630	1,057	2,656,192		
F 6/2-1	580	973	2,445,383	F 6/2	2,234,574
F 6/2-2	480	805	2,023,765		

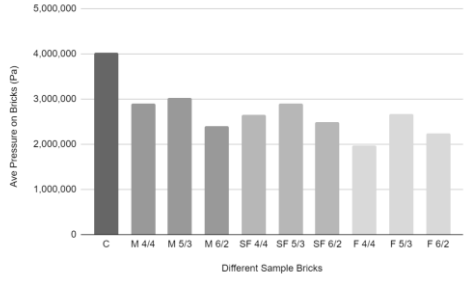

Fig. 11: The average pressure (Pa) on the different sample brick batches at failure

The average compression strength-to-mass value of sample bricks containing exfoliated vermiculite was on average 0.6% lower than the value of the control brick. It can therefore be argued that the results are aligned with the hypothesis.

This average was affected by the size of exfoliated vermiculite used to replace volumes of sand. The average compression strength-to-mass value of bricks containing fine grade exfoliated vermiculite (three different mixing ratios) was 15.5% lower than the value of the control brick. In contrast, the average compression strength-to-mass value of super fine and micron grade ratios respectively 4.9% and 9.1% greater than that of the control brick. These two ratios are then as stated in the hypothesis, as good as the normal cement brick. Table (2) and figure (11) show that the control cement bricks C 1-2 are on average the strongest and sample bricks F4/4 1-2 on average the weakest. It also shows that sample bricks containing vermiculite are substantially weaker.

Table 3: The average compression strength-to-mass ratio of different brick batches

Sample Brick Bathes	Ave Pressure on Brick (Pa) at failure	Average mass (kg)	Compression Strength-to-mass ratio (Pa/kg)
C	4,026,450	0.195	20,683,817
M 4/4	2,909,163	0.140	20,779,733
M 5/3	3,035,648	0.126	24,156,350
M 6/2	2,403,221	0.106	22,743,420
SF 4/4	2,656,192	0.141	18,793,811
SF 5/3	2,909,163	0.125	23,335,529
SF 6/2	2,487,545	0.108	22,961,953
F 4/4	1,981,604	0.143	13,857,368
F 5/3	2,677,273	0.135	19,880,739
F 6/2	2,234,574	0.119	18,725,482

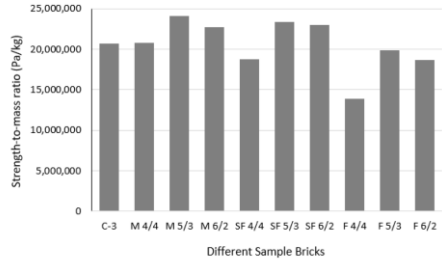

Fig 12: The compression strength-to-mass ratio of different sample brick batches

Table (3) and figure (12) show that the average of the sample brick batch M 5/3 has the highest compression strength-to-mass ratio. The average batch sample bricks with the lowest compression strength-to-mass ratio were F4/4.The average of the batch control sample brick's compression strength-to-mass ratio was the sixth highest.

All the different sample bricks were exposed to a butane flame for 2 minutes and then crushed with the use of a hydraulic press. This was done to simulate the loss of structural integrity or reduction in maximum compression strength after brick is exposed to fire.

The results of this test were as expected. The compression strength-to-mass value of the cement control brick was reduced by 21% (20.7 MPa to 16.3 MPa) after it was exposed to the butane flame. In comparison, the average compression strength-to-mass value of bricks containing exfoliated vermiculite was reduced by 10.6% (20.6 MPa to 18.4 MPa) only. The average compression strength-to-mass value of all sample bricks containing exfoliated vermiculite, after its exposure to a butane flame, was 12.6% (18.4 MPa versus 16.3 MPa) higher than that of the control brick (Table 4 and Fig.13). The hypothesis was confirmed, the sample bricks containing exfoliated vermiculite were substantially stronger than the cement and sand sample bricks. It shows that the control sample brick C-3 after it was exposed to a butane torch flame, weakened the most if compared to the average of the control C. In comparison sample brick F6/2 -3 weekend the least when compared to the average of the sample bricks F6/2. Sample bricks

bricks containing vermiculite weakened by the lowest margin after it was exposed to a butane torch flame.

Table 4: The compression strength-to-mass ratio of burnt and unburnt sample bricks

Burnt Sample Bricks		Unburnt Sample Bricks	
Sample Brick Batches	Compression Strength-to-mass ratio (Pa/kg)	Sample Brick Batches	Compression Strength-to-mass ratio (Pa/kg)
C-3	16,334,932	C	20,683,817
M 4/4-3	17,395,420	M 4/4	20,779,733
M 5/3-3	21,410,281	M 5/3	24,156,350
M 6/2-3	22,005,410	M 6/2	22,743,420
SF 4/4-3	15,517,875	SF 4/4	18,793,811
SF 5/3-3	20,223,943	SF 5/3	23,335,529
SF 6/2-3	22,047,899	SF 6/2	22,961,953
F 4/4-3	13,084,690	F 4/4	13,857,368
F 5/3-3	15,276,007	F 5/3	19,880,739
F 6/2-3	18,536,647	F 6/2	18,725,482

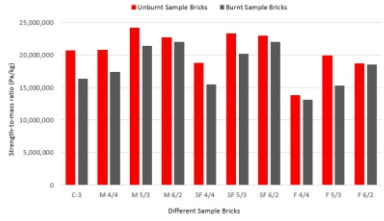

Fig. 13: The compression strength-to-mass ratio of burnt and unburnt sample bricks

A single specimen of each sample size batch was exposed to a butane torch flame until the surface temperature 3cm away from the flame centre reached 400°C. The flame was then removed, and the temperature was measured over 60 seconds at 10-second intervals. The rate at which the temperature reduced was used to test the hypothesis that bricks containing exfoliated vermiculite will have better insulation properties than normal cement brick.

The use of exfoliated vermiculite in the different sample bricks was found to be directly correlated to the length of time it took for the brick to cool down. The temperature of the sample bricks containing vermiculite was on average 34.7% cooler than the control cement sample bricks after 50 seconds. Some sample bricks were more than 40% cooler after 50 seconds (Table 5 and Fig. 14). The data illustrate that the bricks containing exfoliated vermiculite did not absorb as much heat (the core of the sample brick did not heat up as much) and were able to dissipate the little heat build-up at a higher rate. This confirms the hypothesis that bricks containing exfoliated vermiculite will have better insulation properties.

Table 5: The temperature (°C) of the different sample bricks was measured over 60 seconds

Different Sample Bricks	Temp (°C) - 0 sec	Temp (°C) - 10 sec	Temp (°C) - 20 sec	Temp (°C) - 30 sec	Temp (°C) - 40 sec	Temp (°C) - 50 sec	Temp (°C) - 60 sec
C-3	400	210.6	152.8	125.9	114.5	105	89.8
M 4/4-3	400	173.3	124.1	99.1	89.5	77.8	72.3
M 5/3-3	400	142	104.7	82.9	71.2	61.7	58.2
M 6/2-3	400	119.5	91.6	76.6	65.2	56.9	54.1
SF 4/4-3	400	169	125.8	105.2	87.6	76.9	69.9
SF 5/3-3	400	174.3	127.8	105.5	94.6	84.7	75.3
SF 6/2-3	400	154.1	110.1	91	75.2	66	64.1
F 4/4-3	400	170.9	118.1	100.4	79.4	67	62.9
F 5/3-3	400	191	109.9	86.3	74.9	65.1	62.7
F 6/2-3	400	146.3	98.4	77.9	65.5	60.8	56.4

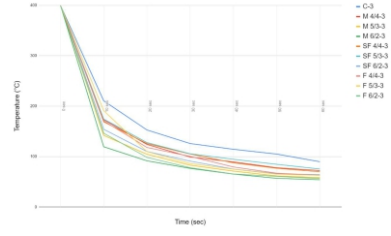

Fig. 14: The temperature (°C) of the different sample bricks was measured over 60 seconds

It shows that the control sample brick C-3 took the longest time to cool down after being exposed to a butane torch flame. Sample brick M6/2 -3 with the highest content of exfoliated vermiculite cooled down the fastest. All sample bricks containing exfoliated vermiculite cooled down at a more rapid rate than the control sample brick C-3.

6. Discussion

This study was undertaken to find the perfect ratio of three common sizes of exfoliated vermiculite each to sand. The aim was to develop a lightweight brick that is still suitable for the construction industry. To be suitable the mixture must render a brick that retains sufficient strength, retains its structural integrity after exposure to an open flame, has good insulating properties and must weigh less than a standard cement brick.

Weighing each sample brick revealed that the sample bricks containing six volume portions of micron grade exfoliated vermiculite had the lowest mass. In other words, six of the eight sand volume portions were replaced by micron-grade exfoliated vermiculite. The average mass of the M 6/2 sample brick batch was 0.106 kg, 42.0% lighter than the average of the control sample brick batch C. The average mass of the control sample brick batch was 0.195 kg and contained eight volume portions of sand. All the sample bricks containing exfoliated vermiculite weighed significantly lighter than any of the control sample bricks C 1-3. The heaviest sample bricks with exfoliated vermiculite contained 50% fine grade exfoliated vermiculite and 50% sand. The average mass of this batch labelled F 4/4 was 0.143 kg. The latter was 24.7% lighter than the average sample brick batch C.

A clear trend was identified in that the lightest group sample bricks all contained six volume portions of exfoliated vermiculite and two volume portions of sand. The second lightest group sample brick contained five volume portions of exfoliated vermiculite and three-volume portions of sand. The heaviest group sample brick contained equal volume portions of sand and exfoliated vermiculite. This highlights the trend that the mass of the sample bricks is related to the volume content of exfoliated vermiculite. Analyzing the sample bricks made with micron exfoliated vermiculite revealed that the reduction in mass is not directly proportional to the volume increase of exfoliated vermiculite. As the volume of exfoliated vermiculite increases by 13% from sample M 4/4 to M 6/2, the average sample brick mass reduced by 10.0% and 5.9%. These results echo those achieved in the research done by Köksal , Coz Diaz , Gencel and Rabanal (2013). Theyfound that by increasing the exfoliated vermiculite to sand ratio in a mixture containing 10% cement the dry bulk density decreased. Increasing the exfoliated vermiculite to sand ratio from 3:1 to 6:1 dry bulk density reduced by 22.8%. Increasing the mixture ratio from 6:1 to 9:1 reduced the bulk density further, this time by 12.4%.

A trend was noticed during the mass tests. Comparing the same ratio mixtures it was clear that the finest grade in a specific ratio blend was the lightest and the largest grade the heaviest. This could not be explained against the bulk density of each grade as the bulk density increases as the exfoliated vermiculite size decreases. Typically, the bulk density of micron and super fine grades exfoliated vermiculite is 125 g/l and that of fine grade exfoliated vermiculite 112 g/l. The only plausible explanation is that a measured volume of micron grade vermiculite contained more particles than the coarser grades of exfoliated vermiculite. This is supported by the Particle size

distribution (PSD) analysis mentioned earlier in the report. And because the ratio blends were done per volume measure the finest grade displace more sand particles.

A pure strength test revealed that sample bricks containing vermiculite were on average 35.7% weaker than the average of the control sample bricks C, as shown in Table 2. The strongest sample brick was as expected the control cement brick C-1. The strongest sample brick containing exfoliated vermiculite contained five volume portions of micron exfoliated vermiculite and three-volume portions of sand and is labelled M 5/3 -2 .

The weakest sample brick labelled F 4/4 -1 contained 4 volume portions fine grade exfoliated vermiculite to 4 volume portions of sand. This unexpected trend was also noticed in other blend sizes. It was thought that this ratio would be the strongest. It was thought that the higher volume of sand in the sample bricks will increase their strength.

A trend was identified showing that the 5:3 ratio (five volume portions of exfoliated vermiculite to three volume portions of sand) was consistently the strongest ratio of each exfoliated vermiculite size range . The strength of the sample bricks also gradually decreased as the exfoliated vermiculite used in the mixtures increased in size and volume, from micron (finest) to fine (coarsest) grade and from a mix ratio of 5:3 to 6:2. These results are built on past research done by Georgiev, Yoleva, Djambazo\v, Dimitrov, Ivanova (2017). The researchers found that baked clay bricks with exfoliated vermiculite as an additive affected the strength of clay bricks as the volume percentage of vermiculite increased. The compression strength of baked clay bricks was on average 24 MPa and reduced to 17 MPa, 15 MPA and 12 MPa as the percentage of exfoliated vermiculite in the mixture increased from 3% to 5% and 8%. This trend was also evident in this research and compression strength was reduced when the mix ratio, vermiculite to sand increased from 5:3 to 6:2. The compression strength of the micron mixture was reduced by 20.8%, super fine by 14.5% and fine by 16.5%.

The trend was reversed when a compression strength-to-mass analysis was done. Reviewing the compression strength-to-mass analyses the strongest average sample brick by mass was the M 5/3 sample bricks. Of all the sample bricks tested, the batch average of the control sample bricks, labelled C, rated sixth. As with the strength analyses, the 5:3 ratio sample bricks were the strongest in each exfoliated vermiculite size category, followed by the 6:2 ratio, placing the 4:4 ratio last again. The sample bricks containing micron exfoliated vermiculite were again stronger by mass than the sample bricks containing super fine exfoliated vermiculite, which in turn was stronger than the sample bricks containing fine (largest size) exfoliated vermiculite. This analysis provides new insight into the strength review of bricks containing exfoliated vermiculite as it would suggest that taller structures could be built with these bricks. A quick calculation reveals that 9,291 control sample bricks C having a 0.0045m² area of compression can be stacked one on top of the other before the bottom sample brick reaches its failure compression strength of 4.026 MPa. In comparison a staggering 10,841 (M 5/3) sample bricks can be stacked one on top of the other before the bottom sample brick reaches its failure compression strength of 3.035 MPa.

The open flame structural integrity test results showed a significant reduction in structural integrity after a sample brick was exposed to a 1,400°C butane flame. Noticeable was that the strength of all sample bricks containing exfoliated vermiculite was less affected by the open flame test. The compression strength-to-mass of sample brick C -3 was reduced by 21.0% compared to an average reduction of the vermiculite samples of only 10.6%. Sample bricks containing 5 volume portions of exfoliated vermiculite to 3 volume portions of sand were on average the strongest before the burn test. Once exposed to the butane flame burn test its average compression strength-to-mass value was below that of the 6:2 ratio sample bricks. The compression strength-to-mass value of the 6:2 sample bricks was reduced by the lowest average percentage of 2.7% compared to 16.0% of the 5:3 mix ratio and 13.9% of the 4:4 mix ratio sample bricks. This can be explained by its high exfoliated vermiculite concentration as it benefited from the insulation properties of this material.

The experiment provides new insight into the use of exfoliated vermiculite in construction. No research articles were found in which the structural integrity of bricks containing exfoliated vermiculite was studied after it was exposed to fire. In the insulation test, the volume of exfoliated vermiculite used in the different sample bricks influenced the rate of heat loss. The results from heating each brick till the measuring point reached 400°C and then letting it cool down in a room at 20°C are summarized .

After 50 seconds the surface temperature of the exfoliated vermiculite sample was on average 34.7% cooler than the control sample brick C-3. The highest variance after 50 seconds compared to the sample brick C-3 a was 48.1°C. The test result highlighted a clear trend, the bricks containing vermiculite cooled down faster. This trend further increased as the volume ratio of exfoliated vermiculite increased in the sample bricks. The cooling down tempo relates to how much heat energy was stored in the sample brick. Therefore, a sample brick that cooled down faster stored less heat energy and therefore had better insulation properties. This view is supported by D Green, R Perry (2015).

Sample brick M 6/2 -3 had the best insulation properties and it coincided with the largest volume ratio of exfoliated vermiculite. This sample brick also contained the smallest size of exfoliated vermiculite which in theory replaced the largest amount of sand particles. These findings build on existing evidence of research done by Betty Beal, Audriana Selby, Colin Atwater, Christina James, Christopher Viens, and Catherine Almquist (2019). The study found that at a 25% concentration of the mass fraction made up of exfoliated vermiculite in clay bricks, the thermal conductivity decreased by 20%.

This was also the finding in the paper, by Köksal , Coz Diaz , Gencel and Rabanal (2013), The study found that the thermal conductivity measured in W/mK of a cement brick reduced as the volume of exfoliated vermiculite increased. At a fixed 10% cement by total volume the exfoliated vermiculite volume ratio to sand was increased from 3:1, 6:1 and 9:1. Thermal conductivity reduced from 0.536 W/mK to 0.514 W/mK and then 0.377 W/mk respectively. This study found a similar trend, the heat loss measured in degrees Celsius over the first 10 seconds was the greatest with a mix ratio of 6:2 followed by 5:3 and then 4:4. The temperature reading reduced respectively by 65.0%, 57.7% and 57.2%.

Having analysed all the test results, it can be seen that there is no one, clear way to choose the best performing sample brick. A statistical scoring system was therefore devised and presented in Table (6). In this table, a score of 10 was assigned to the best performing sample brick and a score of 1 to the worst performing sample brick. This was

done for each test and subsequent derivative. To maintain consistency, the control sample brick made from sand and cement only was included in the scoring system.

Table 6: Statistical Scorecard

Sample Bricks Batches	Mass Test	Compression Strength-to-mass ratio Unburnt	Compression Strength-to-mass ratio Burnt	Insulation Test	Total
C	1	5	4	1	11
M 4/4	4	6	5	3	18
M 5/3	6	10	8	8	32
M 6/2	10	7	9	10	36
SF 4/4	3	3	3	4	13
SF 5/3	7	9	7	2	25
SF 6/2	9	8	10	6	33
F 4/4	2	1	1	9	13
F 5/3	5	4	2	5	16
F 6/2	8	2	6	7	23

As can be seen from the above table the sample brick batch M 6/2 reflected the highest score. This sample brick scored the highest in two categories, namely mass and insulation and performed the second best in the compression strength-to-mass test after the sample bricks were exposed to a butane flame. It can therefore be deduced that based on this scorecard the sample bricks M 6/2 were on average the best performing brick.

7. Limitations and Errors

Some limitations in the testing equipment were identified the greatest of which was the hydraulic press. The fact that it was a manual, hand pump version, resulted in an uneven pressure increase. Ideally, a hydraulic press with a hydraulic pump would have been preferred as such a unit would have resulted in an even pressure gradient increase.

There were also pressure gauge limitations on the unit, the dial scale of the gauge was almost three times the range required meaning sighting errors crept in as it was necessary to estimate values when the pointer was between markings on the dial. A lower pressure gauge would have resulted in more exact readings.

8. Recommendations for Future Research

To better understand why a 50:50 (exfoliated vermiculite to sand) ratio sample brick was weaker than the 5:3 and 6:2 ratio (exfoliated vermiculite to sand) bricks, more studies could be done to confirm or refute this finding.

A more conclusive insulation test should be performed to test the insulation properties of bricks containing exfoliated vermiculite. Linking to this test a real fire simulation under controlled conditions would confirm if bricks containing exfoliated vermiculite are indeed more structural intact after a fire as this research project concluded.

9. Conclusion

The research aimed to prove a hypothesis. The perfect ratio for a suitable lightweight brick is such that exfoliated vermiculite will replace 50% of the volume of coarse sand used in a standard 8:1 (sand to cement) ratio cement brick. The compression strength-to-mass value of this lightweight brick will be as good as that of normal cement brick, but its mass will be significantly less, have better insulation properties, and its compression strength-to-mass value will be greater than that of a standard cement brick after both have been exposed to a simulated fire, and the series of tests did exactly that. The original hypothesis was generally correct.

It was found that the best performing batch of sample bricks, M 6/2 replaced 75% sand with exfoliated vermiculite. The hypothesis predicted 50%. The sample bricks containing exfoliated vermiculite were substantially weaker than the control sample brick batch C when reviewing the compression strength data only. However, when the failure pressure was reworked as a function of mass, sample brick batch M 6/2 was 9.96% stronger than the control batch C.

The tested mix ratios increased beyond the hypothesis which would strictly nullify the winning batch M 6/2 which weighed 45.8% less than the control batch C. To compensate for this, 50% ratios as per the hypothesis was analysed and it was determined that the average mass of the batch containing 50% exfoliated vermiculite still weighed 27.5% less than the standard batch C. This is again in line with the hypothesis.

The compression strength-to-mass value of the best performing batch M 6/2 was 9.96% above that of the control batch C. The compression strength-to-mass value of control brick C-3 was reduced by 21.0% after the simulated fire test compared to a mere 3.2% reduction of sample brick M 6/2 -3. It is therefore deduced that bricks filled with expanded vermiculite will be stronger per mass than normal cement brinks even after it has been exposed to a fire. This deduction is also in line with the hypothesis.

The research illustrated that a fine, exfoliated vermiculite is a better filler material than a coarser grade if used as a filler to reduce the mass of standard cement brick. More importantly, the study demonstrated that when the replacement volume ratio of sand exceeds 60% the bricks are stronger by mass than a standard cement brick. The significance of this was mentioned in the report. Due to the lightness and relative strength of the bricks, regulatory brick layer height can be achieved therefore such bricks have no limiting factor in normal wall construction. The significant mass saving would then also assist in drawing more women into this male-dominated market which will empower women and transfer skills to a new social grouping.

Acknowledgements

Throughout the writing of this report, I have received a great deal of support and assistance. I would first like to thank my teacher, Mrs Milandré Bezuidenthout, whose expertise was invaluable in formulating the research questions and methodology. Her insightful feedback pushed me to sharpen my thinking and brought my work to a higher level. I would also like to thank André Huysamen and Tanya Huysamen, my parents, for their wise counsel, a sympathetic ear, and assistance in writing, designing and editing this report.

References

[1] Alberternst, R., 2020. How many bricks can a bricklayer lay in a day?. [online] Findanyanswer.com. Available at: <https://findanyanswer.com/how-many-bricks-can-a-bricklayer-lay-in-a-day> [Accessed 7 March 2021].

[2] Beal, B., Selby, A., Atwater, C., James, C., Viens, C. and Almquist, C., 2019. A comparison of thermal and mechanical properties of clay bricks prepared with three different Pore-Forming additives: Vermiculite, wood ash, and sawdust. Environmental Progress & Sustainable Energy, 38(6), p.13150.

[3] Georgiev, A., Yoleva, A., Djambazov, S., Dimitrov, D. and Ivanova, V., 2018. Effect of exfoliated vermiculite and exfoliated perlite as pore forming additives on the physical properties and thermal conductivity of porous clay bricks.

. J. Chem. Technol. Metall, 53(2), pp.275-280.

[4] Grant, A., 2021. Gardening With Vermiculite - Vermiculite Uses And Information. [online] Gardening Know How. Available at: <https://www.gardeningknowhow.com/garden-how-to/soil-fertilizers/vermiculite-growing-medium.htm> [Accessed 2 July 2021].

[5] Grunert, J., 2021. [online] Garden.lovetoknow.com. Available at: <https://garden.lovetoknow.com/wiki/Vermiculite_for_Gardening> [Accessed 14 June 2021].

[6] Koksal, F., del Coz Diaz, J.J., Gencel, O. and Alvarez Rabanal, F.P., 2013. Experimental and numerical analysis of new bricks made up of polymer modified-cement using exfoliated vermiculite. Computers and Concrete, 12(3), pp.19-36.

[7] Mandovalvermiculite. 2021. Mandoval | Passive Fire Protection Products. [online] Available at: <https://www.mandovalvermiculite.co.za/> [Accessed 5 July 2021].

[8] McMahon, M., 2021. What is Vermiculite? (with pictures). [online] All Things Nature. Available at: <https://www.allthingsnature.org/what-is-vermiculite.htm> [Accessed 10 June 2021].

[9] Rabello, L.G. and da Conceição Ribeiro, R.C., 2021. A novel vermiculite/vegetable polyurethane resin-composite for thermal insulation eco-brick production. Composites Part B: Engineering, p.109035.

[10] Rashad, A.M., 2016. Vermiculite as a construction material–A short guide for Civil Engineer. Construction and Building Materials, 125, pp.53-62.

[11] Shiffler, A., 2021. Vermiculite: Uses for growing plants, safety, and comparison to Perlite. [online] Herbs at Home. Available at: <https://herbsathome.co/what-is-vermiculite/> [Accessed 2 July 2021].

[12] Sutcu, M., 2015. Influence of exfoliated vermiculite on physical properties and thermal conductivity of clay bricks. Ceramics International, 41(2), pp.2819-2827.

[13] The Editors of Encyclopaedia Britannica, 2021. Vermiculite | mineral. [online] Encyclopedia Britannica. Available at: <https://www.britannica.com/science/vermiculite> [Accessed 4 April 2021].

RESEARCH ABOUT EQUIPOTENTIAL LINES IN ELECTRICITY

Kiana Kamalipoor Shiraz, Farzanegan 2 high school, Tehran, Iran, kiana.k83@gmail.com

ARTICLE INFO

Participated in IYPT 2022, Romania

Advisor: Dr. Mohammad Shariatmadar

Selected by Ariaian Young Innovative Minds Institute , AYIMI

http://www.ayimi.org ,info@ayimi.org

ABSTRACT

To investigate equipotential lines, two electrodes are inserted into water and particles movement in electric field due to high voltage are illustrated. A supply and a voltmeter are used to determine electric potential at various locations to investigate how equipotential lines deviate from our expectations for different conditions and liquids.

Keywords :*Equipotential Lines, Liquid, Electric Field*

1. Introduction

Equipotential lines of each type of electrode are illustrated to find particles movement in electric field due to a high voltage electrodes. Any significant variation in shape of potential lines in different conductivity of different liquids should be considered and theoretical assumptions with experimental data will help to analyze the results.

2. Materials and Methods

To observe this phenomenon we have used several liquids such as tap water, water with salt, alcohol and oil and different types of electrode (Fig. 1).

Fig. 1: Types of electrode

When two electrodes are connected to a high voltage (Fig. 2), potential lines are observed which differ in various liquids.

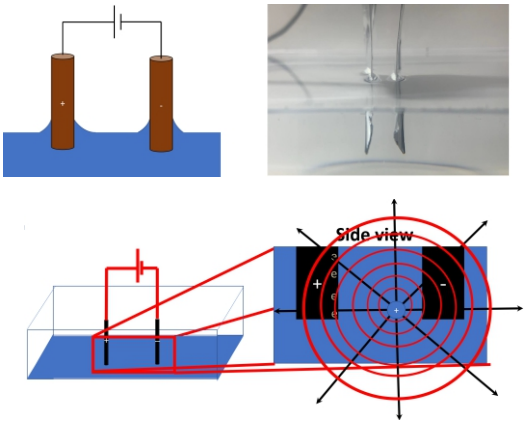

Fig. 2: Electric Potential Lines

Electric Potential lines are shown in macroscopic and microscopic view (Fig. 3).

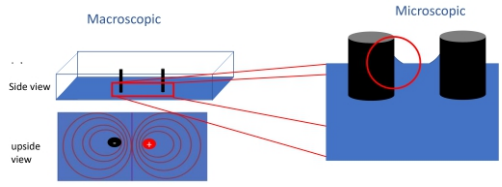

Fig. 3: Macroscopic and Microscopic view

3. Theory

As Poisson's Equation (Eq. 1):

$$\nabla . E = \frac{\rho}{\varepsilon_0} \qquad E = -\nabla V \tag{1}$$

Therefore potential relates to charge density by Poisson's equation (Eq. 2) which for charge free space it is zero (Eqs. 2 and 3).

$$\nabla^2 V = -\frac{1}{\varepsilon}\rho \tag{2}$$

$$\nabla^2 V = 0 \tag{3}$$

The potential of each point (Eqs. 4-6):

$$\psi = \frac{q}{|r - r_0|} + \frac{-q}{|r - r_0'|} \tag{4}$$

$$= \frac{q}{\sqrt{(x-x0)^2+(y-y0)^2+(z-z0)^2}} - \frac{q}{\sqrt{(x-x0)^2+(y-y0)^2+(z-z0)^2}}$$

$$dA = dx\, dy$$

$$\frac{\partial \psi}{\partial n} = -\frac{\partial \psi}{\partial z} = \frac{-2qz_0}{[(x-x0)^2+(y-y0)^2+z0^2]^{\frac{3}{2}}} \tag{5}$$

$$\Phi_{(r0)} = \frac{1}{4\pi}\int dxdy\Phi\ (z = 0 \tag{6}$$

and Electric field (Eqs. 7-9):

$$\nabla \times E = 0 \qquad \Rightarrow E = -\nabla V \tag{7}$$

but in electro dynamics (Eqs. 8-11):

$$\nabla \times E \neq 0 \tag{8}$$

$$\nabla . B = 0 \tag{9}$$

$$\nabla \times E = \frac{-\partial B}{\partial t} \quad \Longrightarrow \nabla \times E = \frac{-\partial\,(\nabla \times A)}{\partial t} \tag{10}$$

$$\Longrightarrow \nabla \times (E + \frac{\partial\,(\nabla \times A)}{\partial t}) = 0$$

$$\text{so } E = -\nabla V - \frac{\partial A}{\partial t} \tag{11}$$

Green's Theory: It states that any two scalar (Φ, ψ) inside a volume (V)having a boundary surface A satisfies the following relationship (Eqs. 12- 13):

$$\int_V dV(\Phi \nabla^2 \psi - \psi \nabla^2 \Phi) = \oint_A dA(\Phi \frac{\partial \psi}{\partial n} - \psi \frac{\partial \Phi}{\partial n}) \tag{12}$$

$$\nabla^2 \psi = -4\pi q \delta^{(3)}(r - r_0) \tag{13}$$

$\delta^{(3)}$: Delta function in three-dimensional space
Φ : electric potential
ψ: auxiliary field

Potential of each point (Eqs. 14-15)

$$\Phi_{(r0)} = -\frac{1}{4\pi q} \oint_A (\Phi \frac{\partial \psi}{\partial n} - \psi \frac{\partial \Phi}{\partial n}) \mathrm{dA} \tag{14}$$

Boundary conditions for Φ :

Dirichlet $\Longrightarrow \psi = 0$

Neumann $\Longrightarrow \nabla \psi = 0$

then (Eq. 15):

$$\Phi_{(r0)} = -\frac{1}{4\pi q} \oint_A \Phi \frac{\partial \psi}{\partial n} \mathrm{dA} \tag{15}$$

4. Experiment

In this research we have used linear , point and Concentric electrodes in liquids (Figs. 4-8).

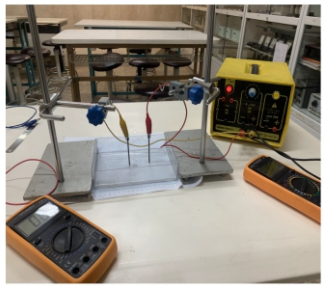

Fig. 4: Experimental setup

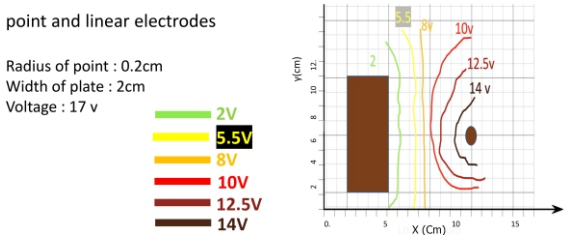

Fig. 5: Potential lines in Point and linear electrodes

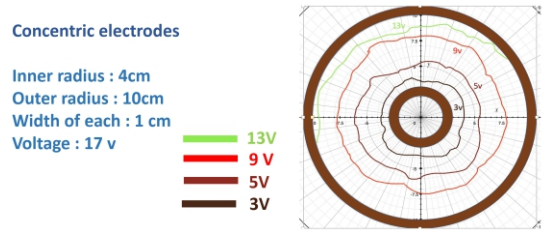

Fig. 6: Potential lines in concentric electrodes

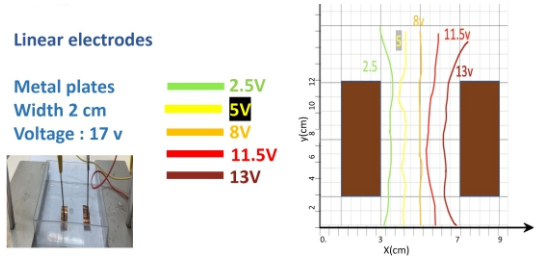

Fig. 7: Potential lines in linear electrodes

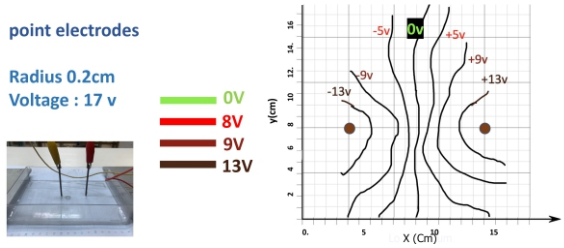

Fig. 8: Potential lines in point electrodes

This experiment is done with various liquids and the results are analyzed (Fig. 9).

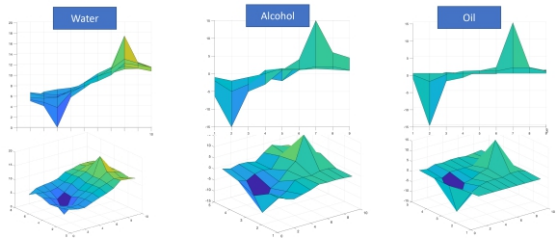

Fig. 9: Analysis of experiments in different liquids

By simulation all the results are compared in different electrodes (Figs. 10-13).

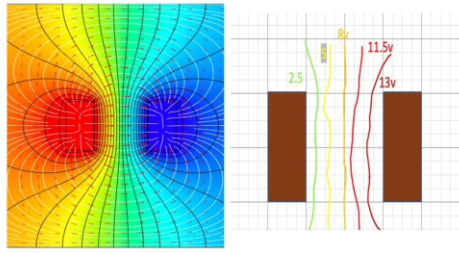

Fig.10: Simulation and experiments comparison in linear electrode

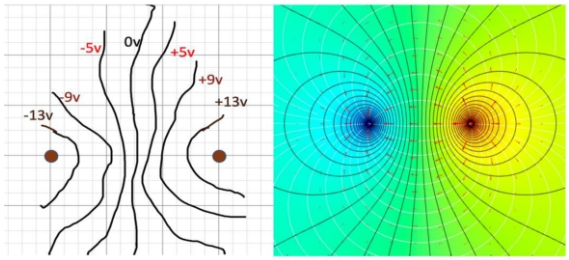

Fig.11: Simulation and experiments comparison in point electrode

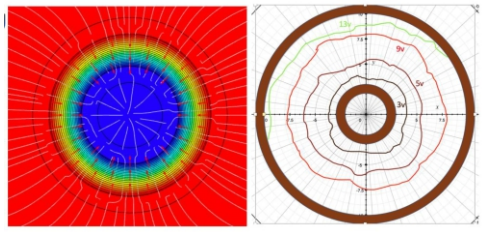

Fig.12: Simulation and experiments comparison in concentric electrode

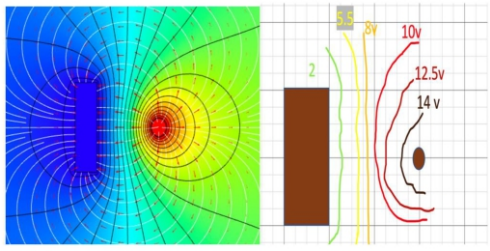

Fig.13: Simulation and experiments comparison in linear/ point electrode

5. Conclusion

Equipotential lines of each type of electrode were illustrated . There wasn't any significant variation in shape of potential lines in different conductivity of liquids. By changing dielectric constant of liquid potential lines varied. Theoretical expectation and experimental results were compared.

References

[1] D.Halliday ,In: Fundamentosde Física :eletromagnetismo (LTC, Rio de Janeiro, 2009), v. 3, p. 81

[2] Griffiths , David j introduction to electrodynamics / David j. Griffiths-3rd-ed

[3] Feynman, R. P., Leighton, R. B., Sands, M., The Feynman Lectures on Physics, Volume 2, Addison-Wesley, 1977

[4] Distribution of Charge and Potential in an Electrolyte Bounded by Two Plane Infinite Parallel Plates

[5] A theoretical method of electric field analysis for dielectrophoretic electrode arrays using green's theorem

APPLE BROWNING

Eileen Hemmati, Farzanegan 2 high school, Tehran, Iran

ARTICLE INF

Participated in PYNT 2017

Advisor: Dr. Mohammad Qorbani

Accepted by Ariaian Young Innovative Minds Institute , AYIMI

http://www.ayimi.org ,info@ayimi.org

ABSTRACT

This problem is about apple turning brown after being cut or bruised. We need to find ways of preventing browning. To find chemical reactions and parameters which are important in this phenomenon, Several experiments are designed . Some of the substances such as citric acid, and salt are studied and the duration which it takes the color of the fruit (apple) is changed. The objective of the present work was to quantify enzymatic browning and PPO activity and identify and quantify target polyphenols in apple. Fruit which contains acid, it is helpful in stopping the enzymatic browning and somehow paralyzes the polyphenol cells.

Keywords : *, Enzymes ,Polyphenols, Browning, Fruit*

1. Introduction

Polyphenols are one of the most important and certainly the most numerous among the groups of phytochemicals present in the plant kingdom.

Currently, over 8000 phenolic structures have been identified, of which more than 4000 belonging to the class of flavonoids, and several hundred occur in edible plants.

However, it is thought that the total content of polyphenols in plants is underestimated as many of the phenolic compounds present in fruits, vegetables and derivatives have not yet been identified, escaping the methods and techniques of analysis used, and the composition in polyphenols (Fig. 1) for most fruits and some varieties of cereals is not yet known.

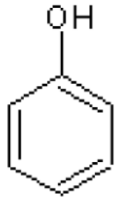

Fig. 1: Polyphenol molecule

The term polyphenols refers to a wide variety of molecules that can be divided into many subclasses, subdivisions that can be made on the basis of their origin, biological function, or chemical structure. Chemically, they are compounds with structural phenolic features, which can be associated with different organic acids and carbohydrates. In plants, the most part of them are linked to sugars, and therefore they are in the form of glycosides. Carbohydrates and organic acids can be bound in different positions on polyphenol skeletons.

Among polyphenols, there are simple molecules, such as phenolic acids, or complex structures such as condensed tannins, that are highly polymerized molecules.

2. Material and Methods

2.1. Polyphenol Oxidase

Polyphenol oxidase (tyrosinase) (TY) is a bifunctional, copper-containing oxidase having both catecholase and cresolase activity (Malmström and Rydén 1968) (Fig. 2).

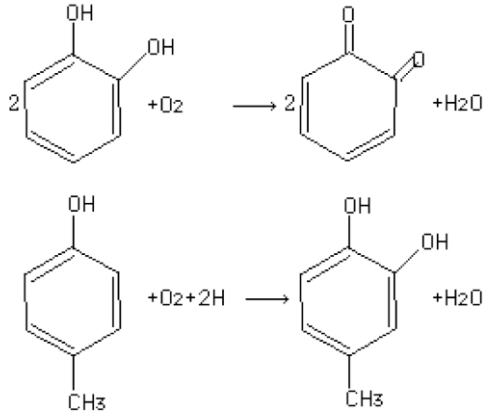

Fig. 2: Polyphenol oxidase

Jolly et al. (1974) refer to it as oxygen and 4 electron-transferring phenol oxidase. It is responsible for browning reactions throughout the phylogenetic scale.

Although a tyrosine from Neurospora crassa has been purified (Fling et al. 1963), most work has been done with the mushroom enzyme, even though yields and consistency are poor; its multiplicity was shown by Smith and Krueger (1962). Bouchilloux et al. (1963) obtained four enzymes. See review by Nelson and Mason (1970).

Inhibitors: Compounds that complex with copper. The enzyme is also inhibited competitively by benzoic acid with respect to catechol and by cyanide with respect to oxygen (Duckworth and Coleman 1970).

Activity: Polyphenol oxidase is an oxygen transferring enzyme. Besides using O2 to catalyze the dehydrogenation of catechols to orthoquinones and the orthohydroxylation of phenols to catechols, a peroxidase activity has been reported on by Strothkamp and Mason (1974). Kinetic studies have been reported by Kertész et al. (1971). See also the review by Malmström and Rydén.

Specificity: A large number of parasubstituted catechols areoxidized (Duckworth and Coleman 1970).

Stability: The lyophilized preparation is stable for 6-12 months when stored at -20°C.

2.2. Enzymatic Browning

Enzymatic browning is one of the most important reactions that occur in fruits and vegetables, usually resulting in negative effects on color, taste, flavor, and nutritional value. The reaction is a consequence of phenolic compounds' oxidation by polyphenol oxidase (PPO), which triggers the generation of dark pigments. This is particularly relevant for apples, which are rich in polyphenols and highly susceptible to enzymatic browning. The objective of the present work was to quantify enzymatic browning and PPO activity and identify and quantify target polyphenols in apple [Malus ×sylvestris (L.) Mill. var. domestica (Borkh.) Mansf.] pulp in the cultivars (cvs.) Aori27, Elstar, Fuji, and Mellow at three fruit developmental stages (FDS).Enzymatic browning showed significant among cvs. and FDSs and interaction between both factors. PPO activity showed significant difference among cultivars and FDSs. A significant difference was evidenced for polyphenol content among cultivars and FDSs with interaction between both factors (Fig.3).

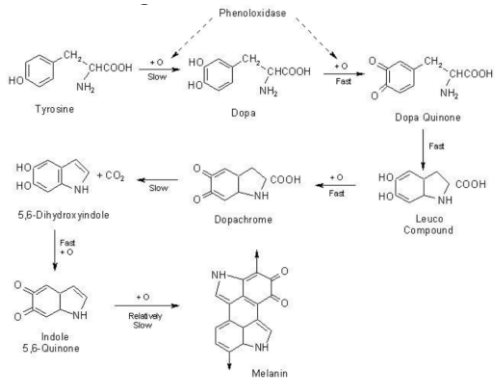

3. Experiment

3.1. Lemon Juice

Lemon juice is another traditional and popular way of preventing this procedure. Lemon juice with the pH of 2 to 2.60 is considered as a fruit which contains acid, which is really helpful in stopping the enzymatic browning and somehow paralyzes the polyphenol cells. But there's a problem! We need a general way to prevent, but lemon juice changes the taste and color of the apple slices (Fig. 4).

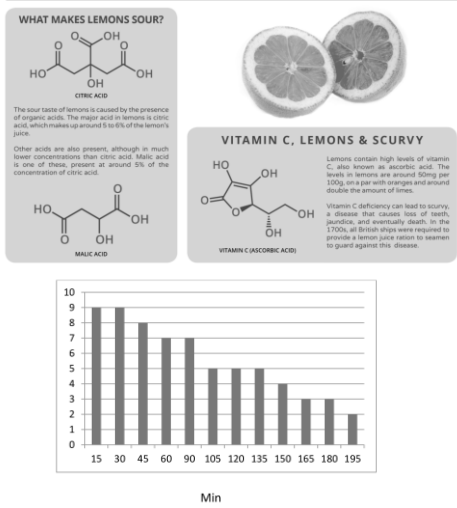

Fig. 4: Stopping the enzymatic browning vs time by Lemon juice

3.2. Tap Water

You probably know water's chemical description is H2O. A water molecule consists of one atom of oxygen bound to two atoms of hydrogen. The hydrogen atoms are "attached" to one side of the oxygen atom, resulting in a water molecule having a positive charge on the side where the hydrogen atoms are and a negative charge on the other side, where the oxygen atom is. Since opposite electrical charges attract, water molecules tend to attract each other, making water kind of "sticky." The side with the hydrogen atoms (positive charge) attracts the oxygen side (negative charge) of a different water molecule. All these water molecules attracting each other mean they tend to clump together. This is why water drops are, in fact, drops! If wasn't for some of Earth's forces, such as gravity, a drop of water would be ball shaped -- a perfect sphere. Even if it doesn't form a perfect sphere on Earth, we should be happy water is sticky. Water is called the "universal solvent" because it dissolves more substances than any other liquid. This means that wherever water goes, either through the ground or through our bodies, it takes along valuable chemicals, minerals, and nutrients(Fig. 5).

Pure water has a neutral PH about 7, which is neither acidic nor basic.

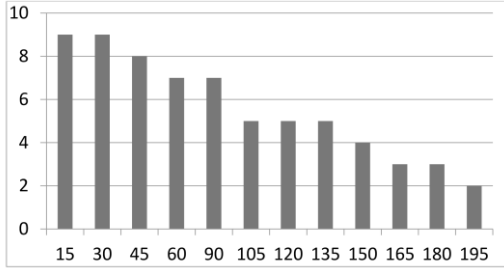

Fig. 5: Stopping the enzymatic browning vs time by Tap Water

3.3. Citric Acid

As we know citric acid is a nearly strong acid which could destroy our apple So I used one with higher pH which is 4.8, but I used it in two forms, crystals and liquid. To estimate what form works the best, I tested both of them. The pH of this acid is 4.8 and the chemical FormulaC6H8O7.

We used 50 g of Crystal form of Citric acid and sprinkled it all over the bare part of apples. It ruins the surface and gives it a chemical taste which makes it uneatable and it is more harmful than the liquid form.

In other experiment we poured 50 g acid on the surface. It makes red color but after 1 hour it stayed still and it was better than crystals (Figs.6 and 7).

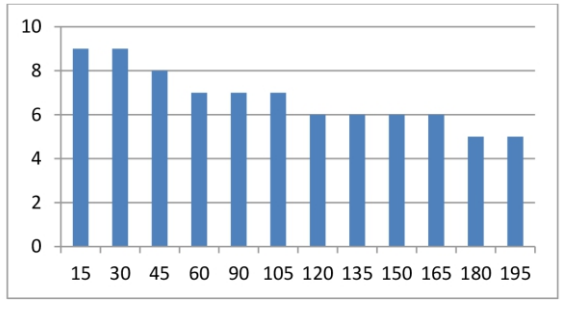

Fig. 6: Stopping the enzymatic browning vs time by liquid citric acid

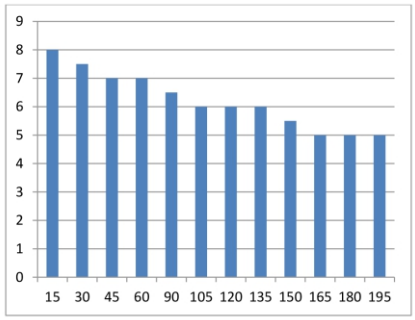

Fig. 7: Stopping the enzymatic browning vs time by crystal citric acid

3.4. Salt

Sodium chloride is the most common salt, the common table salt used for the seasoning of food. It forms in cubic crystals apparent even in table salt. It occurs commonly in the mineral form, halite, also called rock salt. It can be formed by the acid-base reaction of hydrochloric acid and sodium hydroxide:

$HCl + NaOH \rightarrow H2O + NaCl$

As a solid, sodium chloride is crystalline and forms a cubic lattice. The bonding of the sodium and chlorine atoms is one of the classic examples of ionic bonding. In aqueous solution it ionizes to Na+ and Cl- ions and forms an electrically conducting solution.

The ionic bonding of NaCl can be visualized in terms of Lewis diagrams.

When the diameters of sodium and chlorine and their ions are measured, they offer some confirmation of the picture of ionic bonding.

When sodium loses an electron to form Na+, its effective size decreases to about half. When chlorine gains an electron to produce the octet structure Cl-, its size increases to almost double (Shipman, et al).

Sodium chloride exists on the earth in great abundance in sea water and is an important part of the fluid electrolytes of humans and other living organisms (Fig. 8).

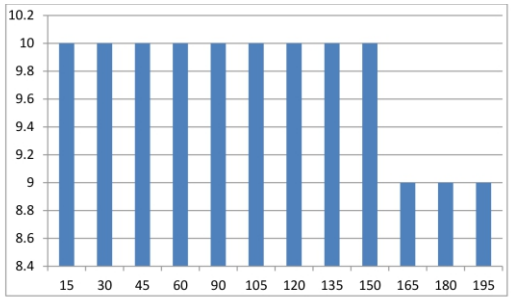

Fig. 8: Stopping the enzymatic browning vs time by salt

4. Results

Due to diagrams salt was the substance we were looking for, by a small calculation we realize that it's the best possible way. Because when we sprinkle a small amount of this chemical on the surface, it keeps it white for a long time and has 2cm penetration after 3:45 hours. But the disadvantage in that it soaks in the water and makes it like jelly.

So the solution changes, we need a physical way of preventing which is blocking the oxygen which is physical. Because it's general and can be used by companies and for shipping this fruit to long distances.

Fig. 9: Different slices with salts to prevent browning

5. Conclusion

After all the progress in our experiments , still we haven't found an adequate and general chemical substance that can be used in some jobs such as shipping fruits like apple or pear over long distances.

But the answer is a physical change and not a chemical one. Because any chemical change, changes the substance and that physical change that I considered , is blocking the oxygen because oxygen helps the process of oxidizing the polyphenols by polyphenol oxidase so it needs to be taken away.

IN SILICO DESIGN OF COMPETITIVE INHIBITORS USING DEEP REINFORCEMENT LEARNING

Lukas Dubsik , Gymnazium Brno-Reckovice university, Czech Republic, Contact: xdubs@gyrec.cz,

ARTICLE INFO

Gold medalist in BUCA IMSEF 2022

Consultant: Mgr. Ondrej Schindler – Masaryk

Awarded by Ariaian Young Innovative

Minds Institute , AYIMI

http://www.ayimi.org ,info@ayimi.org

ABSTRACT

The aim of this work is to design a program capable of rapid and accurate design of new drugs. Enzymes and their interacting competitive inhibitors have been chosen as the focus. However, the final model can also be applied to other reactants. Several additional models were also built to achieve the goal, namely NDock which is responsible for faster molecular docking. Several libraries were also created in Python, C# and C++ programming languages to facilitate the manipulation of the files describing each structure. The molecule that is given the highest score using molecular docking (NDock used here) moves on and is edited in a stepwise fashion.

Keywords : *Accurate Design, Molecular Docking, Enzymes ,Competitive Inhibitors*

1. Introduction

Enzymes are proteins that are involved in most biochemical reactions in organisms. The aim of this work is to design a program capable of rapid and accurate design of new drugs based on enzyme inhibitors. An inhibitor is a molecule that binds to an enzyme more strongly than its substrate and therefore prevents the enzymatic reaction of the substrate. Examples of enzymes include the well-known Ibuprofen.

The input of the prediction program is a protein - enzyme and its already known ligand - substrate. Using deep feedback learning methods, the program attempts to find a molecule that binds to the protein more strongly than the provided substrate and thus acts as an inhibitor of the protein. The process is iterative, and at each iteration the inhibitor candidates are suitably adjusted to maximize the binding between the enzyme and the inhibitor.

The program is designed to be general so that it can be easily extended to other enzymatic reaction types. Several additional programs have been designed to achieve the goal. Examples include NDock (Neural Molecular Docking), which is responsible for accelerated molecular docking, or libraries for easier manipulation and handling of molecular structure information files.

The predicted molecules are stable and bear similarity to the experimental inhibitors, but neither their synthesis nor subsequent experimentation was part of the work. The accuracy of the program is close to the accuracy of the classical Autodock 4 method. The main advantage of the developed program is its speed and low computational power cost. The library itself (under the name BIP - Bioinformatic Python) and its various functions, such as force fields, searching for non-covalent interactions or working with chemical files, is applicable in other programs.

2. Method

Today's medicine is usually concerned with synthesising drugs that can be used for the largest possible proportion of the population. However, some fields of medicine require highly specific treatments tailored to the patient. An example is cancer, where the increase in mutations is so rapid and their properties so different that an effective cure for all is almost unattainable. However, a large, highly accurate and sufficiently fast bioinformatics apparatus is needed to design specific drugs.

After the disease-causing protein is discovered and its structure is also found, it can be inserted into the program itself. Here, important information such as electrical charge, aromaticity or free energy is first extracted and then entered into the database. The molecule then goes into a structure modification program that uses deep feedback learning. Here, the structure is iteratively refined over time. As a result, there are several possible, competitive inhibitors. These candidate inhibitors undergo testing to see if they are indeed inhibitors, so as not to further propagate possible errors. Candidates that pass the test are given a score, which is the sum of the free energies obtained using the NDock program. This score tells us how good a competitive inhibitor the inhibitor is. Only the molecule with the highest score is re- entered into the database for structure modification. This iteration continues until the number of iterations specified by the user is completed or the final molecule is found.

The steps of the program, and the results, are summarized below.

2.1. Program to Modify Molecule

At each step of the model, the molecule goes through 3 main processes. First the molecule is treated, then it is classified, and finally it is given a score that tells how good an inhibitor it is. There are 4 separate deep feedback networks operating within the modification, each responsible for one part of the modification (Fig. 1).

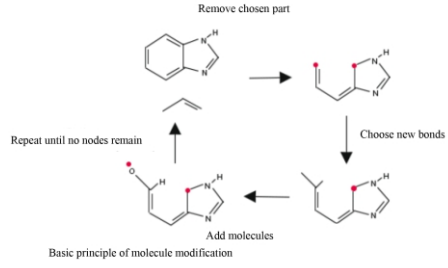

Fig.1: Basic principle of molecule modification

First, all the interconnected parts of the molecule are selected, which, even after their removal, leave the molecule as a single unit. Their maximum size is determined by the user, with a size of 3 for smaller molecules and up to 7 for larger ones. However, the time and computational power requirements increase exponentially with larger size (Fig. 2).

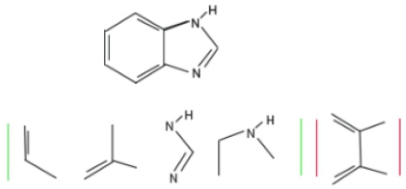

Fig. 2: Allowed and disallowed parts of a molecule, disallowed parts are those that split the molecule into multiple parts.

For each selected part, a decision is then made whether or not to remove it. This is done by the first model. The atoms that have bonded with the removed atoms are then taken as the nodes from which the new part of the molecule will be built. These nodes are then given a score based on the number of bonds they can form (Fig. 3).

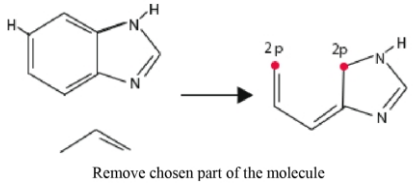

Fig. 3: Remove part and add nodes

Each node is then assigned links that are selected based on both its score and the output of the other model. Atoms or links are then selected to the bonds with the help of the third model. In the case of a link, this node is connected to another node with the help of the fourth model. If any of the newly added atoms has a score greater than zero, that atom then becomes a new node.

The ligand is modified by the model until no nodes remain. This happens gradually by selecting hydrogens as atoms, which always have a score of 0, or by joining nodes. In the initial stages of training, however, the ligand size may grow exponentially, but this can be avoided by setting limits on the start and removing them gradually (Fig. 4).

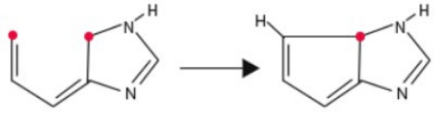

Fig. 4: Possible disappearance of the nodes of the molecule by adding hydrogens or joining, formation also ends when the possible limit of atoms is reached

3. Classification

Using free energy, it is possible to determine how strong the ligand binding is in the active site, but it is not possible to tell if it is an inhibitor or a substrate. If we assume that the binding is strong enough, it is necessary to know the outcome of the reaction. Instead of the complicated and tedious calculation of the ligand reaction result, it is much simpler to use neural networks. For ligand resolution, a dataset was constructed from the KEGG, RCSB PDB, PubChem and ZINC databases. The dataset contains a set of proteins and their substrates, inhibitors and activators. Each protein and ligand were transformed into an N-Cube representation and then added together with its protein to the neural network model.

The model uses convolutional learning, kernels (matrices used as filters in CNNs) are applied to both protein and ligand and then combined into a single linear layer with a uniform result.

The initial dataset was split into training, validation, and test datasets, with the final results summarized below. The result was surprising, achieving up to 97% accuracy (Fig. 5).

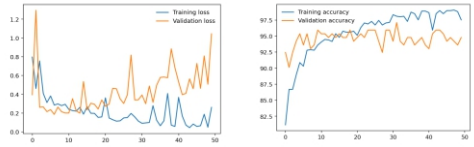

Fig. 5: Loss and accuracy of classifier training after transfer learning of convolutional networks

4. Molecular Docking to Detect Competitive Inhibition

During enzymatic reactions, both the binding of ligands to enzymes and the eventual conversion of these substrates into products and termination of binding occur. Using the equilibrium constant Keq we are able to represent both reactions. Here, I have chosen free energy for the calculation, as we would require complex simulations for the kinetic constants.

There are 3 basic methods to estimate the free energy itself. Using the full scheme requires an evaluation of the free energy at each point, and hence complex integrations. Using a finite point, like the full scheme, requires knowledge of the neighborhood of the ligand when it is outside the active region of the protein.

$$\Delta G_e = \frac{1}{2}\left[U_{site}^{elec} - U_{bulk}^{elec}\right] + \alpha\left[U_{site}^{vdW} - U_{bulk}^{vdW}\right] + \gamma$$

The best solution, however, is an empirical calculation that only considers the position of the ligand in the active region. The use of this calculation is mostly applied in molecular docking, which tries to determine the position of the ligand in the active site using this very rough approximation of the free energy. Docking scores can be calculated based on the Lennard- Jones potential (taking into account the interaction of atoms, mainly Van der Wals forces), electrostatic forces and solvation parameters (representing the displacement of water during the ligand reaction).

$$\Delta G_e = \sum_i^{prot}\sum_j^{lig}\left(\frac{A_{ij}}{r_{ij}^{12}} + \frac{B_{ij}}{r_{ij}^{6}} + 332\frac{q_i q_j}{\varepsilon(r_{ij})r_{ij}} + (V_i S_j + V_j S_i)e^{\frac{-r_{ij}}{2\delta^2}}\right)$$

$$A_{ij} = 4\varepsilon\delta^{12} \qquad B_{ij} = 4\varepsilon\delta^{6} \qquad S_i = L_i + 0{,}01097q_i \qquad V_i = \frac{4}{3}\pi r_i^3$$

$$\varepsilon(r_{ij}) = F + \frac{H}{\epsilon + ke^{-\mu H r_{ij}}}$$

5. NDock – Neural Molecular Docking

The dataset was compiled using the KEGG database. The protein structure (in both pdb and mmcif format), and subsequently the active site structure, was obtained from the RCSB PDB (Protein data bank) and the ligand structure from PubChem (in sdf format). The larger the dataset, the better the results can be expected. Unfortunately, I did not

have enough computing power to take full advantage of this fact, so I constructed a dataset of average size with the largest possible variation (approximately 3000 entries).

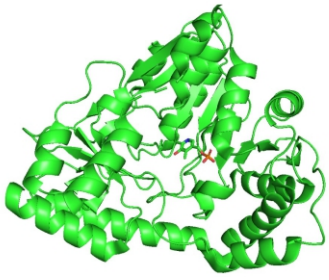

Fig. 6: Example of Protein and its ligand used from my dataset, PyMOL server was used for illustration

Before the data can be used to train a neural network, it must be normalized for a uniform representation. Thus, active sites and their ligands and targets were extracted from each protein. The target here is meant to be the position of the ligand given in the pdb file, the ligand is the position of the downloaded pdf file, so the goal is to get the ligand to the position of the target (Fig. 7).

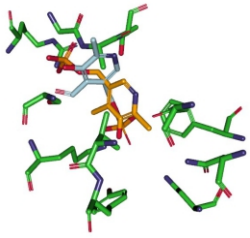

Fig. 7: Active site, target in orange, ligand in light blue

The ligand, target and active site are then normalized to the origin and rotated. The rotation is done by selecting the atom closest to the origin and then rotating it so that all dimensions, except y, are 0. Both the ligand and the active site are rotated in this way. The target is normalized and rotated by the same values as the active site.

The active site and ligand were converted to their respective representations (AMK and SELFIES sheets). A recurrent network was used for each part, which was pre-trained on the encoder/decoder model due to lack of computational resources. The encoder outputs were then combined into a single linear layer. The use of recurrent networks has the advantage that we can have an unspecified number of inputs.

$$RMSD = \sqrt{\frac{1}{N_A}\sum_{i=0}^{N_A}((x_{Ri}-x_i)^2+(y_{Ri}-y_i)^2+(z_{Ri}-z_i)^2)}$$

The output of the model is 6 numbers, these represent the displacement of the centre of the molecule in space and rotation in 3 angles using rotation matrices. The loss of the model is then calculated using RMSD (Root mean square deviation).

6. Using Classification as a Reward System

The program uses feedback learning to modify the ligand and create a competitive inhibitor. However, in order to use feedback learning, we need a reward system by which the model can orient itself and learn how to proceed.

Initially, the ligand must be classified, differentiated into substrate, inhibitor or activator, indicating to the model that the ligand must be changed into an inhibitor. In the case of classification as an inhibitor, the score deals with the measurement of enzymatic reactions and tells us how good the inhibitor is competitively.

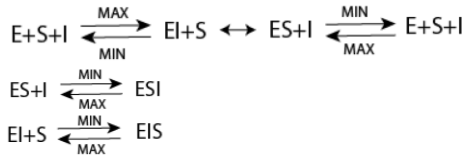

These reactions are evaluated based on a docking score (NDock used here) modelling the free energy and then combined in a final score, in case of a classification other than inhibitor, the program is terminated.

7. Results of the Molecule Modification Program

The goal of the program is rapid and accurate drug design. Therefore, three drugs that act as competitive inhibitors were selected, namely Acetazolamide, Viagra and Methotrexate (Fig. 8).

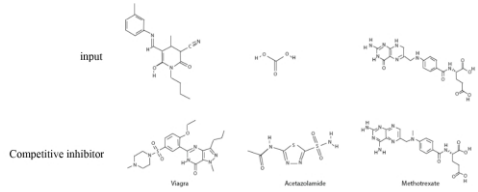

Fig. 8: Demonstration of input molecules, substrates, and experimentally determined competitive inhibitors

First, a dataset of their proteins, active sites and the substrates they inhibit was obtained. This data was entered into a program and 100 possible competitive inhibitors were obtained for each. The results were then divided into 2 categories, those that most closely resembled the experimental results and those that received the highest reward (Fig. 9).

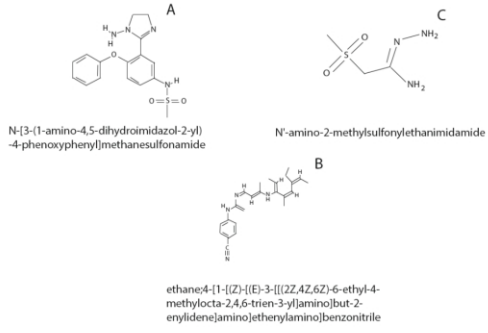

Fig. 9: Molecules with the highest score determined by the program. (A) Viagra. (B) Methotrexate. (C) Acetazolamide.

As can be seen here, the final results with the highest scores do not resemble their experimental counterparts. Even if they have higher programmed scores than the inhibitors themselves, it is difficult to say whether they are better, this could only be determined experimentally or by quantum chemical methods (Fig.10).

The molecules most similar to the experimental ones did not have the highest scores. These molecules, although bearing some similarity, started to form at the beginning of the program, then the further the program went on, the more

the molecules diverged. This phenomenon can also be explained by the fact that as the program goes on it gets better scores, so these molecules, even the experimental ones, are not the best. It's just that the properties of the ligand can be altered by a single changed atom, so concluding this assumption is rather wrong .

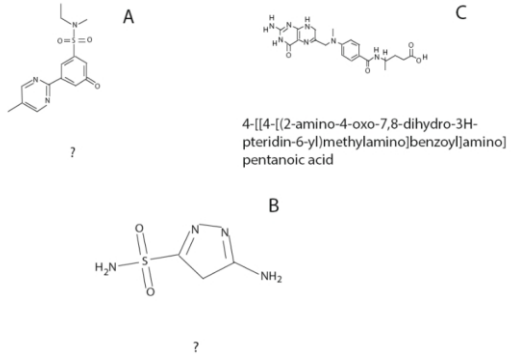

Fig. 10: Molecules with the highest similarity to the experimental results determined by the program. (A) Viagra. (B) Acetazolamide. (C) Methotrexate. Question marks indicate that the molecule was not found in the databases

The molecules generated by the program as possible competitive inhibitors of the previously mentioned substrates were finally compared with the database in PubChem and Zinc to see if they were valid and had already been synthesized. Of the said molecules, I just found 82% (2473 out of 3000 results) and was able to identify them. However, the remaining 18% passed as valid in a force field test to determine spatial arrangement .

8. Comparison of Neural Docking and Classical Methods

The carbanic anhydrase protein (in pdb format under 1dmy) in complex with the competitive inhibitor Acetazolamide, used for example in the treatment of epilepsy or glaucoma, was selected as an example of the results (Fig.11).

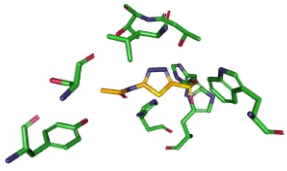

Fig.11: Example of docking target, crystallographically determined structure

To validate the classical methods, AutoDockTools software was first applied to add hydrogens, calculate charges, determine rotating ligand bonds, and determine the search space. The prepared protein and ligand were loaded into Autodock 4. The best result offered had an RMSD loss of 1.456 (Fig. 12).

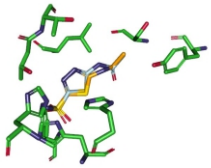

Fig.12: The result of molecular docking using Autodock 4 software, shown here in light blue

Subsequently, I repeated the process in my program. Here the final loss was 2.018 (Fig. 13).

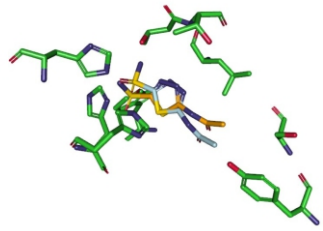

Fig. 13: Result of Neural Docking, here marked in light blue

Then I performed the same process on the extended dataset, each element of this data was not included in the training set for neural docking.

Table 1: Summary results for Autodock 4 and Ndock

Results	Autodock 4	NDock
RMSD	~2.045	~2,854
Time	~3 days	~12,13 min

Even though my loss was higher than the classical methods, it was still acceptable (the difference between the result and the target is such that the free energy calculations and other values are comparable to each other). The speed and efficiency, as expected, exceeded those of the classical methods. In the case of my program, the dataset of 1000 molecules and their proteins took me around a few minutes to run, Autodock 4 took several days.

9. Conclusion

The main goal of the work was to develop a program using deep feedback learning for the design of new competitive inhibitors. To achieve this goal, the program NDock was created using neural docking as a faster but not more accurate alternative to existing methods such as Autodock 4. In my work, I additionally created several libraries, mostly in the Python programming language.

Although NDock does not show the same accuracy as classical methods, its results are sufficient. However, its main advantage is its speed and low computational power cost. The program creates realistic, mostly already synthesized molecules. The library itself and its various functions, such as force fields, searching for non-covalent interactions or working with chemical files (sdf, pdb, mmcif), is applicable to other problems, but at the time of writing the library is far from complete.

The structure of the program itself is very flexible. If the score to be followed is defined correctly, the meaning and the goal can be easily changed. The work itself focuses only on competitive inhibitors, but the exact same procedure is applicable to other inhibitors, even other types of ligands. The idea that the input is the substrate, and the output is the inhibitor is also changeable. The input can be the experimental inhibitor itself and the function of the program becomes the modification of the inhibitor. In this way, the system can be adapted to any work with modification or creation of molecules.

References

[1] Shin, S.H., Bode, A.M. & Dong, Z. (2017). Precision medicine: the foundation of future cancer therapeutics. Dostupné z: https://doi.org/10.1038/s41698-017-0016-z

[2] Bayat A. (2002). Science, medicine, and the future: Bioinformatics. Available at: https://doi.org/10.1136/bmj.324.7344.1018

[3] Hughes, J. P., Rees, S., Kalindjian, S. B., & Philpott, K. L. (2011). Principles of early drug discovery. Dostupné z: https://doi.org/10.1111/j.1476-5381.2010.01127.x

[4] Kanehisa, M. and Goto, S. (2000). KEGG: Kyoto Encyclopedia of Genes and Genomes. Nucleic Acids Res. 28, 27-30.

[5] Kanehisa, M. (2019). Toward understanding the origin and evolution of cellular organisms. Protein Sci. 28, 1947-1951.

[6] Kanehisa, M., Furumichi, M., Sato, Y., Ishiguro-Watanabe, M., and Tanabe, M. (2021). KEGG: integrating viruses and cellular organisms. Nucleic Acids Res. 49, D545-D551.

[7] Kim S, Chen J, Cheng T, et al. (2021). New data content and improved web interfaces. Nucleic Acids Res. 2021;49(D1):D1388-D1395. Available at: https://doi:10.1093/nar/gkaa971

[8] Sterling, Irwin. (2015). J. Chem. Inf. Model. Available at: http://pubs.acs.org/doi/abs/10.1021/acs.jcim.5b00559

[9] H.M. Berman, J. Westbrook, Z. Feng, G. Gilliland, T.N. Bhat, H. Weissig, I.N. Shindyalov, P.E. Bourne. (2000). The Protein Data Bank. Available at: Nucleic Acids Research, 28: 235-242.

[10] RDKIT: Open-source cheminformatics. Available at: http://www.rdkit.org

[11] The PyMOL Molecular Graphics System, Version 1.2r3pre, Schrödinger, LLC.

[12] Morris, G. M., Huey, R., Lindstrom, W., Sanner, M. F., Belew, R. K., Goodsell, D. S. and Olson, A. J. (2009). Autodock 4 and AutodockTools4: automated docking with selective receptor flexibility. J. Computational Chemistry 2009, 16: 2785-91.

[13] Oystein Bjorke, Lunci Hua. (2012). Helix Toolkit WPF.

[14] Bruce Alberts, Alexander Johnson, Julian Lewis, David Morgan, Martin Raff, Keith Roberts a Peter Walter. Molecular biology of the cell. 6. ed. Canada, 2015, s. 1342. ISBN: 978-0-8153-4464-3.

[15] Johnson, K. A., & Goody, R. S. (2011). The Original Michaelis Constant: Translation of the 1913 Michaelis–Menten Paper. Biochemistry, 50(39), 8264–8269. Available at: https://doi.org/10.1021/bi201284

[16] Berg J., Tymoczko J. a Stryer L. (2002) Biochemistry. W. H. Freeman and Company. ISBN: 0-7167-4955-6.

[17] Ouertani A, Neifar M, Ouertani R, et al. Effectiveness of enzyme inhibitors in biomedicine and pharmacotherapy. Adv Tissue Eng Regen Med Open Access. 2019;5(3):85-90. Available at: https://medcraveonline.com/ATROA/effectiveness-of-enzyme-inhibitors-in- biomedicine-and-pharmacotherapy.html

[18] Diesenroth, Faisal a Ong. Mathematics for machine learning. 1. ed. Cambridge, 2020, s. 371. ISBN: 978-1-108-45514-5.

[19] Aurélian Géron-O'Reilly. Hands-On Machine Learning with Scikit-Learn, Keras & TensorFlow. 2. ed. Canada, 2019, s. 819. ISBN: 9781492032649.

[20] Gilbert Strang. Introduction to linear algebra fifth edition. 5. ed. US, 2016, s. 573. ISBN: 978-0-9802327-7-6.

[21] Nie, F., Hu, Z., & Li, X. (2018). An investigation for loss functions widely used in machine learning. Commun. Inf. Syst., 18, 37-52. Available at: file:///C:/Users/-/Downloads/CIS18Aninvestigationforlossfunctionswidelyusedinmachinelearning.pdf

[22] James Stewart. Calculus: Early transcendentals. 7. ed. Brooks, 2008, s. 1170. ISBN: 978-0-538-49790-9.

[23] Jordan, M I. Serial order: a parallel distributed processing approach. Technical report, June 1985-March 1986. US: N. p., 1986. Web. Available at: https://cseweb.ucsd.edu/~gary/258/jordan-tr.pdf

[24] Sepp Hochreiter, Jurgen Schmidhuber (1997). Long short-term memory. Neural Computation. 9 (8): 1735-1780. S2CID 1915014. PMID 9377276. Available at: https://www.bioinf.jku.at/publications/older/2604.pdf

[25] Cho, Kyunghyun; van Marrinboer, Bart; Gulcehre, Caglar; Bahdanau, Dzmitry; Bougares, Fethi; Schwenk, Holder; Bengio, Yoshua (2014). Learning Phrase Representations using RNN Encoder-Decoder for Statistical Machine Translation. Available at: https://arxiv.org/pdf/1406.1078.pdf

[26] Y. LeCun, B. Boser, J. S. Denker, D. Henderson, R. E. Howard, W. Hubbard and L.D. Jackel. Backpropagation applied to handwritten zip code recognition. Neural Computation, 1(4):541-551, 1989. Available at: http://yann.lecun.com/exdb/publis/pdf/lecun-89e.pdf

[27] Sun, Z., Ozay, M., & Okatani, T. (2015). Design of Kernels in Convolutional Neural Networks for Image Classification. Available at: http://yann.lecun.com/exdb/publis/pdf/lecun- 89e.pdf

[28] Mouton, Coenraad; Myburgh, Johannes C.; Davel, Marelie J. (2020). Gerber, Aurona (ed.). Stride and Translation Invariance in CNNs. Artificial Intelligence Research. Communications in Computer and Information Science. Cham: Springer International Publishing. 1342: 267-281. Available at: https://arxiv.org/pdf/2103.10097.pdf

[29] Gholamalinejad, H., & Khosravi, H. (2020). Pooling Methods in Deep Neural Networks, a Review. Available at: http://yann.lecun.com/exdb/publis/pdf/lecun-89e.pdf

[30] Boué, L. (2018). Deep learning for pedestrians: backpropagation in CNNs. Available at: https://arxiv.org/ftp/arxiv/papers/1811/1811.11987.pdf

[31] Francois, V., Henderson, P., Islam, R., Bellemare, M., & Pineau, J. (2018). An Introduction to Deep Reinforcement Learning. Foundations and Trends® in Machine Learning, 11, 219–354. doi:10.1561/2200000071. Available at: https://arxiv.org/pdf/1811.12560.pdf

[32] Richard S. Sutton a Andrew G. Barto. Reinforcement Learning: An Introduction. 2. ed. Cambridge, 2015, s. 352. Available at: https://web.stanford.edu/class/psych209/Readings/SuttonBartoIPRLBook2ndEd.pdf

[33] Burnetas, A., & Katehakis, M. (1997). Optimal Adaptive Policies for Markov Decision Processes. Mathematics of Operations Research - MOR, 22, 222–255. Available at: file:///C:/Users/-/Downloads/MDPS_mor97.pdf

AGE OF THE UNIVERSE , CALCULATION AND CONFIRMATION OF COSMIC DATA

Ghazal Attari, Farzanegan 4 High School,Karaj /Iran, Ghazalattari1386@gmail.Com

ARTICLE INFO

Bronze medalist in International Greenwich Olympiad

IGO 2022, London, UK,

Advisors: Ms. Kabiri, Ms. Johari

Accepted by Ariaian Young Innovative Minds Institute ,

AYIMI, http://www.ayimi.org ,info@ayimi.org

ABSTRACT

Astronomy is a kind of knowledge which is so wonderful for anybody even for non-expertise individuals. Especially if anyone is interested in astronomy, can have a role in this science development. To know the age of Earth we have used spectroscopy method in 12 galaxies as a sample and by using VIREO Virtual Observatory, first we tried to calculate their velocities away from ourselves and then measured the Hubble constant by estimating the distance of these galaxies of course in this way the spectral parallax method was used. Finally, by reversing it and performing a series of single transformations, we get the age of the universe.

Keywords : *Hubble law, VIREO Virtual Observatory, Spectrum, Galaxy, Age of the Universe*

1. Introduction

New cosmology began with Hubble observations the Hubble value, $h_0 \sim 5.3$, obtained by first observations while many current observations indicated, $0.5 \leq h_0 \leq 1$, but the question is here that how these obvious changing occurred during 6 months? So, we can realize that there are still some errors about real amount of these new and important cosmological parameters. Therefore, with using a combination of x ray's signals effect and Sunyaev-Zel'dovich (SZ) we use a large, galaxy cluster dynamically calms by Chandara, Planck and Blockham Observatory.This is the first analysis data related to axis before the overall accuracy of x-ray temperature measurements are marginalized.

While our limitations to the quietest and most systematic clusters minimize physical astrology and for a fixed cosmological model with:

$$H_0 = 67.3 + \ldots \Omega\Lambda = 0.7, \Omega m = 0.3$$

we have to find 21.3-13.3 Km / s Megaparsec which is limited by Temperature calibration uncertainty. We discuss the prospects for reducing the prevailing systematic constraint on this analysis and by x-ray calibration or accurate measurement of the relative (SZ) effect it provides an acceptable path for H_0 level constraints (GT, Van et al., January 2012).

In this task we suggest a kind of independent method and non-local cosmological model to limit Fixed Hubble which has been inspired by H0-independent, quasi-cosmopolitan features of the Hubble Modified HIIGx HII galaxy, defined by Jenny T. Wan al et (2016) and they could analysis it with Hubble diagram from the type of SN Ia (Ia) supernova to obtain an inference from the Fixed Hubble. It is shown as:

$H_0 = 71 \pm 20$ Km / s Megaparsec and this method used by other Hubble diagram in upper red shift but it expands unreal H0 results. (Jian-Chen Zhang et al. January 2021) also we can provide a measurement H0 fixed Hubble from the oscillation distance of the SBF surface brightness for 63 bright galaxies, mostly of the primary type up to 100 megapixels observed with the sub-channel in the Hubble Space Telescope .HST distances reach the Hubble Current, and most galaxies are in the 80-50 MPa range but the average statistical uncertainty in individual measurements is 4% for this reason we have made IR SBF Hubble diagrams by these distances and H0 will be limited by these 3 different galaxy velocity treatments.

We limit H_0 using three different galaxy velocity treatments. From the average weight of white calibration (TRGB)we can obtain $H_0 = 73.3 \pm 0.7.2.4$ Km/s Megaparsec, because it reflects some error bars related to statistical uncertain and systematic.

This kind of result is in good agreement with recent H0 measurements of type Ia supernovae with time delays in lens quasars multiplied and reservoirs are compatible (John P. Blakeslee et al January 2021) we attempt to use some VIREO data and important H0 Parameters to calculate the age of the universe.

2. The Importance and Necessity of this Research

In order to provide a compatible model with description of the universe first we should know the age of this universe then we can find some parameters related to age of universe of course some parameters in this field are as follows:

- Rate with the melody of the universe
- The abundance of cosmic elements and the nucleation cycle

The compatibility of cosmological models with the age of the universe is measured, while the age of the universe should be compatible with the age of the components within the universe and not less than that for example, we have a set of observations related to some physical astronomical performances that are older than the age of the universe based on cosmological methods, and for this reason we say this is an inconsistency. In this regard, some cosmological models attempt to remove this inconsistency but in overall we believe that if we have no idea about the real and exact age of this universe, thus we cannot make a consistent model to describe the universe.

In fact, based on Friedmann's equations, the age of the universe is related to the rate of expansion and the densities of matter and energy, it can also limit the frequency and constituent content of the universe. So, the main propose of this research:

- to measure Fixed Hubble based on virtual observatory data
- to calculate the age of universe

and also, Questions with research hypotheses are:

1) Is the amount of Fixed Hubble exact?

2) Is the age of the universe compatible with the age of its components?

3) Are the models presented in the description or geometry of the universe compatible with the age of the universe?

3. Background Knowledge

First, the measurement of the velocity of a galaxy used by Wesno Slyfer in 1912/1291, and next decades was followed more fundamentally by Adville Hubble. In 1929/1308, the first one who measured the distance between galaxies was Adobe Hubble when he plotted these distances at the speed of each galaxy, he could achieve something unusual. When we go farther away from the Milky Way galaxy, the faster it gets away. But there is a question that is there anything special about our place in the universe that makes us a center of cosmic repulsion?

Of course, it was a significant discovery and it was believed that this expansion today is the result of a huge explosion that occurred between 10 and 20 billion years ago.

In a project by (John P. Blakeslee al et. January 2021) SBE method was introduced. This method measures the spatial difference with small-scale oscillations in the polarity of the pixel intensity of the image for the discrete nature of stars consisting of a galaxy then finally, they can collect a large sample of high-quality distances that have a coma cluster in a relatively moderate amount of time.

4. Research Method

Given this current article to obtain the age of the universe using virtual observatory data it is able to discover the facts and realities of the world of creation, therefore, for the nature of the subject, the method of this research is descriptive and fundamental type.

4.1. Population

The statistical population of this study is the spectrum of the hydrogen line and the calcium line in the 12 known astronomical galaxies (the names of the galaxies are numbered in the astronomical culture) which placed in well-known 12 galaxies (in this case the hydrogen and calcium lines have been studied statistically) (Fig. 1).

4.2. Measurement Tools for VIREO Data Analysis

The virtual observatory provides access to a variety of data analysis tools that can be used to view and analyze data collected by telescopes and various instruments.

These include spreadsheets and image processing programs that can be specified in user settings and called from the VIREO program. VIREO also contains several programs for analyzing and displaying its specific data. Using the TOOLS option in the menu bar, they are easily accessible through the virtual observatory control panel.

VIREO tools option includes: Spectral classification tool, displays stored spectra and makes them available for comparison to standard spectral atlases.

Spectrum Measuring Tool: Includes stored spectra that allow users to measure wavelength and intensity.

Radio Pulsar Analysis: indicates the recording of signals from a maximum of three VIREO radio receivers and allows users to measure the input time and power of the input pulses.

HR Diagram Analysis: Displays metering data for star clusters and enables the user to measure the distance between redness and cluster age.

Fig. 1: The statistical population

4.2.1. Measurement the Spectrum of Galaxies with VIREO

After installing the program, we follow the following steps in order to select a desired galaxy (Fig. 2):

Login - File - entering your favorite name

Run Exercise – The Hubble Redshift- Distance Relation

Fig. 2: Steps to select a desired galaxy

Due to our study which is about the estimating the age of the universe, we choose the transition to Hubble red, next we choose our telescope. From the three available options, we have to select a telescope with an aperture of 1 meter and then press the open key to open the aperture of the telescope.

We can see the sky from a telescope, Now, we have to select the object with the galaxy we want so that the telescope orifice is in front of it.

A) with turning on the tracking button always causes the telescope to move with the desired mass so that it does not come out of the telescope aperture.

B) Then by selecting the slew option and the Observation Hot List, which is one of the 13 available galaxies we have to be patient till the telescope starts its rotation and focused on the object.

(Note: of course, in this current study, all work steps have been done for 12 galaxies)

A) selecting Telescope option from View part

B) selecting ACCESS option

Now a window based on the figure opens in front of us. When we press the Go button, the light of the desired galaxy enters the telescope for the desired time and draws its spectral diagram.

(Note: In this research, the diagrams are drawn in a time interval of 3 minutes)

Save the drawn page and select the spectrum measuring option from the main window menu and re-read the saved chart file that we drew.

eventually We read the wavelength λ line of the element calcium and hydrogen from the graph and put it in the corresponding table and perform the calculations.

5. Descriptive Data Analysis

In this case we say the wavelength obtained is for

Hydrogen line (based on diagrams) and we have to reduce the amount in the laboratory in this way the difference of Wavelength of the element hydrogen obtained and same factor is used for calcium to indicate the difference of wavelength for the element of calcium then based on the following Equitation some amount obtained by this method shown in the related tables.

1) obtaining this amount and the difference of wavelength is following:

$\Delta\lambda_H = \lambda\ obtained - \lambda\ laboratory$ for hydrogen line
$\Delta\lambda_K = \lambda\ obtained - \lambda\ laboratory$ for calcium line

- The laboratory wavelength of the K calcium line is equal A3933.7
- The laboratory wavelength of the H calcium line is equal A3968.5

2) Obtaining speed of galaxy

$V_H = C \times \frac{\Delta\lambda_H}{\lambda_H}$ the speed of galaxy based on hydrogen line data
$V_K = C \times \frac{\Delta\lambda_K}{\lambda_K}$ the speed of galaxy based on calcium line data

3) obtaining average speed: For each galaxy, add the velocities from the calcium line and the hydrogen line and divide by 2 to obtain the average speed of galaxy then we show it as V avr.

4) obtaining the amount of Fixed Hubble: We put the average velocity number obtained from the previous step in Hubble's law. by this method we can get the Fixed Hubble as following below:

H=V/D

NOTE: in this relation the amount of D which should be galaxy distance we don't have it but in this particular case we have to use of Spectral parallax equation which means:

$$m - M = 5logd - 5$$
$$logD = \frac{m-M+5}{5}$$

Symbol M: is the absolute magnitude of the galaxy, which in this study is considered to be 22.

Symbol m: is the apparent magnitude of the galaxy, the value of which is specified in the plots (Table 1).

Table 1: Fixed Hubble value for 12 Galaxies

H	D(pc)	logD	m	V_{avr}	V_b	V_R	Name of the galaxy	
45.10	331.33	8.52	15.60	14937.1	14792.94	15081.26	36747	1
49.27	363.07	8.48	15.80	14621.41	14690.74	14552.09	36773	2
49.25	301.99	7.98	15.40	14875.76	15199.43	14552.09	36805	3
73.60	95.49	7.9	12.90	7028.78	7140.60	6916.97	NGC4874	4
82.58	79.43	8.98	12.50	6559.95	6505.32	6614.58	NGC4889	5
40.81	954.99	8.6	17.90	38981.26	38917.55	39044.97	51976	6
52.42	398.10	8.78	16.90	20872.19	20766.70	20977.69	54876	7
39.30	602.55	8.66	16.30	23681.59	23588.47	2203.03	54875	9
48.35	457.08	8.22	14.10	22100.32	22164.62	11628.82	54891	10
58.32	165.95	8.34	14.70	12760.64	11767.54	12813.40	NGC7499	11
69.56	218.77	2.28	14.40	13254.57	12707.88	13216.32	NGC7503	12

$\Delta\lambda_K$	$\Delta\lambda_H$	λ_K	λ_H	Name of the galaxy	
193.97	199.5	4127.67	4168.00	36747	**1**
192.63	192.5	4126.33	4161.00	36773	**2**
199.3	192.5	4133.00	4161.00	36805	**3**
93.63	91.5	4027.33	4060.00	NGC4874	**4**
85.3	87.5	4019.00	4056.00	NGC4889	**5**
510.3	516.5	4444.00	4485.00	51976	**6**
272.3	277.5	4206.00	4246.00	54876	**7**
309.3	314.5	4243.00	4283.00	54875	**8**
290.63	291.5	4224.33	4260.00	5491	**9**
154.3	153.83	4088.00	4122.33	NGC7499	**10**
166.63	169.5	4100.33	4138.00	NGC7501	**11**
174.3	174.83	4108.00	4143.33	NGC7503	**12**

6. Discussion and Conclusions

From the values obtained for the fixed Hubble in Table (1), we take the average to consider a certain value for the Hubble constant. The average = H obtained for 12 galaxies based on the description of the measurement and the expansion of the universe / return to the big bang, if we invert the number obtained for the Hubble constant, the age of the agent is obtained, i.e.:

$$H = 55.8375\ ,\ 1\ km = 3.2407792 \times 10^{-20} S$$
$$\rightarrow H = 180.95700858 \times 10^{-20} \frac{1}{s}$$
$$\frac{1}{H} = age\ of\ universe\ {}^{SMpc}/_{Km}$$

age of universe = $0.0055261745 \times 10^{-20} s$

From the dividing this number by the light year in kilometers gives the value of 13.08, which is equal to the age of the universe. Therefore, the age of our universe is 13.08 billion years .

Acknowledgment

I would like to express our gratitude and thanks to all the loved ones who sincerely and without any expectations helped me in this project particularly from Ms. Dr. Kabiri and Dr. Rokni, the supervisor, Ms. Johari, in charge of research, in Farzangan 4 high school.

Reference

[1] Narlikar, Gianni Vishnu, 2009 Introduction to Cosmology,

[2] Ingleb, Mike, 2013 Astrophysics for Observers

[3] Redpi, Jan, 2012 Star and Space Atlas,

[4] Kolb, Peter 1394 Cosmology

[5] Gregory, Zilik 1396 Basic Astronomy and Astrophysics Volumes 1 and 2

[6] Croatia, Lavarteb 1396 Jahani e Nish

[7] Mansouri, Reza, 2007 Textbook on Cosmology

[8] VIDEO Virtual Observatory Guide.

[9] Authentic Internet shadows, including the Big Bang

EXPERIMENTS TO FIND CHARACTERISTIC OF THE SOUND IN A DRUM

Seyed Zahra Hosseini , Alghadir high school, Kish Island, Iran, thetomycat@gmail.com

ARTICLE INFO

Participated in PYPT, IYPT 2022

Silver Medalist in IMSEF 2022, Izmir, Turkey

Advisor: Alireza Noroozshad

Accepted in country selection by Ariaian Young

Innovative Minds Institute,AYIMI,http://www.ayimi.org ,info@ayimi.org

ABSTRACT

The problem states that, when dropping a metal ball on a rubber membrane stretched over a plastic cup, a sound can be heard. As the experiment represents, the metal ball on a specific membrane with a specific elasticity, starts going up and down which after a while will stop. Following the membrane deformation and an overview of theories, a model is designed with ANSYS to obtain graphs as tension and strain over time. Number of collisions for each ball, frequency of the sound, the difference between the stretched mode and the normal version of membrane are investigated by Tracker, MATLAB and Besel equation.

Keywords : *Sound, Bouncing membrane, Characteristics*

1. Introduction

The problem states that, when dropping a metal ball on a rubber membrane stretched over a plastic cup, a sound can be heard therefore to find the origin of this sound and explore how its characteristics depend on relevant parameters some experiments are done. As the experiment represents, dropping a metal ball on a membrane with a specific elasticity, causes it starts going up and down on membrane and the speed of the movement will slowly starts to decrease and after a while, the ball will stop on the membrane (Fig. 1 & 2). The frequency of the sound is tracked to find different relevant parameters.

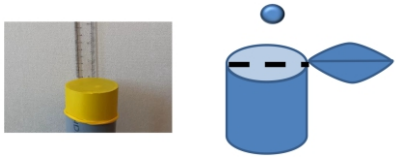

Fig.1: The ball movement on the membrane

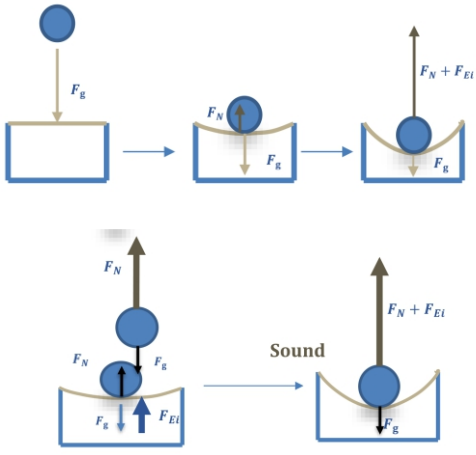

Fig. 2: Free- body diagram of bouncing of the ball on membrane and producing the sound

2. Materials and Methods

Following the membrane deformation and an overview of theories, a model is designed with ANSYS to obtain two graphs known as tension and strain over time (Fig. 3).

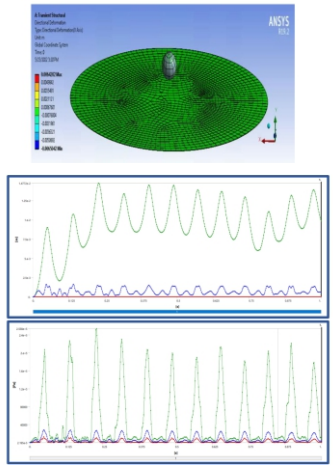

Fig 3. Tension and strain over time by ANSYS modeling

Applied forces to the system are studied to clarify the origin of the sound. Before the ball hits the membrane, there is a gravitational force and by releasing the ball, the potential energy starts to decrease. When the ball goes up again due to the elastic deformation and the accumulated energy in the membrane, a sound can be heard which its origin is the air pressure difference.

The wave characteristics in the membrane by hitting the ball are frequency, speed, amplitude, and wavelength. To obtain the frequency , function of Bessel equation is used (Eqs. 1-6).

$$\frac{\partial^2 T}{\partial t^2} = c^2 T k \tag{1}$$

$$T = A\cos(cst) + B\sin(cst) \tag{2}$$

$$f = \frac{1}{T}$$

$$f = \frac{cs}{2\pi} \tag{3}$$

$$\rho^2 \frac{\partial^2 R}{\partial \rho^2} + \rho \frac{\partial R}{\partial \rho} + (\rho^2 - n^2)R = 0 \tag{4}$$

$$r^2 \frac{\partial R}{\partial r^2} + r \frac{\partial R}{\partial r} + (s^2 r^2 - n^2)R = 0 \tag{5}$$

$$R = EJ_n(\rho) \tag{6}$$

Now to obtain the coefficient S and then frequency, there is a boundary conditions if the ball hits or bounces on the edge of the cup (Eqs. 7-11)

$$u(a,\theta,t) = 0 \tag{7}$$
$$r = a$$
$$u = RT\theta \rightarrow R(a) = 0 \tag{8}$$
$$R = EJ_n(sr) \rightarrow J_n(as) = 0 \rightarrow as = \alpha_{nm} \rightarrow S = \frac{\alpha_{nm}}{a} \tag{9}$$

$$u = \sum_{n,m} E_{n,m} J_n\left(\frac{\alpha_{n,m}}{a} r\right)\left(A\cos\left(\frac{C\alpha_{n,m}}{a} t\right) + B\sin\left(\frac{C\alpha_{n,m}}{a} t\right)\right)(C_n\cos(n\theta) + C_n\sin(n\theta)) \tag{10}$$

$$f = \frac{c\alpha_{n,m}}{2\pi a} \tag{11}$$

The difference between the normal membrane and the stretched one over the cup is related to the elasticity (ε) as an important characteristic (Eq. 12).

$$\varepsilon = \frac{l_1 - l_0}{l_0} \tag{12}$$

l_0= normal membrane

l_1 =stretched membrane

3. Experiments

The setup consists of three different balls to measure the frequency for different mass and a covered cup with a stretched membrane (Fig. 4). Spectroid,is used to have a visualized site of the movements for the ball therefore when a metal ball starts bouncing on the specific membrane over the cup the frequency and intensity of the sound which is heard changes and the red diagram shows the maximum holder and the natural frequency for the specific elasticity of the membrane.

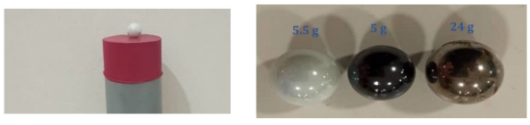

Fig 4. Different balls in our experimental setup

MATLAB is used for the spectrums in each ball at different heights and different elasticities and Tracker to count the number of collisions for each ball and the thump hearing sound that is possible to be recognized by the given diagram for x versus time (Fig.5).

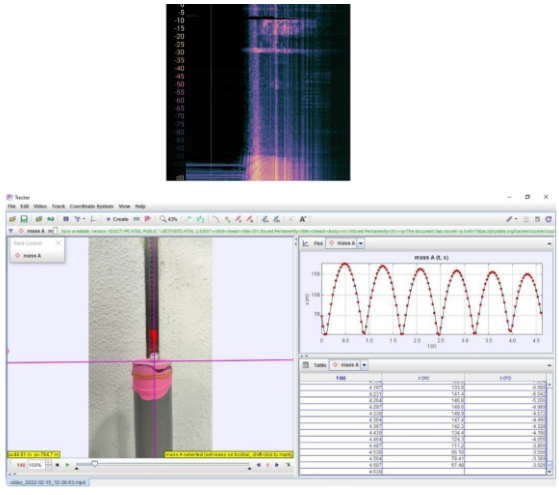

Fig. 5: Frequency vs change of elasticity (ε)

Membrane with different tensions (ε=0.71-3) are used in our experiment to analyze the data related to the number of collisions, frequency and amplitude.

There are three different sounds, which originate from the movements of the ball on the membrane, the cup itself and lastly the surroundings. However, as the theory, the main sound we hear is the sound from the movements of the ball (the max point in spectroid diagram) (Fig. 6).

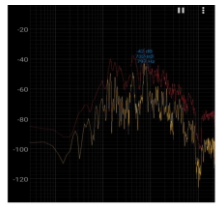

Fig. 6: Spectroid diagram

4. Results

Three different diagrams are analyzed, amplitude verses time, amplitude verses frequency and frequency versus time for three different balls but in constant membrane and height of releasing. It is observed that the most fluctuations are in the period of 500 Hz to1000 Hz (Fig.7).

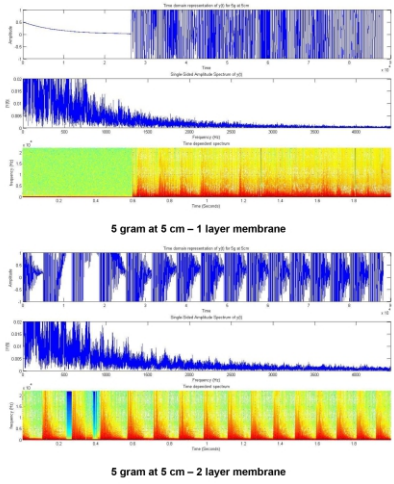

Fig. 7: Amplitude verses time, amplitude verses frequency and frequency versus time for three different balls

The average range of frequency in each different tensions, that starts with 0.7 and ends up to 3 shows the least frequency would be the one for ε=0.71 and as much as the epsilon is increasing it is possible to observe an increasing trend of frequency (Fig. 8).

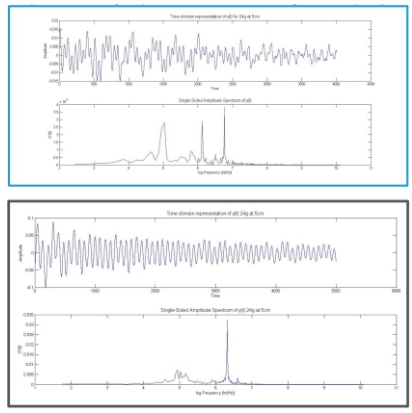

Fig. 8: The average range of frequency in each different tensions

By increasing the distance between ball and membrane, number of collisions will increase (Fig. 9).

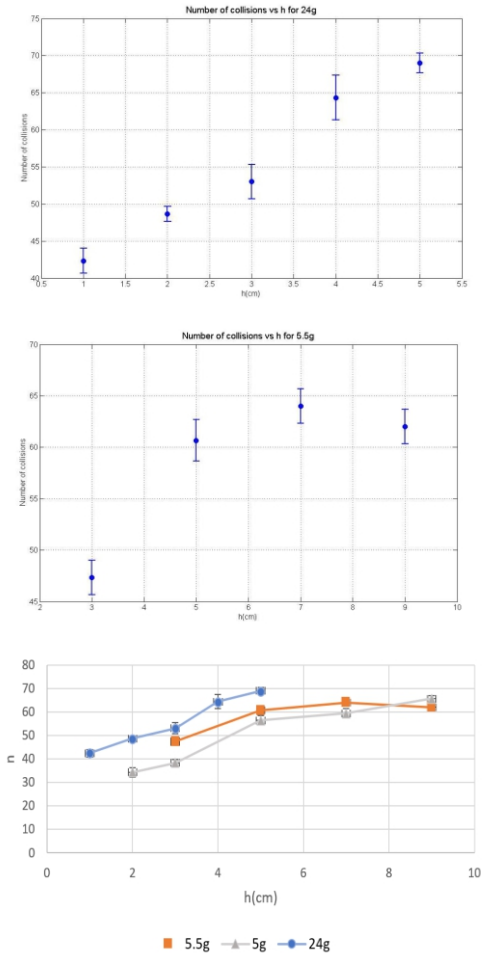

Fig. 9: Number of collisions in different heights and comparing with different masses of balls

5. Discussions

We assumed that by changing the weight and distance between membrane and ball the frequency shouldn't change, and the plots of frequency versus distance and weight, in different weights (5 g to 24 g) proves that the frequency in each distance is almost constant and is a straight line which is a good agreement with the theory (Fig.10).

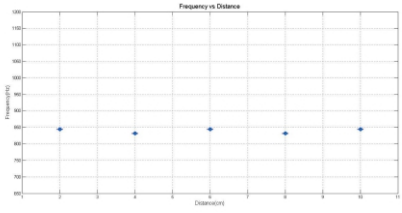

Fig. 10: Frequency versus distance

It is the same for the amplitude of the sound but in different tensions the frequency will change too but the amplitude will be constant. It is observed the change of the amplitude is very small because of the errors in the experiment and surrounding voice.

It can be reported that experimental result and the theory of frequency of the sound have a good agreement with each other (Table 1). We observed a schematic and a real version of the setup and how the system works, and for the experiment we tried different layers of membrane, with latex balloon and a Nitrile rubber material, aluminized plastic and rubber for the toy balloon and different balls (5-5.5-24 g).

Table 1: The average frequency based on the graph for changes of the ε

	ε						
Frequency	0.71	1	1.35	1.46	1.6	2	3
	610	680	770	850	820	880	1080

References

[1] https://www.compadre.org/osp/EJSS/4495/280.htm

[2] ttps://courses.physics.illinois.edu/phys406/sp2017h/Student_Projects/Spring09/Knud_Sorensen/K_SorensenPhys498POM_Spring09_Final_Report.pdf

[3] https://courses.physics.illinois.edu/phys406/sp2017Lecture_Notes/P406POM_Lecture_Notes/P406POM_Lect4_Part2.pdf

[4] https://journals.aps.org/pre/abstract/10.1103/PhysRevE.82.016203

INVESTIGATION OF PHYSICAL AND CHEMICAL PROPERTIES OF CAOUTCHOUC

Atena Outokesh, Farzanegan1 School, atenaoutokesh@yahoo.com

ARTICLE INFO

Participated in PYNT 2020

Advisors: Rozhin salmani , Hedieh pourghasem,

Accepted in country selection by Ariaian Young Innovative Minds Institute , AYIMI

http://www.ayimi.org ,info@ayimi.org

ABSTRACT

Rubber has existed since ancient times, and some plant fossils date back three million years. It is interesting to know that over 400 types of latex plants produce a different percentage of rubber. Trees like Hua, Sapphire and Balata, in particular Brazilian air tree (Hevea brasiliensis) has the largest share in the production of rubber base materials in the world . Among its producing lands is the United States. Rubber is a white syrup that comes from rubber trees, also called latex or elastomer. This material has many applications in industry and in this article we intend to examine its.properties carefully.Physical and chemical natural rubber.

Key Words : *Caoutchouc, Lastomer, Physical Properties , Chemical Properties*

1. Introduction

Have you ever thought which properties in Caoutchouc have effect on its usage?

By studying and examining the physical and chemical properties of Caoutchouc, we found rubber is one of the most essential materials in it. Due to its excellent elasticity, rubber is used in the manufacture of a different products including hospital supplies, home appliances and toys.

2. Research Methodology

The physical properties of Caoutchouc in six samples and the chemical properties of Caoutchouc in three samples have been studied, and we discuss the importance of each according to their application in industry.

2.1. Physical Properties

2.1.1. Electrical conductivity

This critical percentage of the additive in which the polymer (elastomer in this study) changes is called permeability or penetration. The higher the permeability, the lower the electrical resistance and the higher the electrical conductivity in the material. The penetration rate for soot in different experiments is 16%. As a result, due to the low permeability of the soot, the rubber has little electrical conductivity.

2.1.2. Strength

Strength is the amount of the force a material can withstand.

Strengths			
Tensile strength	Yield strength	Flexural strength	Compressive strength

Tensile strength: The maximum stress that an object can withstand when stretch from the sides. Tensile Strength or UTS (Ultimate tensile strength), Equals the maximum load divided by the initial cross-sectional area of the sample.

$$s_u = \frac{P_{max}}{A_o}$$

Tensile strength determination is simple and repeatable and useful for purposes such as characterization and product quality control. Caoutchouc molecules have a high tensile strength due to its stretch and being the chain. Gaps in the chains and disordered arrangement of the chains may be the reason for this particular behavior in the tires. The more vacancies there are, the more room for chain mobility. The more disordered the chains are, the greater the ability to repel and revert to their initial state after the force is applied.

Adding sulfur	Adding soot
Increased strength	Increased strength and elasticity

2.1.3. Hardness

It is defined as the ability of a material to withstand the permanent deformation or penetration to its surface. Material hardness is measured by Hardness meter (Fig. 1).

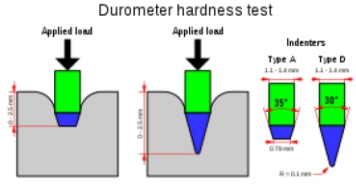

Fig. 1: Hardness meter

Hardness meter of Rubber (Durometer) are usually used to measure the hardness of rubber, elastic polymer materials. In the durometer, such as metal hardness meter, gauges and various units are used, the most commonly used are shore A and shore D. Shore A is used for softer plastic materials and shore D is used for harder specimens (Fig. 2).

Fig. 2: Hardness meter of shore A
Usage: Rubbers hardness measurement

This tool is for materials such as elastomers, rubber, leather, PVC, silicone, Teflon, neoprene and more.

2.1.4. Elasticity

Tensile properties have a reversible (elastic) deformation of the environment and materials, and are also called viscoelastic. The elasticity of the environment cause the rebound forces to be created by any part of the environment that has shifted from its equilibrium state. Adding carbon soot to the raw rubber increases its elasticity.

2.1.5. Damping

In physics this property reduces the amplitude of oscillations in oscillator systems, especially in the consonant oscillator. In general, the part that lowers something's energy is called a damper. (Reduces its oscillation).

Damping				
Radiation damping	Hysteresis damping	Friction damping	Viscose interior damping	External viscous damping

2.1.6. Viscose Interior Damping

This damping is due to the adhesion of the material and is proportional to the speed. As the building's natural frequency increases, the damping ratio increases. Internal viscosities can easily and routinely be involved in dynamic analysis . This damping is the most popular type of Damping.

Internal viscosity damping in rubber is high. That is, due to its oscillation due to the high viscosity between the particles the internal oscillation ends very quickly.

2.1.7. Failure Resistance

Rubber is highly resistant to wear and tear. In fact, it can be said that rubber performance is high and works well for a long time. This is due to soot, sulfur and other substances added to improve natural rubber.

3. Chemical properties

Caoutchouc is Polymers composed of the isoprene organic compound with partial impurities of other organic compounds and water. Like other polymers, it consists of long molecular chains. It is insoluble in water and soluble in alcohol and ether.

Chemical name: Polyisoprene Hydrocarbon Chemical formula: (C_5H_8)

Molecular weight: 2×10^5 - 4×10^5

It is an elastomer (an amorphous polymer which is also called rubber).

amorphous polymer	
Thermoplastic	Elastomer

Whether an amorphous polymer is thermoplastic or elastomer depends on the glass transition temperature or it's Tg. This is the temperature at which the polymer becomes soft, flexible and hardened under the glass. If an amorphous polymer has a Tg below room temperature, that polymer can be an elastomer because it is soft and rubber at room temperature. If the amorphous polymer has a Tg above room temperature, it will be a thermoplastic polymer because it is hard and glassy at room temperature. Thus, in general, it can be said that amorphous polymers below Tg are thermoplastic and above it are elastomer.

The Tg of Caoutchouc is very low at about -70 degrees Celsius. As a result, according to the text above, the rubber at room temperature is soft and elastically.

4. Elastomers' properties

1- flexibility 2-The property of wasting energy 3-Resistance to adverse conditions such as: abrasion, solvents, oils, ozone, acids and alkalis without penetration of water and air.

5. Thermal Behavior

From the scientific point of view, the most useful part of polymers is based on their thermal behavior. (Also called thermodynamic response).

Polymers and their thermal behavior	
Thermoset	thermoplastic

- thermoplastic: There are substances that are fully reacted or polymerized. These materials become soft when exposed to heat, and pressure causes them to flow and can form and, after cooling, stabilize their shape. Incomplete and scrap forms can also be re-melted and reshaped. Due to heat and pressure they become soft and flow to become hardened by the cold and take the form of mold, and this cycle can be repeated several times without reducing the polymer properties .

-thermoset: They are substances that do not fully react and do not fully polymerize and are complemented by effective factors such as reaction heat. Products made of these materials have a lattice structure and do not soften with warming, so they cannot be reprocessed and re-fabricated. These polymers react with warming. Cross links are made in them and converted to solid polymers. These polymers are usually available in powder, liquid or pre-polymer molds and are formed by heat and pressure .

According to the text above, the rubber has a very good thermal behavior, also called the "Goss Joule" effect, and is a thermoplastic (meaning it is liquid at high temperature and can shaped with pressure) . In this effect, unlike other materials due to rapid deformation, it has a temperature rise that is also called "anthropic elasticity" .

6. Swelling Against the Solvent

Rubber is swollen by some solvents such as benzene, gasoline, carbon tetrachloride and some vegetable and mineral oils. The intermolecular bonds of the raw rubber when exposed to these broken materials form a granular or gel-like solution. But if there are cross links in the material, they prevent the rubber from swelling. In fact, it can be said that the volcanization improves the resistance of the rubber to the solvent. It also reduces the elasticity of the rubber after a while (rubbers dry).

7. Discussion and Analysis

Due to the role and application of natural rubber in industry, it can be said that the most important physical property of rubber is its elasticity (enhanced by sulfur and soot). The good thermal behavior of the rubber has the highest efficiency in its chemical properties. In general, the physical properties of tires are more important than their chemical properties .

Due to the high strength, toughness and tensile strength of many materials with similar properties, depending on its application, it is often in a position to be highly resistant to these three factors.

Also considering other properties mentioned, tires are the

natural rubber in industry are eliminated during the manufacturing process. Natural rubber is also used in the manufacture of glasses and shoes because of its easy shaping properties .

8. Conclusion

The highest consumption (more than 60%) of this material is in the manufacture of tire types. As mentioned earlier, rubber has many applications in a variety of industries including aircraft manufacturing, hospital equipment, toys and home appliances due to its elastic properties.

References

[1] https://books.google.com/books papers+about+caoutchouc&source

[2] https://books.google.com/books soot+in+caoutchouc&hl

VISUAL AND GAME SUPPORTED GLOBAL WARMING AWARENESS PROJECT

Aysenur Bayer, Turkey, Aysenurbayer.2006@gmail.com

ARTICLE INFO

Gold medalist in BUCA IMSEF 2022

Awarded by Ariaian Young Innovative

Minds Institute , AYIMI

http://www.ayimi.org ,info@ayimi.org

ABSTRACT

Climate change causes chain problems affecting each other in the world day by day. The problems caused by global warming not only endanger the natural resources necessary for human life, but also affect social life, cultures, socio-economic structure, In this project; Before the game, which is in the prototype stage, was developed, a test was made to groups of all ages. As a result of the test, it was seen that most of the people had insufficient knowledge about global warming, and as a result, it was aimed that as many people as possible could reach the right information while having fun with minimum effort.

Key Words :*Climate change, Game, Global warming*

1. Introduction

The aim of this project is to increase the sensitivity of people by supporting the information taught audibly in school with visuals and animations and observing the effects of global warming on the individual. Thanks to this game, the person will be able to have fun while learning about the threat waiting for themself and the world, and they will be able to comprehend the negative effects of global warming more effectively by directly observing the events that can be done unconsciously and invisible to the eye every day.

1.1. Global Warming

Climate change is formed by the increase of gases that hold heat, and these gases create a greenhouse effect in the world. The greenhouse effect is a beneficial effect for the world, but if this effect reaches to dangerous levels, it may cause global warming to increase. Due to these gases, carbon emissions are increasing in the world; therefore, the sensibility of the greenhouse effect increases. According to BBC data, Turkey has started to rank 15th among the first 15 countries in 2020 (BBC, 2020).In their new report, the world's leading climate scientists announced that the struggle to keep global warming below 1.5 degrees Celsius has become "now or never" (NTV, 2022).

Global warming, which started to increase as a result of the Industrial Revolution that started in 1760, poses a great threat to the world. The main source of many problems such as acid rain, famine that has started to appear in various countries, and the melting of glaciers is global warming. This trend must be stopped for both the present and the next generation. In order to stop this trend, all people in the world should be made aware, not just a certain group. Because, as the name suggests, this problem is not a national one, but a global one.

1.2. Games and Learning

Today, the dominance of technological devices in our lives has led to a significant strengthening of our visual memory. Such dominance of technology has prepared the environment for people to turn to visually rich and interesting games (Meb Akademi Uzem, 2020). For this reason, if the education shown in schools is not supported by visuals and interacted with the learning audience, it will most likely not attract the attention of the target audience and will not make learning fun, nor will it ensure that learning is permanent. In other words, changing learning methods and interests as a result of the benefits of technology play a role in increasing the importance of the game in education.

The game arouses curiosity and pushes the player to take lessons. It presents what needs to be known in an interesting way in front of the player. Concepts in the game are taught through a series of stories that help players learn faster. The immediate feedback people receive during the game not only accelerates and perpetuates learning, but also helps them feel confident about their newly acquired skills.

Game-based education enables learning by encouraging logical thinking that stimulates intellectual growth and problem-solving abilities. It guides the lives of individuals in different ways according to their content and helps to relate the learning experience to real life. For this reason, games are much more effective when compared to traditional education methods. The game; It attracts the attention of the player with interesting activities, enables them to learn the skills they need to perform in a daily context, and motivates them by giving positive feedback (Meb Akademi Uzem, 2020).

1.3. Awareness

Awareness; The state of being able to look at themselves and what are related to them from the outside with a different eye is the logical awakening process.

Individual awareness; It enables the person to see the negativity approaching and take action, and causes an important development in the formation of social awareness in case of interaction with the person's close environment.

From the past to the present, the people have governed their own behavior. Therefore, nature, over which humanity has dominated since its existence, takes shape and reacts according to the attitudes of the people living in that region rather than the authorities who are constantly in search of solutions to environmental problems. Scientists can come up with various solutions to a problem that directly concerns the environment, but they can have an impact to a certain level. A solution that can provide

permanence for a problem that concerns the environment in which the society lives can be provided with social awareness activities that will cause a change in the behavior of the society itself.Today, there are ongoing awareness-raising activities for global warming, but since global warming has not yet had a direct impact on people's lives, they do not realize this big problem that awaits them and do not do the necessary work. Since the education provided in schools mostly covers the environmental effects, it cannot attract the attention of young individuals and cannot confront them with the danger of the situation.

The lack of awareness-raising activities manifests itself even in very simple problems that we witness in our daily lives. For example:

According to the 2016 data of the World Health Organization (WHO), diseases caused by environmental pollution cause 12.6 million deaths every year (AA,2017).

According to the data, the vast majority of people also fail to fulfill their responsibilities to the environment, which has been repeated to them since their childhood.

As mentioned before, this indifference of people to the situations taught to them aurally, the visual memory strengthened as a result of the dominance of technological devices in our lives, and the tendency of people to learn with visuals for the same reason.

Games supported by visuals and animations are more preferred by young people and if this situation is used in a positive way, this deficiency in education can be closed.

When used correctly, games are entertaining and instructive. Especially today, in these times when people are preparing their own end step by step, people need an instructive resource that will meet their orientation for "awareness", which is the most important factor in order to stop the terrible scenarios we are approaching. For these reasons, the game is of great importance today.

1.4. Awareness with Game

In the designed game, both the entertaining and instructive functions of the games were utilized. The game, which assigns the player to ensure the satisfaction of the public and to take care of the city, which consists of four areas, in this way, gives the player a fun time and instills a sense of responsibility; In addition, it is aimed that the gamer is informed about the problem by providing the operation of the game through questions.

1.5. Main Goal in The Game

The player's goal is to keep the satisfaction rate (percentage rate) and population as high as possible. The person who can answer the most questions correctly out of the two players and who can meet these two criteria the most, wins the game. The reason for choosing the population number as one of the main criteria is that the message to be given in the game is transferred to the player with numerical data. The reason why the satisfaction rate is determined as the main criterion is that the player can understand the changes created by global warming better by adopting their city.

Apart from these two criteria that will determine the winner in the game, 4 instructive criteria have been determined in order to observe that global warming has a direct effect on the life of the individual with a chain plot. These criteria are not taken into account when determining the winner, but they are necessary so that the basic criteria can be observed concretely.

1.6. Visuality in Game

One of the main differences in teaching with games is to attract attention with visuals. For this reason, it is aimed to effectively convey the problems that may be caused by globalwarming with striking visuals in the game, and to raise awareness by arousing the empathy of the player by processing the effects of all problems through an avatar.

To appear in the game; Avatar images were created, standing at the head of the dried- up lake in swimming clothes, standing across the barren field, looking into the space in front of it, and watching the food warehouse that was emptied as a result of animal deaths. With these visuals, it is aimed that the player can observe a possible life and bring the player face to face with his future.

1.7. Life at The Game

The four areas chosen to be in the game are among the most basic elements that make up a city. In addition, these areas were thought to be the areas that would best tell the player that global warming directly affects human life. These four areas are designated as schools and hospitals (required public areas), farms and fields (food supply sources), tourist attractions (lakes, seas, oceans, forests), and accommodation.

Hospitals:

Even if global warming is unobservable, it directly affects human health. It is an obvious fact that a disruption caused by global warming – which can happen in food supplies, water resources, farms or fields – causes serious health problems. For example, evidence that fires resulting from global warming affect human life with a chain effect are given below:

The world has entered a vicious circle. As global warming increases, forest fires increase. Global warming increases as forest fires increase (Milliyet, 2021). As a result of the combustion of natural biomass after forest fires, thousands of separate pollutants and components such as carbon dioxide, water vapor, carbon monoxide, hydrocarbons and other organic chemicals, nitrogen oxides and trace minerals are released (Euronews, 2021). According to the research published in the European Heart Journal, this number is more than the number of people who die from tobacco consumption in the world. Scientists said that about 800,000 people in Europe end their lives an average of more than 2 years earlier each year due to polluted air (BBC,2019).

Many people are hospitalized as a result of these negativities that are not directly diagnosed as "global warming". However, especially in recent days, due to the health problems it causes, "global warming" has started to be diagnosed as a diagnosis.

A Canadian doctor diagnosed "climate change" for the first time in history to an elderly patient who had difficulty breathing due to the extreme heat in the country, and announced that the patient was suffering from clşşşşimate change (Euronews, 2021).

Schools:

Schools; they are one of the basic places in a city for the construction of the future in society and therefore for the development of efforts to stop global warming. If the education in schools can provide the right learning, science and awareness will dominate the society.

Farm and Field Areas:

In a city, people's food is largely derived from livestock and farmland. If the functioning of these two is not carried

out correctly, the problems that will arise in food supply or product efficiency will negatively affect human life.Global warming, the rapid drying of wetlands, and the resulting decrease in agricultural production pose a serious threat to the nutrition of the world's population. It is estimated that the world population, which was approximately 7 billion 500 million in 2016, will exceed 9 billion in 2050. The Food and Agriculture Organization (FAO), affiliated to the United Nations, warns that if the global warming level exceeds 2 degrees, the number of 800 million people suffering from hunger and 1 million 200 thousand people living in poverty will increase (Retail Turkey, 2017).

Problems such as excessive rains caused by global warming, unexpected weather events and infertility of the soil will cause disruption in these areas and directly affect human health.

The global climate crisis deeply affects the ecological balance… The deterioration of the ecological balance brings with it significant yield losses in agricultural productivity... We see the greatest impact of global climate change with the increase in temperature. The increase in temperature greatly affects plant growth. The reason for the increase in temperature is expressed as carbon emissions (TRT, 2021).

Tourist Attractions:

Many factors such as drought, fires, disasters and high temperatures caused by global warming are destroying many places that attract attention by the society and foreigners. These areas also include areas that are necessary for life, such as public parks, freshwater lakes and forests.

The decrease in water resources due to climate change will have a negative impact on agricultural production. The total amount of water in the world is 1.4 billion km3, of which 97.5% is salt water and the remaining 2.5% is fresh water. With the increase in population in the world, the amount of usable water per capita is gradually decreasing. With the pollution of clean and drinkable water resources, water scarcity is increasing day by day (Apelasyon,2016).

Accommodation Area:

The direct effect of global warming on human life with this chain of events can be observed in accommodation areas. The progress of climate change in today's way will cause a visible negative change in accommodation areas. Animals are affected by high temperatures, the fields become unproductive due to weather events, dry water sources dry out as a result of drought and air pollution as a result of fires.

2. Method

2.1. Research Method

This research is a research in the causal comparison method, which is the subtitle of quantitative research, in terms of aiming to reveal the existing situation.

Causal comparison is a research method that tries to determine the causes of an emerging or previous situation, the variables that affect these causes, or the consequences of an effect (Metin, 2014).

2.2. Universe & Sample

All provinces of Turkey were included in the research universe in the pre-test phase. In the final test phase after the game was played, the research universe was chosen as the province of İzmir. The sample that can represent both universes was selected by easy sampling method.

The purpose of easy sampling includes everyone who wants interested (Kılıç&Ural, 2011).

2.3. Data Collecting Process

The scale is a list of questions prepared according to a certain plan in order to understand the feelings, thoughts and experiences of certain people or groups on a subject. The questionnaire, on the other hand, does not give a symbolic numerical data, but rather gives results that can be interpreted differently from person to person.

In this project, after various researches, the scale in the thesis prepared by Gökdere, M., Sontay, G., Usta, E. (2015) was used. 22 questions about global warming and 17 questions about global warming, which are perception determination questions, were included in the scale, and a total of 39 questions. The data collection process was carried out in an online way. The data were carried out in two stages, which are the pre-test and post-test stages.

2.4. Game Design

Programs such as Adobe Photoshop CC 2020, Adobe XD CC 2022, Adobe Illustrator CC 2021, Figma were used in the production of the game's interface, menu, character and map visuals. The use of minimalist, eye-catching and compatible themes/colors is one of the most important goals of the game's visual design process. The primary colors used (#8580f6, #84c990, #ffffff) have been prioritized to provide an experience that is both modern and simple and evokes nature. Another important point is that the fonts used in the same way can be compatible with each other in the game, thus creating a theme. The main fonts used in the theme are as follows: Inter Font Family, Gotham Rounded Bold, SF Pro Display.

The images used in the game were first designed in a vector environment in Illustrator, so that the visual quality could support all platforms, regardless of their size. In order for the player not to be bored, eye-catching, simple but remarkable character designs were preferred. In addition to aesthetics, the game provides instant access to the solution of the questions in terms of providing an effective learning process.

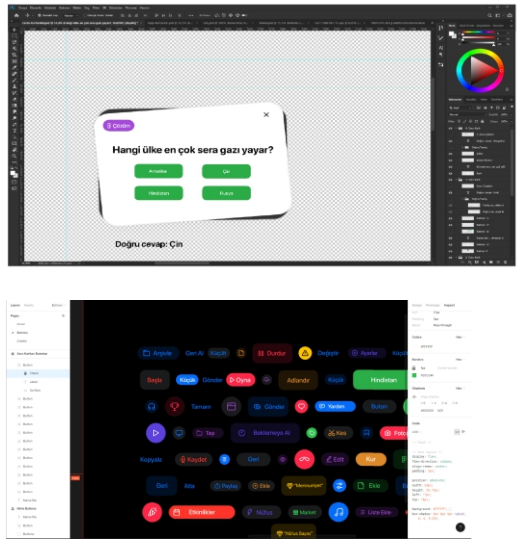

Fig. 1: Images From The Game Design Process

2.5. The Stage of Transforming the Designs into Games

After the designs are completed, the game engine chosen for the creation of the game is Unity. It is designed as a 2D (2D project) with vector designs. The “Start Menu” in the above image is designed as Stage 1, the Map and the part where answers to the questions are given as Stage 2. “Amount of food per person”, “Amount of water per person”, “Air pollution rate” etc. specified in the operation part of the game. Variables that take value according to the progress of the game are defined in Stage 2. Questions are defined as different objects in Unity. In order not to ask the questions asked again, these question objects contain a control variable. When the player answers a question, the "Ask" variable will take the value 0 instead of 1. Thus, it was ensured that the questions did not repeat themselves. 8 The answers to the questions change the values of basic criteria and instructive criteria. When these changes reach a certain size, visual changes occur on the map. While making visual changes, methods such as animation triggering and light regulation were used.

2.5. Participants

There are 299 people in the pre-test study.

According to figure (2a), there are 161 men and 138 women in the study.

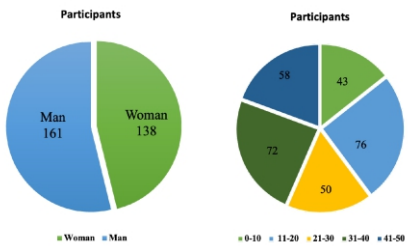

a b

Fig. 2: a and b)Participants by gender and age (pretest data)

According to figure (2b), there are 43 people between the ages of 0-10, 76 people between the ages of 11-20, 50 people between the ages of 21-30, 72 people between the ages of 31-40, 58 people between the ages of 41-50.

According to figure (3), in the study, 108 from İzmir, 74 from Ankara, 34 from Istanbul, 30 from Manisa, 8 from Aydın, 8 from Antalya, 4 from Muğla, 4 from Balıkesir, 3 from Kayseri. 3 from Samsun, 3 from Bursa, 2 from Sakarya, 2 from Ağrı, 2 from Afyonkarahisar, 1 from

Edirne, 1 from Adana, 1 from Sivas, 1 from Yalova, 1 from Bingöl , 1 from Muş, 1 from

Çanakkale, 1 from Eskişehir, 1 from Erzurum, 1 from Giresun, 1 from Kahramanmaraş, 1 from Isparta, 1 from Kocaeli, 1 from Kütahya, 1 from Ordu , 1 person from Konya, 1 person from Zonguldak, 1 person from Ardahan, 1 person from Niğde.

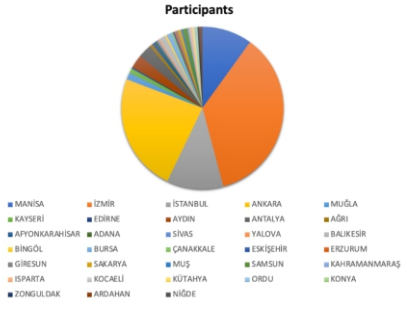

Fig. 3: Participants by Cities

There are 155 people in the final test study after playing the game. According to figure (4a), there are 89 males and 66 females in the study.

According to figure (4b), there are 33 people between the ages of 0-10, 38 people between the ages of 11-20, 32 people between the ages of 21-30, 27 people between the ages of 31-40, and 25 people between the ages of 41-50.

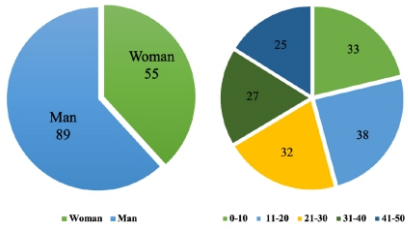

a b

Fig. 4: a and b Participants by Gender and Age

Table 1: Work planning by time chart

	Months				
Job description	**September**	**October**	**November**	**December**	**January**
Literature Review	X	X	X		
Data Collection and Analysis		X	X	X	
Programming the Application		X	X	X	
Project Report Writing			X	X	X

2.6 Game Flow

When the player enters the game, the player will see a menu that reflects the theme of the game with its colors and will be able to learn about the basic features of the game. When the play the game option is pressed, the player will be directed to the map, which forms the basis of the game, where they can observe the effects of global warming. Apart from the basic criteria that will determine the winner in the game - satisfaction rate and population, instructive criteria have been determined in order to observe that global warming has a direct effect on the life of the individual with a chain plot. These criteria are not taken into account when determining the winner, but they are necessary so that the basic criteria can be observed concretely. These criteria are as follows: amount of food per capita (initially determined as 1000 kg.), amount of water per person (initially determined as 1000L.), air pollution rate (initially determined as 0%.), total number of trees (initially 1000 trees. The number of people in the hospital (initially determined as 0 people.), the number of product varieties produced in the field (initially determined as 1000 varieties.), the total number of farm animals (initially determined as 1000 animals.).

The effects of these determined instructive criteria on the playgrounds are as follows:

Schools and Hospitals: In cities where schools cannot be active, development and public satisfaction cannot be mentioned. For this reason, the number of people in the schools of the person who answers the questions correctly increases, which causes an increase in the basic and instructive criteria that enable the game to be won by improving awareness and technology. In the wrong

answer, there is a decrease in the criteria for the same reasons.

The existence of hospitals, on the other hand, is intended to reinforce the view that is intended to be told to the player with numerical data and to make the learning permanent. For this reason, answering the questions correctly or incorrectly and thus changing environmental conditions will cause a decrease in the number of people in the hospital.

Farm and Field Areas: Global warming greatly affects human health in this area, as in other areas. For this reason, in case of incorrect answers to the questions, increases and decreases are observed in instructive criteria such as the amount of food per capita, the number of people in the hospital, the number of product varieties produced in the field and the total number of farm animals.

Areas Attracting Tourists: The disappearance of these socioeconomically important public areas, which are preferred by people for entertainment and activity, will undoubtedly reduce the satisfaction of the people. In addition, the changes in the lakes, forests and parks included in these areas, besides affecting the basic criteria; It also affects instructive criteria such as the amount of water per capita, 11 air pollution rates, the total number of trees and the number of people in the hospital.

Accommodation Area: The player has a king avatar symbolically in the accommodation area. This area is intended to be the player's living space. Thus, if the player does not take steps to stop the impending threat, he will be able to observe the effects of the disaster that awaits him in his own living space. In addition, some features have been added so that the player can adopt this virtual environment as a living space. Thanks to these features, the player will be able to decorate his house, take care of his garden, and in case of wrong answers, he will be able to see concretely the effects of the decisions he made after losing the decor items he installed in the house.

2.7. Cards

At game; cards have been prepared in order to ensure effective learning, to comprehend information visually as well as verbally, and to make learning permanent.

Prepared question cards contain questions that determine the flow of the game. In this way, the player will be able to learn about the subject verbally as well as visually. Besides, it is thought that the information that causes changes about the player's own city will attract the attention of the player more.Solution buttons are placed in the upper corners of these question cards, where the answer can be learned. In this way, the player will be able to immediately learn the information; will be able to receive instant feedback with changes taking place in the city.

In addition to the question cards; cards that verbally explain the changes that will take place in the city appear on the screen right after the question is answered and the answer is learned by these cards; the main idea of the game and the chain of negatives caused by global warming in the city was explained to the player directly and verbally. In this way; the events taking place in the city and the changes on both basic and instructive criteria can be showed to the player in more understandable way.

3. Results

In the pre-test phase, 43% of the 22 information-determining questions about global warming were answered correctly, while 57% were incorrectly answered In 17 perception-determining questions about global warming, 54% of people answered "I agree", while the remaining 46% answered "I am undecided" or "I do not agree".

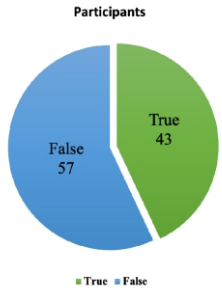

Fig. 5: True-False Graph of the First 22 Problems (Pre-test)

In the final test stage after playing the game, 78% of the 22 questions about global warming were given correct answers, while 22% were incorrectly answered.

In 17 perception-determining questions about global warming, 73% of people answered as "agree", while the remaining 27% gave answers as "undecided" or "disagree" (Fig. 6).

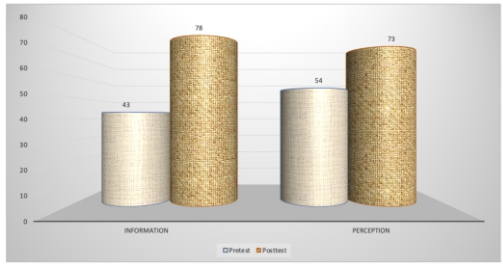

Fig. 6: Graph of the final test

4. Conclusion

The game is intended for every individual of the society, regardless of age. This situation is also seen in the scale made.Data were obtained from each individual between the ages of 0-50, both in the pre-test and post-test phases. As a result of the pre-test, it was seen that more than half of the people did not have the necessary knowledge about global warming, and most of them did not work on this issue.

Considering that these data are obtained from a wide age group, it is possible to say that both the education given in schools about global warming and awareness activities for adults are insufficient.

It is thought that this situation is caused by the absence of visuals in ongoing works so the learning can't be permanent, and the way that global warming issues are told, that people can not adopt the information and emphatize.

In addition to informing the society, in order to encourage people to develop solutions to the global climate change problem, the gaming industry, which is the leading use of technological tools today, has been utilized; Protect Your City with the objectives of “effective, fun minimum effort/maximum learning, learning that appeals to everyone”! developed. In order to achieve these goals, the methods mentioned in the project were developed and the game was played with a sample that could represent the universe.

After the game was played, a final test was administered to these people. As a result of the applied test, a great

difference is observed between the pre-test data and post-test data both in knowledge and perception question parts. That shows that the improved game, increased the awareness about global warming.The applied method is similar to the method of the studies conducted by Bakar Fındıkçı (2021) and Kınam Dokuzlar&Uçar (2018).

"Questionnaire" was used as a data collection tool in the project. Although it is easy to answer the questions, the disadvantage of the project is that some people may answer randomly. However, since the number of data in the project is high, the project is not affected by this disadvantage.

5. Suggestions

Problems related to global climate change and its effects on people are increasing; poses a great risk to all of us. That's why, to develop solutions is a great importance.

- Effective visuality and an accessible, user-friendly game flow should be given importance in order to attract people's attention in advertising, marketing and games which are made for social awareness.
- The place of this type of visually oriented games in education can be increased and they can be played as an activity in schools, at the end of the relevant units.
- The game; The number of questions will be increased, the features that will personalize the city will be increased, and more people can access the game by being developed and implemented in a way to interact with other players.
- The game can be put on official education platforms and provide more students to get information.
- The game can be transformed into more individual-oriented works that are presented with more impressive visuals by transferring to virtual reality platforms.

References

[1] Akgün, H., Koyuncu, M.(2018); Interaction Between Livestock and Global Climate Change, U. Ü. Journal of the Faculty of Agriculture (32), 151-164.

[2] Arıkan, R., (2004) Research Techniques and Report Preparation, Asil Publishing, Ankara.

[3] Bakar Fındıkçı, M. (2021); Examining Sustainability as Awareness Through Graphic Design Products, UlakBilge Sosyal Bilimler Dergisi, (67), 1435-1446.

[4] BBC(2019,March) "Air pollution causes about 8.8 million premature deaths worldwide each year." ; retrieved from https://www.bbc.com/turkce/haberler-dunya-47537853.

[5] BBC(2019, July) "Which country produces how much garbage and how much does it recycle?"; retrieved from https://www.bbc.com/turkce/haberler-dunya-48851661#:~:text=Endekse%20g%C3%B6re%2C%20d%C3%BCnya%20genelinde%20her,

[6] BBC (2021, October) "The climate crisis: what is COP26, what to expect from the conference in Glasgow?" ; retrieved from https://www.bbc.com/turkce/haberler-dunya- 56829395.Büyüköztürk, Ş., (2008) Manual of data analysis for social sciences, Pegema Yayınları, Ankara.

[7] Congar, K., (2021, August) "How can we protect ourselves from air pollution and poisoning caused by forest fires?"; retrieved from https://tr.euronews.com/2021/08/06/orman-yang-nlar-–n-sebep-oldugu-hava-kirliliginden-ve-zehirlenmelerden-nas-l-korunuruz.

[8] Congar, K., Limb, L. (November, 2021) "A Canadian doctor 'diagnosed climate change' for the first time in the world"; retrieved from https://tr.euronews.com/green/2021/11/12/kanadal-bir-doktor-dunyada-ilk-defa-bir-hastaya- iklim-degisikligi-teshisi-koydu.

[9] Dursun, E., (2022); Effects of Global Warming on Living Beings, Kocaeli Üniversitesi, Tıp Fakültesi, Kocaeli. Retrieved from http://www.obi.bilkent.edu.tr/bultenorta/20172018/ekoilk23032018.pdf

[10] DW(2021,May) "China is the biggest contributor to greenhouse gas emissions"; retrieved from https://www.dw.com/tr/sera-gaz%C4%B1-emisyonlar%C4%B1n%C4%B1n-en-b%C3%BCy%C3%BCk-sorumlusu-%C3%A7in/a-57457474.

[11] Gökkur, S.(2016); Impact of Climate Change on Water Resources, Apelasyon Dergisi, (34).

[12] Gökdere, M., Sontay, G., Usta, E. (2015); The Study of Scale Developing Related To The Environmental Literacy Component on the Secondary School Level, Necatibey Eğitim Fakültesi Elektronik Fen ve Matematik Eğitimi Dergisi (EFMED), (9), 49-80.

[13] Güneş, M., Sevinç, M. (2019, December) "Water resources are decreasing day by day due to global warming, climate change and many human-induced factors. 36 lakes have dried up in 50 years in Turkey. Here are the most critical ones among those lakes…"; retrieved from https://www.trthaber.com/haber/turkiye/turkiyenin-kuruyan-golleri-444292.html.

[14] Haberler(2019,September) "Will you succeed in this global warming test?"; retrieved from https://www.haberler.com/quiz/bu-kuresel-isinma-testinde-basarili-olabilecek-misin-885/. Meb Akademi Uzem (2020, February) "Game Based Activities and Trainings in Education"; retrieved from https://uzem.mebakademi.com/oyun-temelli-egitimler.htm.

[15] İşbank(2021,June) "What is the Greenhouse Effect and What are the Consequences?"; retrieved from https://www.isbank.com.tr/blog/sera-etkisi-nedir.

[16] Katanich, D. (2020,March) "The number of endangered rhinos in Africa is increasing year by year"; retrieved from: https://tr.euronews.com/2020/03/26/afrika-da-nesli-tukenmekte-olan- gergedanlar-n-say-s-her-gecen-y-l-art-yor.

[17] Kılıç, İ., Ural, A. (2011) Scientific Research Process and Data Analysis with SPSS, Detay Yayıncılık, Ankara. Kınam Dokuzlar, B., Uçar, T.F. (2018); Graphic Design Applications in the Context of a Social Awareness Project, Faculty of Fine Arts Art Journal, (11).

[18] Meb Akademi Uzem (2020,February) "Game Based Activities and Trainings in Education" ; retrieved from https://uzem.mebakademi.com/oyun-temelli-egitimler.html.

[19] Metin, M.(2014); Scientific Research Methods in Education from Theory to Practice, Ankara, Pegem Akademi Yayıncılık.

[20] NTV(2022, April) "Global warming ultimatum from climate scientists: It's now or never"; retrieved from https://uzem.mebakademi.com/oyun-temelli-egitimler.html.

[21] Özcan Chocardelle, P. (2021, November) "Easy climate test 1: How well do we know about climate change?"; retrieved from https://hthayat.haberturk.com/test/873-kolay-iklim-testi-1- iklim-degisikligini-ne-kadar-taniyoruz.

[22] Reis, M. (2017, June) "Strategic importance of food and agricultural products in the world"; retrieved from https://retailturkiye.com/mehmet-reis/dunyada-gida-ve-tarim-urunlerinin- stratejik-onemi/

[23] Sayın, E. (2021,June) "Global climate change moves from farm to fork"; retrieved from https://www.trthaber.com/haber/cevre/kuresel-iklim-degisikligi-tarladan-sofraya-yanasiyor- 585728.html.

[24] Sputnik Türkiye(2021, August) "Hawking: Tell climate change deniers to go to Venus, I'll pay for it"; retrieved from https://tr.sputniknews.com/20180111/hawking-iklim-degisikligi- venus-1031771875.html.

[25] Şencan, H., (2007)Scientific Research in Social and Behavioral Sciences, Seçkin Yayıncılık, Ankara.

[26] Türk Yurdu (2016,June) "Awareness Consciousness" ; retrieved from https://www.turkyurdu.com.tr/yazar-yazi.php?id=2669.

[27] Türkiye Uzay Ajansı(2022,May) "VENUS"; retrieved from https://www.turkyurdu.com.tr/yazar-yazi.php?id=2669.

[28] Yıldırım, S. (2021,August) "Forest fires will increase as global warming continues"; retrieved from https://www.milliyet.com.tr/ekonomi/kuresel-isinma-surdukce-orman-yanginlari- artacak-6565416.

FINGER TRAINING ROBOTIC DEVICE (FTRD)

Romina Sedigh, West Vancouver Secondary School, Vancouver/Canada, rominasedighh@gmail.com

ARTICLE INFO

Bronze Medalist in International Greenwich Olympiad IGO 2022,,London/ UK

Silver medalist in BUCA IMSEF 2022, Izmir, Turkey

Awarded by Ariaian Young Innovative Minds Institute,AYIM, http://www.ayimi.org ,info@ayimi.org

ABSTRACT

A vast majority of people with significant stroke and significant disorders such as weakness and spasm have experienced severe impact on their daily activities. To evaluate hand performance, there are few criteria that are needed. The goal of this project with Finger Training Robotic Device (FTRD) is to help people with finger and hand disabilities to recover faster and to gain back their ability of finger movement. With robotic devices, rehabilitation can be increased in intensity and frequency, standardized, and provide a controlled multisensory stimulation to help patients move as they need while avoiding inappropriate movements.

Key Words :*Hand Recovery, Rehabilitation Robotics, Stroke, Finger Movements*

1. Introduction

Most stroke patients develop significant disorders such as weakness and spasticity that have a severe effect on their daily activities. The ability to perform Daily Life Activities (DLA) is highly dependent on hand function, and those who suffer from hand injuries are less able to perform DLA and thus reduce their quality of life. In severely ill patients, the injured hand often has difficulty along the fingers and no marked improvement over time, which makes restoring hand function one of the biggest challenges in stroke rehabilitation. Rehabilitation of finger function after stroke has changed significantly in recent decades. Robotic devices allow to increase the amount and intensity of treatment, standardize treatment, provide a complex but controlled multisensory stimulation. It helps the patient to perform the required task and at the same time prevent inappropriate movements.

2. Materials and Methods

Finger Training Robotic Device (FTRD) is an effective mechatronic robotic device that is specifically designed for hand treatment (Fig. 1).

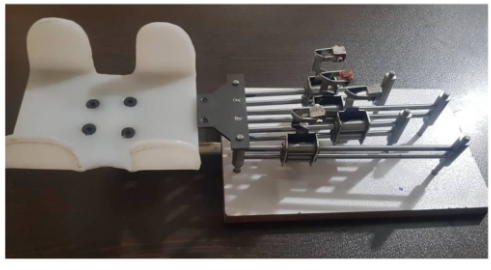

Fig. 1: Finger Training Robotic Device

It measures the patient's isometric strength for each finger separately as well as the strength of the hand. Furthermore, it improves finger or hand strength and reduces spasms. Thus, patients can regain a normal range of motion in their hands as much as possible. This robot can be used for various types of hand disabilities that have been described as follows.

2.1. Cerebral Palsy

This physiotherapy program is designed to help people with cerebral palsy control hand stiffness, perform voluntary movements, and prevent hand deformity with this device and physiotherapy knowledge.

2.2. After Hand Surgery

This device can be used to perform physiotherapy and rehabilitation after hand surgeries.

I Upper limb repair and transplant surgery:

Repairing and transplanting damaged nerves in the upper limbs, including the arm and shoulder, caused by stretching, tearing, stabbing, and similar injuries.

II Tendon repair and transplant surgery:

I For tendon repair and transplant surgeries (Tendon Replacement), physiotherapy is essential for quickly returning to pre-injury activities, moving limbs, and preventing premature adhesions.

III Fractures of the hands and fingers:

To improve the range of motion and opening of the fingers, return muscle strength to grasp objects, and improve the range of motion of the fingers after fractures of the hands or fingers, physiotherapy is required.

2.3. Paralysis of One or Both Sides of the Body, Stroke, and Brain Injury

These diseases lead to a loss of muscle control (Ataxia), laxity, and in many cases excessive stiffness, which results in unintended side effects, including reduced functionality, limited range of motion, and side effects.

Review of the purposeful movements of the mechatronic rehabilitation system for fingers and wrists (Fig. 2) [1].

I Radial deflection/wrist ulnar
II Bending/stretching the wrist
III Bending/stretching fingers
IV Forearm pronation/supination

3. The Main Parts of FTRD

Different parts in FTRD system are included as (Fig. 3):

1) Finger holder steel sheet

2) Finger holder magnet
3) Double-sided rail holder
4) Power transmission belt controlled by a stepper motor
5) Longitudinal motion guide
6) Step motor for each finger

I) Each of the mechanisms is used individually for each finger

II) FTRD has 6 servomotors - left and right hand

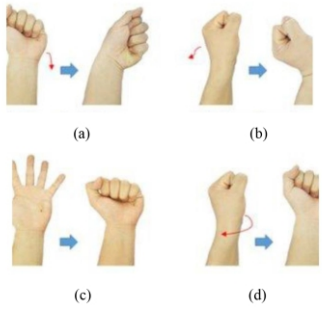

Fig. 2: a) Ulnar Deviation; b) Extension of wrist; c) Flexion of fingers; d) Supination

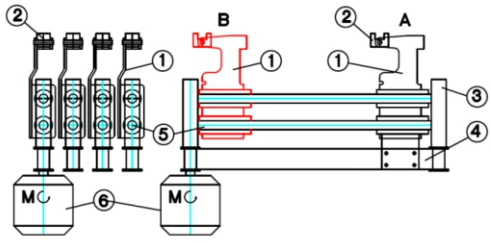

Fig. 3: Main Parts of FTRD

This device is designed so that a servomotor can control each movement mechanism at different speeds. It also has a reciprocating motion in the form of a rail and movement (guide bar and sliding liner). Each of the fingers of the device is moved by a mechanism that, by way of an independent servomotor, converts the pulley rotational motion into a reciprocating linear motion that causes the fingers to move. For each finger movement, a mechanism is designed that is converted to a reciprocating linear motion by a Foley-era servomotor, causing the fingers to move. With the PLC- programmable system of this device, each finger can get the desired amount of speed and power. A magnet is installed in each cubic block of the moving part of the device for each finger. To attach the fingers to the robot, a metal is taped to the fingers, which allows the user to attach to the mechanism and move the fingers correctly when the user places their fingers on the device. To hold the forearm, adjustable support has been installed in different directions (Fig. 4).

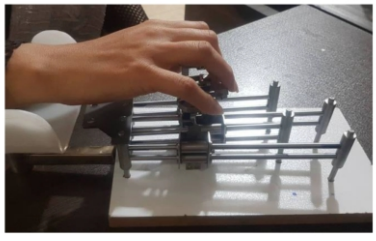

Fig. 4: Adjusting of FTRD with finger movement

4. Conclusion

A significant number of individuals with motor impairments are among the stroke survivors. In fact, in the initial motion, all post-stroke survivors and patients with hereditary conditions may experience hand function impairments. The hand is one of the foremost vital limbs of humans; it consists of five fingers and a wrist. In general, to manage the stroke's debilitating impact on patients' upper limbs, particular finger and wrist exercises may help. Robotic devices allow to increase the amount and intensity of treatment, standardize treatment, provide a complex but controlled multisensory stimulation. This device is an effective mechatronic robotic device specially designed to treat the hand. The proposed four-finger rehabilitation robot with simplified design and low manufacturing cost could be used in robotic applications in home care for disabled people.

Acknowledgement

I would like to thank my father who guided me in doing this project. He provided me with invaluable advice and helped me in difficult periods. His motivation and help contributed tremendously to the successful completion of the project.

References

[1] https://www.researchgate.net/figure/Eight-motions-of-the-wrist-and-fingers-a-and-b-radial-and-ulnar-deviation-of-the_fig4_336527108

DESIGNING A MOBILE ELECTROSPARK COATING SYSTEM FOR PRODUCING FUNCTIONAL SEMI-CONDUCTOR NANOPARTICLES

Feza Güngör, Turkey, fezagungor68@gmail.com

ARTICLE INFO

Gold medalist in BUCA IMSEF 2022

Awarded by Ariaian Young Innovative

Minds Institute , AYIMI

http://www.ayimi.org ,info@ayimi.org

ABSTRACT

In order to improve the standard electro-spark coating system, semiconductor metal oxide NPs; It was planned to design a control unit that controls the size distribution on the surface and provides limited accumulation to the linear region on the preferential axis. This control unit in the robotic platform provides the linear movement of the substrate in an axis during the spark, as well as the coaxial movement of the selected metal electrode pair. This project is considered to be successful in material production system design including robotic control unit, NP production and testing its effect on properties.

Key Words :*Electro-Spark Coating, Semiconductor,Robotic*

1. Introduction

The production of materials at the nanoscale enables the making of functional devices whose physical, chemical and biological properties can be changed and making these devices usable in our daily lives. Although composed of the same atoms, formations in different geometries create different material properties with different behaviors. This situation reveals how important the material production techniques can be, as it enables us to reach new and useful technologies.

Semiconductor metal oxide materials, on the other hand, arouse great interest in researchers working on nano-scale semiconductor devices, as they can be produced in various nanoscales, as well as being easy to manufacture. Moreover, these materials show unexpected properties when produced in different forms. For example, the optical and electrical properties of metals such as copper (Cu), gold (Au) are very different at the macroscopic and nanoscale. At the macroscopic scale, gold is yellow in color for its optical properties, but red at the nanoscale. Copper is opaque at the macroscopic scale (it absorbs more light) and quite transparent at the nanoscale. Bismuth, which has semimetal properties in macroscopic form, is semiconductor in nanowire form. The optical and electronic properties of materials vary greatly depending on their size. In that case, it will be possible to control many physical properties and functions of materials whose size can also be controlled.

The "moving electrospark coating system on robotic platform" designed in this project study and the translational movement of the substrate along a preferential axis during the spark, instead of the traditional "immobile substrate feature" in the coating technique, which is one of the plasma-based material preparation techniques, causes semi-metal oxide nanoparticle formation and physical effects on its properties were investigated.

In the standard electrospark coating technique, a high voltage difference is applied between two high purity metal electrodes, which are at a critical distance from each other. In this way, the spark formed between the electrodes vaporizes the electrode tips and metal particles are released. The next step is important from here. Because the process of depositing these metal particles on the substrate as metal oxide nanoparticles by combining with the oxygen in the atmosphere is the reason for the emergence of this project. Since the subject of our interest is the production of semiconductor metal oxides, it is very important to be able to deposit the resulting NPs into the desired template area. Thus, a more comfortable working area will be created on a suitable surface for applications such as diodes and sensors.

In this study, one of the most important parameters in the semi-metal oxide nanoparticle generation system is the size of the electrostatic energy stored in the capacitor. Capacitor energy is highly dependent on the voltage difference between metal electrodes. When capacitor energy is released, direct current (dc) creates a high temperature plasma arc between the ends of the two electrodes. In the examination of the NP production system and the resulting product material, separate experiments should be carried out for certain values of the voltage difference between the electrodes. This process is necessary because, depending on the magnitude of the voltage difference applied between the electrodes, there are differences in the shapes of the nanoparticles deposited on the substrate surface.

It is possible to create many properties and application areas by succeeding in controlling the structure of semiconductor nanoparticles. Therefore, an interface design was carried out to control the size distribution of the semiconductor metal oxide NP and to be linearly oriented and deposited to a preferential region. This interface gives the substrate an axial movement capability controlled by Arduino UNO, and it produces NPs for different spark voltage values at certain intervals, at once, with the systematic movement of the substrate. Accumulation of nanoparticles at the desired line length and concentric smooth placement on the target area on the substrate surface in one go, on the preferential axis, has been successfully achieved. The interface designed in this study works as a functional robotic control component that performs both operations at the same time and enables NPs to be deposited into millimetric or micro channels (template). Since the same component moves the substrate during spark, NP production is provided in independent, parallel and linear channels (template) on the substrate surface, and it is possible to cover the substrate surface with

homogeneous semiconductor nanoparticle channels. The critical element in this process; It is the accumulation of nanoparticles in a homogeneous and preferential region of the substrate surface with identical dimensions. If the homogeneous distribution of nanoparticles on the substrate surface and size control cannot be achieved, effective optical and electrical properties cannot be achieved. Therefore, the most important feature of this robotic component is to create electronic and/or electrooptical paths on suitable surfaces.

It covers measurement systems that will determine the application areas. Once it is understood that the properties of materials change depending on their size, they are very valuable for many application areas such as electronics, computers, aviation, space, health, energy, defense and food. There are various studies on the antimicrobial properties of gold and silver NPs (Singh et al., 2014; Habiboallah et al., 2014; Nambiar et al., 2010) to ZnO (zinc oxide) NPs on their capacity to act as gas sensors (Singh et al., 2010). ., 2014). The fact that nanoscale materials are lighter, more robust, and programmable means that the same or more processes can be performed with less material compared to large-size material. This also means less energy, cost and hassle.

There are different techniques to produce materials at the nanoscale. These are generally material preparation techniques created in solution, plasma or vacuum systems (Rane et al., 2008). Plasma-based techniques are frequently used to produce materials such as particles and wires at nanoscale. Electro-spark also; It is a technique with different arc capacity depending on the type of electrodes used, cross-sectional area and work function. Although it is a very simple technique, the cost for the needs may vary. After the first studies for the purpose of producing materials, applications were made in the normal atmosphere environment without the need for vacuum (Schwyn et al., 1988). In various researches, this technique; carbon nanoparticles (Horvath et al., 2003), carbon flakes (Tabrizi et al., 2009), metals (Tabrizi et al., 2010), metal oxide nanoparticles (Kim et al., 2005; Vons et al. , 2011), semiconductor nanoparticles, Si nanoparticles (Kumpika et al., 2008), Zinc-Oxide nanoparticles (Güngör et al., 2017), Copper-Oxide nanoparticles (Güngör and akd., 2019).

In this study, it is aimed to increase the capacity of the system to be used in semiconductor nanomaterial production and semiconductor device applications by adding interfaces such as robotic control unit to a standard electrospark coating system. Thus, the mobile electrospark coating system was installed on the robotic platform, the details of which are given in the "Methods" section, and thin films consisting of nanomaterials produced with this system were examined optically, surface and electrically.

2. Materials and Methods

In this study, the system designed to produce functional semiconductor metal oxide NP basically consists of two main units. The first is the robotic control unit that simultaneously provides the axial movement of the substrate controlled by the Arduino UNO and the concentric movement of the metal electrode pair. The other is the high voltage unit used to create the plasma-based arc between the electrodes.

High voltage unit; It consists of a variac that provides 0-220V output and a DC high voltage source whose output voltage can be adjusted between 0-6kV, the capacitor used to store energy and the switch used to adjust the spark number (Fig.1a). Here, the 0.2 µF/5kV capacitor is charged with a voltage difference of 3kV, 4kV and 5kV, and the stored 0.9J, 1.6J and 2.5J electrical energy is discharged between the electrodes. High purity Zn, Ag and Cu electrodes were used in the experiments. Spark speed is set to be 1 every 3s. Thin film sample group consisting of each semi-metal oxide nanoparticle was prepared with a spark number of 10. Microscope glass was used as substrate. The position of the metal electrodes is adjusted relative to the horizontal axis. The vertical axis distance between the glass substrate and the metal electrodes is approximately 1 mm.

The robotic control unit, on the other hand, has two freedoms of movement at the same time. One of them is related to the axial movement of the substrate during the spark. Axial movement was controlled by microcontroller (Arduino Uno) and step-motor driver unit with the values determined by the user for the number of steps. For this control process, in addition to the micro-step feature and 1, 2, 4, 8, 16 and 32 steps, the pitch value of the mechanical system is taken into account. In this way, the linear regions (lines) on which nanoparticles are coated on the substrate surface are separated from each other. Another feature of the robotic control unit is that it can provide planar motion control not only in one axis, but also in both axes for a fixed spark voltage value (Fig.1b). Thanks to this feature, it will be possible to produce devices such as optical and electrical circuit elements by coating semiconductor nanoparticles on special template surfaces. The other motion controlled by the robotic unit is related to the concentric motion of the metal electrode pair. In concentric motion, it was decided to use an intermediate element (M8X1) with metric-8 right and left threads to control the distance between metal electrodes and combined with a second step-motor driver unit with Arduino Uno. Thus, the step-motor completes 1.8 degrees with different steps (up to 6400 steps), which are multiples of 2. It is possible to control the distance between the electrodes in the order of 10-6m. The schematic representation of the rsystem designed and used in the project is given in Figure (1c).

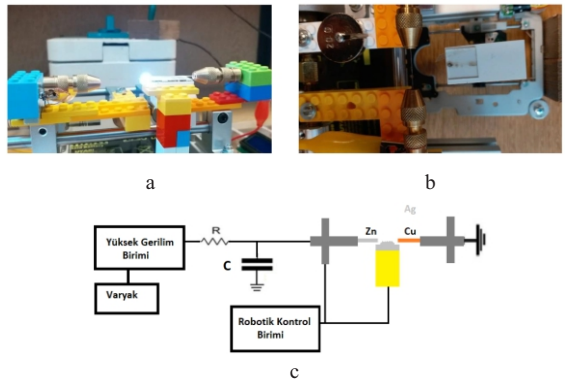

Fig. 1: Photographs taken during electro-sparking in the nanoparticle deposition system (a) and during the movement of the substrate with a single axis robotic control unit (b), Schematic representation of the system (c)

In order to examine the optical properties of semiconductor metal oxide nanoparticles produced with the system controlled by Arduino UNO-based, optical transmittance spectra in the wavelength range of 300-1100 nm were obtained at room temperature. For this, a UV-Vis spectrophotometer (Seeman 3000) with CCD (Charge Coupled Device) detector was used. Experimental optical transmittance spectra of thin films in the uniaxial linear region where semi-metal oxide nanoparticles accumulate

on the substrate were obtained. The optical constants of the material (such as film thickness, refractive index, optical band gap) cannot be obtained directly from the experimental optical transmittance spectra obtained in a certain wavelength range. Therefore, theoretical spectrum curves obtained by calculation are fitted to the experimental spectrum by means of utilities in the computer environment. In this study, the program that provides us this convenience is a computer program that works on the basis of the unconstrained minimization algorithm by Birgin (Birgin et al., 1999). In this way, theoretical optical transmittance spectra, which give the best agreement with the experimental optical transmittance spectra, were obtained. Then, information such as film thickness, refractive indices, optical band gap of the samples were obtained from these theoretical spectra. Scanning electron microscope (SEM, FEI Quanta FEG 250) was used to examine the surface properties and energy dispersive spectroscopy (EDS, Energy Dispersive Spectroscopy) analyzes were used to determine atomic concentrations. Electrical measurements; were made using 4-point technique for Ag doped ZnO and Cu doped ZnO samples at room temperature. For this, an optical microscope (USB connection, x1000) and current-voltage unit were used to observe the movement of these types at the micrometer scale during the measurement with two tungsten types (Fig. 2 a, b and c).

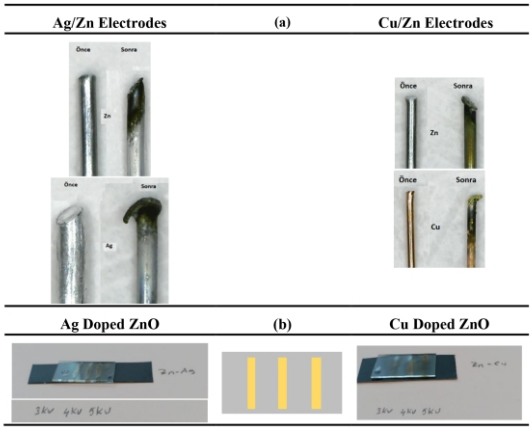

Fig. 2: Photographs of Ag/Zn and Cu/Zn metal electrodes before and after electro-spark (a) and photographs of thin-film samples formed from Ag-doped ZnO and Cu-doped ZnO nanoparticles obtained with the rHESK system, and schematic representation showing the linear sample regions on the substrate surface (b)

The experimental optical transmittance spectra of the samples produced for each different spark voltage in the system are shown in Figures (3) and (4). Accordingly, the Cu-doped ZnO nanoparticle thin film formed with 4kV spark voltage is highly optically permeable, that is, quite good transparent, compared to the samples obtained for other spark voltages. The Cu-containing sample obtained when 3kV spark voltage is applied is not sufficiently optically permeable compared to the other samples in this group. However, Ag-doped ZnO samples showed high optical transmittance for the wavelength of the light used in optical transmittance measurements greater than 550nm.
The graphs in Figures (5) and (6) show the theoretical spectra of Ag-doped ZnO and Cu-doped ZnO thin films obtained when a spark voltage of 4kV is applied between the electrodes, which is consistent with the experimental optical transmission spectra. Just like the experimental optical transmittance spectra obtained for each sample separately, the theoretical optical transmittance spectra for each sample were obtained separately.

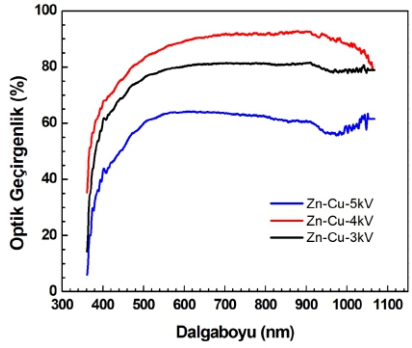

Fig. 3: Experimental optical transmission spectra of thin films of Cu-Zn-Oxide nanoparticles obtained with Cu/Zn metal electrode pair for different spark voltages.

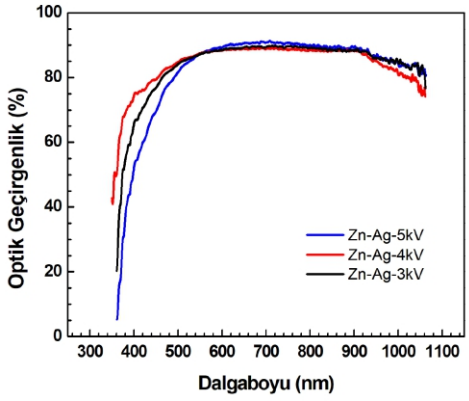

Fig. 4: Experimental optical transmission spectra of thin films composed of Ag-Zn-Oxide nanoparticles obtained with Ag/Zn metal electrode pair for different spark voltages

The film thicknesses and optical band gaps determined by using these spectra obtained for three different spark voltages of the Ag-containing and Cu-containing ZnO sample groups are given in Table (1). From this information, it was observed that the optical band gap in both Cu-containing and Ag-containing metal oxide NP sample groups increased with spark voltage. The thickness of the thin films formed by nanoparticles varies in the range of 74-196nm.

Table 1: Parameters of metal oxide nanoparticles produced with the system designed in the project. Thickness t, optical band gaps Eg, average NP size D and electrical resistances of elements obtained from EDS analyzes R of thin film samples formed from nanoparticles obtained for different spark voltages

Elektrot Couples	Sample	V_{spark} (kV)	t (nm)	E_{gap} (eV)	D (nm)	Ag amount (%)	Cu amount (%)	Zn amount (%)	R (kΩ)
Ag/Zn	Ag-ZnO	5	181	3.1630	50	0.05	--	2.78	33
		4	196	3.0700	60	0.05	--	2.52	12
		3	183	3.0600	60	0.18	--	5.41	56
Cu/Zn	Cu-ZnO	5	95	3.1045	20	--	0.38	3.05	4000
		4	74	3.0780	70	--	0.30	3.97	8000
		3	174	3.0580	60	--	1.04	1.52	12000

SEM images of the samples obtained with Ag/Zn and Cu/Zn electrode pairs in the rHESK system, depending on the spark voltage values (5kV, 4kV and 3kV), are shown in

in Figures (7) and (8).

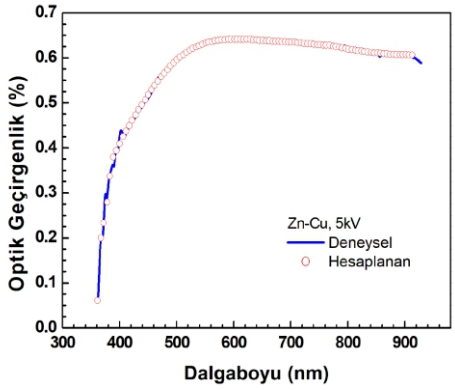

Fig. 5: Experimental (-) and theoretical (o) optical transmittance spectra of thin film consisting of Cu-Zn-Oxide nanoparticles obtained with Cu/Zn metal electrode pair for 5kV spark voltage

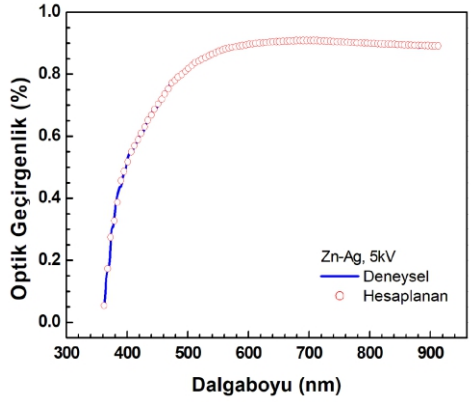

Fig. 6: Experimental (-) and theoretical (o) optical transmittance spectra of thin film consisting of Ag-Zn-Oxide nanoparticles obtained with Ag/Zn metal electrode pair for 5kV spark voltage

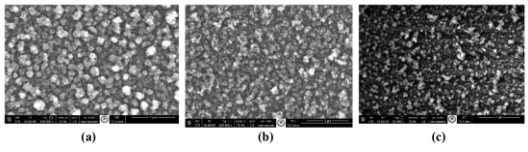

Fig. 7: SEM images of Ag-Zn-Oxide nanoparticle films obtained with Ag/Zn electrode pair for spark voltages of 5kV (a), 4kV (b) and 3kV (c)

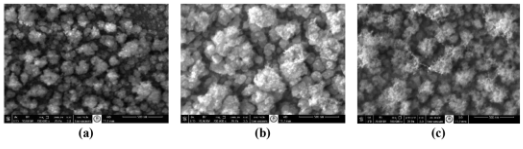

Fig. 8: SEM images of Cu-Zn-Oxide nanoparticle films obtained with Cu/Zn electrode pair for spark voltages of 5kV (a), 4kV (b) and 3kV (c)

When 5kV spark voltage is applied to Ag/Zn electrodes, groups with an average diameter of 60nm and groups with diameter distribution in the 40-230 nm range, which can be distinguished from each other, were observed. When 4kV spark voltage is applied, NPs of 30-80nm dimensions were observed. While an average NP size of 60nm was observed in the sample obtained when 3kV spark voltage was applied, it was observed that NPs overlapped (agglomeration) in places.

When 5kV spark voltage was applied to Cu/Zn electrodes, the lowest 20 nm NPs were observed, while pellets with an average diameter of 180 nm were also observed due to overlapping NPs. When 4kV spark voltage was applied, the average NP size was determined as 70nm and the NPs were more evenly distributed on the surface. In the sample produced with 3kV spark voltage, a fringed formation formed by nanowires and NPs of different lengths and approximately 10nm in width was observed.

SEM images made us think of other possibilities. The work-functions of the electrodes used during the sparking process (4.33eV for Zn, 4.26 eV for Ag and 4.65 eV for Cu) are different from each other. Due to the high energy values stored in the capacitor with high spark voltages and the high kinetic energies gained by the nanoparticles formed while discharging during the arc, it is considered that NPs may jump to different positions on the substrate surface or, if they are lower, may not complete the nanoparticle shaping, adhere to the surface or clump. The elemental analysis values of the EDS measurements made by selecting a specific region on the surfaces of the samples produced with Ag/Zn and Cu/Zn electrode pairs are shown in Table 1. In Figures (9) and (10), EDS spectra of Ag-containing and Cu-containing ZnO samples produced with 4kV spark voltage are shown as examples. In these analyzes, it was understood that Ag ions entered the ZnO structure in a very small amount, but Cu ions relatively more. The electrical measurement results are shown in Table (1). The electrical resistances of Cu-containing ZnO samples in the order of M decrease as the spark voltage increases. Ag-containing ZnO samples, on the other hand, have resistances of the order of k, the resistance values change depending on the amount of Ag ions in the ZnO structure.

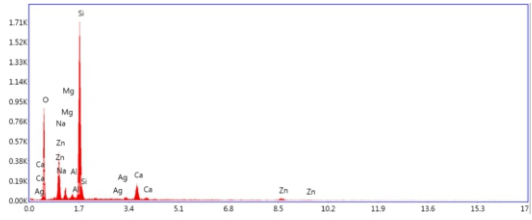

Fig. 9: EDS analysis of a thin film sample consisting of Ag-Zn-Oxide nanoparticles for 4kV spark voltage with Ag/Zn electrode pair

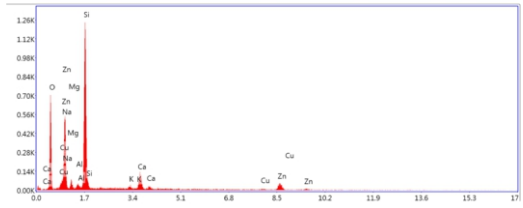

Fig. 10: EDS analysis of the film sample consisting of Cu-Zn-Oxide nanoparticles for 4kV spark voltage with Cu/Zn electrode pair

3. Conclusin and Discussions

New technologies are required to produce materials at the nano-scale and to study their properties. In this project study, the standard electrospark coating system, which is a plasma-based material preparation technique in which nanomaterials such as nanoparticles and nanowires can be prepared, was developed to produce functional semiconductor nanoparticle structures that can be used as a

device, its applications were made and its physical properties were examined. Therefore, the project studies were planned in three main groups.

The first group; It includes the design and installation of the material production system and the software of the robotic control unit. In the standard electrospark coating system, the substrate surface on which the nanomaterial will be coated is immobile, and the nanoparticles that emerge thanks to the spark between the electrodes accumulate on the substrate surface. Physical properties of materials; Since it changes according to the size, shape and arrangement on the surface, designs were made to ensure the formation of homogeneous semiconductor paths on the substrate surface, and the first prototype of a new electrospark coating system called sHESK emerged. The second group of work; involves the production of semiconductor nanomaterials. With the designed system, Ag doped ZnO and Cu doped ZnO samples were produced. By applying different spark voltages with this system, the formation of independent, parallel, linear regions consisting of semiconductor nanoparticles on the substrate surfaces has been successfully achieved.

Last group work; It includes the examination of the physical properties of the produced samples. The Cu-doped ZnO nanoparticle thin film produced with 4kV spark voltage is highly optically permeable compared to the samples obtained for other spark voltages. Ag-doped ZnO samples, on the other hand, showed high optical transmittance for the wavelength of the light used in optical transmittance measurements greater than 550nm.

Thicknesses of thin films formed by Cu-containing and Ag-containing metal oxide nanoparticles vary in the range of 74-196nm. In both sample groups, the optical band gap increases with the spark voltage. It has been observed that the nanoparticle sizes vary in the average range of 20-70nm. In sample structures from SEM images; In addition to nanoparticle forms, it has been observed that nanowire forms are also formed. In the test experiments carried out according to the EDS analysis, it was understood that Ag ions entered the ZnO structure in very small amounts, but Cu ions relatively more. The electrical measurement results showed that Cu-containing ZnO samples had resistances in the order of M, while Ag-containing ZnO samples had resistances in the k order.

In this project work; Optical, surface and electrical properties of thin film materials obtained with Ag-containing and Cu-containing ZnO nanoparticles were investigated depending on the spark voltage values between the electrodes. In these experiments, the spark number and the translational velocity of the substrate were kept constant. In the rHESK system, which was developed for the production of nanoparticles and other forms, it was observed that nanoparticle sizes, shapes, and therefore optical and electrical properties can be changed by changing the spark voltage, spark number and substrate velocity in the first place. Physical properties can be controlled with rHESK system parameters and these semiconductor films made of metal oxide nanoparticles; It can be used in the construction of devices such as LED, solar cell, diode, sensor, varistor, capacitor. These devices can be evaluated in many areas such as space, energy, defense, health and food.

4. Suggestions

The designed rHESK system can also be used by planning different nanomaterial production parameters apart from the works within the scope of the project. In the system used in the atmosphere, the area where the arc occurs can be closed and the surface coating experiments can be repeated with electrospark in an appropriate and inert (non-reacting) gas environment. By using different substrate surfaces, substrates with different surface energies can be coated with metal oxide nanoparticles. Because the adhesion of an energetic particle to every solid surface does not occur under the same conditions. The effect of substrate on nanoparticle formation can be investigated.

Acknowledgements

In this study, photographs of the physical changes of Zn, Ag and Cu metal electrodes in the system before and after electro-spark are given in Figure 2 (a). Wear, melting and sedimentation were observed at the ends of the metal electrodes after electro-sparking. Photographs of thin film samples consisting of metal oxide nanoparticles formed on the glass substrate surface are shown in Figure 2(b). In these photographs, it is seen that independent, parallel, semiconductor linear regions consisting of Ag doped ZnO and Cu doped ZnO nanoparticles form on the substrate surfaces.

References

[1] Birgin, E.G., Chambouleyron, I., Martinez, J.M. (1999). Estimation of the optical constants and the thickness of thin films using unconstrained optimization, Journal of Computational Physics, 151(2), 862-880. doi:10.1006/jcph.1999.6224.

[2] Greiner, M., Lu, ZH. (2013). Thin-film metal oxides in organic semiconductor devices: their electronic structures, work functions and interfaces. NPG Asia Mater 5, e55. doi:10.1038/am.2013.29.

[3] Güngör, E. Güngör, T, Çalışkan, D. Özbay, E. (2019). Cu Doping Induced Structural and Optical Properties of Bimetallic Oxide Nanodots by the Vertical Spark Generation, Acta Physica Polonica A,135(5), 857-862. doi:10.12693/APhysPolA.135.857.

[4] Güngör, E. Güngör, T, Çalışkan, D. Özbay, E. (2017). Synthesis and optical properties of Co and Zn-based metal oxide nanoparticle thin films, Acta Physica Polonica A, 131(3), 500-503. doi: 10.12693/APhysPolA.131.500.

[5] Habiboallah, G., Mahdi, Z., Majid, Z., Nasroallah, S., Taghavi, A.M., Forouzanfar, A., & Arjmand, N. (2014). Enhancement of Gingival Wound Healing by Local Application of Silver Nanoparticles Periodontal Dressing Following Surgery: A Histological

[6] Assessment in Animal Model. doi:10.4236/MRI.2014.33016

[7] Horvath, H., Gangl, M. (2003). A low-voltage spark generator for production of carbon particles, Journal of Aerosol Science, 34, 1581-1588. doi:10.1016/S0021-8502(03)00193-9.

[8] Kim, J.T., Chang, J.S. (2005). Generation of metal oxide aerosol particles by a pulsed spark discharge technique, Journal of Electrostatics, 63, 911-916. doi:10.1007/s11051-008-9407-y.

[9] Kumpika, T., Thongsuwan, W., Singjai, P. (2008). Optical and electrical properties of ZnO nanoparticle thin films deposited on quartz by sparking process, Thin Solid Films, 516, 5640-5644. doi:10.1016/j.tsf.2007.07.062.

[10] Nambiar, D., & Bhathena, Z. P. (2010). Use of silver nanoparticles from Fusarium oxysporum in wound

dressings. Journal of Pure and Applied Microbiology, 4(1), 207-214.

[11] Rane, A.V., Kanny, K., Abitha, V.K., ve Thomas, S. (2018). Synthesis of Inorganic Nanomaterials, Methods for Synthesis of Nanoparticles and Fabrication of Nanocomposites. Synthesis of Inorganic Nanomaterials içinde (121–139). Woodhead Publishing. doi:10.1016/b978-0-08-101975-7.00005-1.

[12] Schwyn, S., Garwin, E., Schmidt-Ott, A. (1988). Aerosol Generation by Spark Discharge, Journal of Aerosol Science, 19, 639-642. doi: 10.1016/0021-8502(88)90215-7.

[13] Singh, R. and Sing, D. (2014). Chitin membranes containing silver nanoparticles for wound dressing application, International Wound Journal, 11(3), 264-268. doi: 10.1111/j.1742-481X.2012.01084.x

[14] Singh, A. K. Rapid and eco-friendly synthesis of copper nanoparticles, AIP Conference Proceedings, 1591 (1) (2014) 372-373. doi:10.1063/1.4872606

[15] Tabrizi, N.S., Ullmann, M., Vons, V.A., Lafont, U., Schmidt-Ott, A. (2009). Generation of nanoparticles by spark discharge, Journal of Nanoparticle Research, 11, 315-332. doi:10.1007/s11051-008-9407-y.

[16] Tabrizi, N.S., Xu, Q., van der Pers, N.M., Schmidt-Ott, A. (2010). Generation of mixed metallic nanoparticles from immiscible metals by spark discharge, Journal of Nanoparticle Research, 12, 247-259. doi:10.1007/s11051-009-9603-4.

[17] Vons, V.A., de Smet, L.C.P.M., Munao, D., Evirgen, A., Kelder, E.M., Schmidt-Ott, A. (2011). Silicon nanoparticles produced by spark discharge, Journal of Nanoparticle Research, 13, 4867-4879. doi:10.1007/s11051-011-0466-0.

BUILDING A PACKAGE TO RESCUE EGGS

Fatemeh Kiani , Mahsan Ferdosi, Absal School , Tehran, Iran

ARTICLE INFO

Participatedin PYPT 2017

Supervisor: Hassan Bagheri Valougerdi

accepted by Ariaian Young Innovative Minds Institute , AYIMI

http://www.ayimi.org ,info@ayimi.org

ABSTRACT

The purpose of this paper is to design an effective structure that protects an egg when drops from 2.5 meters height. To build an effective structure all natural involved mechanisms such as air resistance, gravity, and physical properties of the egg should be taken into account. The effort is to calculate and minimize all the forces against the egg when it crashes the floor combining physics and mathematics. So we are going to invent a passive device that will provide safe landing for an uncooked hen's egg . The device must fall together with the egg.

Key Words : *Egg , invention a device, safe landing*

1. Introduction

Egg is a spherical shape material with a thin and vulnerable crust. Thus, it must be carried in such a safe boxes during loading to reduce the risk of being cracked in potential falls. This will economically help both producers and sellers. The height of trucks is usually between 2 to 2.5 meters which makes it necessary to save the eggs when it falls (Fig. 1). As seen in figure (2) the egg has a spherical structure . Egg contains different layers and parts shown in figure (2). The layers and components of the egg are: eggshell, air cell, internal and external membrane, thin and thick egg white (albumen), germinal disk, vitellina membrane, chalaza, yolk covered with a soft egg shell (crust) .

Fig. 1: Egg's car transportation

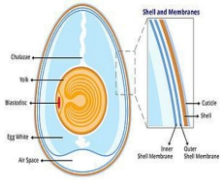

Fig. 2: The different layers of eggs [3]

Considering the shape of egg different type of containers have been built (Fig. 3).

Fig. 3: Box of eggs

Spherical shape of the eggs make it resistance to the chicken (hen) body weight when the chicken lay down on it. Also, this structure makes the egg to move along a curve path when leave it on a flat surface instead of a straight path. When the egg is being carried in a vertical state it can bear the maximum pressure compared to horizontal, therefore care must be taken to hold the egg vertical in the container during transportation. Due to the arch-shaped design the applied pressures will evenly be distributed and because of that eggs are most resistance when the pressure applies to their ends. Experiments show that egg can stand up to 15 kg.

2. Materials and Methods

We want to design an instrument that will enhance the strength of eggs in falling. This could help efficient and more secure transport of eggs by trucks, as we know the height of normal trucks are 2.5 m so it can protect the eggs against the falling and reduce the financial damage.
Velocity and time are two important factors that could help to reduce the hit impact.

3. Theory

Force distribution on an arc-shape structure is shown in figure (4) .Gravity is the force that attract a body with smaller mass toward the earth which has bigger mass.

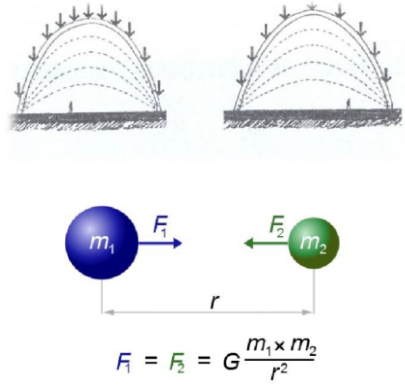

Fig. 4: Forces are applied on eggs

All bodies will fall with the same acceleration, unless air

friction or other forces affect them. Acceleration is the velocity changes per unit of time. If two different body masses fall from the same height they will land on the earth at the same time. If a body with the mass of "m" falls the force affecting that is equal to F=m.g, in which, g is the gravitational acceleration; and is 9.81 square meter per second . If a net force of "F" affects an object, that object will gain an acceleration that has a reverse relation to the mass of the object (the second law of Newton) and also the velocity from falling a height (Eqs. 1 and 2).

$$F=ma\,,\ F=\frac{dp}{dt} \quad (1)$$

$$v=\sqrt{2gh} \quad (2)$$

According to the equation by reducing the velocity or increasing the impact time one can decrease the force and also one can use a protection as a guard for example: spongy and …

Important factors to decreasing the force:

- Reducing the velocity,
- Increasing the time of impact,
- Height, local gravity, the area and the cross section of the falling object is important.
- Gravity, the word "gravity" refers to the force that pulls an object to another object. More specifically, it is the force that the Earth or another heavenly body exerts on people or objects, pulling them toward it. The gravitational acceleration of Earth is 9.807 m/s^2.

The kinetic energy of an object is the one that it possesses because of its motion ($K=1/2.m.v^2$) and the potential energy is the energy stored in an object because of its position relative to a reference position. Depending on the amount of object mass and gravitational acceleration the potential energy is calculated (U=m.g.h).

In fact when the egg is falling the potential energy is continuously converting to kinetic energy. The more the eggs getting close to surface the less the potential energy and the more the kinetic energy become. Therefore, we need to design a structure that not only acts as a buffer but also increase the air friction force e.g., parachute.

Friction is the force resisting the relative motion of two solid surfaces against each other. The lower the friction the faster two surface will move against each other. The air resistance against the falling objects is a friction force. Therefore, the air friction should be taken into account in the calculations .

Impulse is the product of the force acting on an object during a time interval. Therefore, during the egg fall we need to reduce the impulse from the surface. The designed structure should have a good buffer against the impulse. The bufferingmaterial used to reduce the impulse force can be an umbrella, spring, foamy stuff, air cushions, or even hanging the eggs, or suspending it in a gelatin .

4. Structures

Structure and its strength play a main role in the distribution of the forces and reduce the impulse. Structures are like cubical, pyramids, unsymmetrical shapes.

As mentioned earlier due to arch-shaped nature of egg is better to let the egg to hit the ground on it either end in order to increase its strength against the impulsion force.

4.1. The First Idea

Idea taken from the nature is very useful in solving every day's life problems. We took our structural idea by looking at the honey bee hexagonal nest architecture. The hexagonal architecture is the most effective shape of the nesting compared to square or triangular shaped structures. Since the bees body is spherical shaped, in order to reduce the ineffective spaces, it will be ideal to make the hexagonal cells (Fig. 5). In a hexagonal structure each cell each has at least three connections with neighboring cells (cell number 2 to 7 with the central cell and adjacent cells). This fact makes the cell stronger and also makes it less time consuming to build the nest. In reality when we put six cells next to each other we have built an extra bonus cell (cell number 7) for free. In a mathematics expression using 30 matches we build seven hexagonal cells; in other word we should have 42 matches to be able to make seven hexagonal cells but we were able to save 12 matches.

If we are going to save only one egg, we need one hexagonal cell which has less cost. Compared to one egg with the mass of m, when a box containing 7 eggs hits the ground the impulse force is seven times greater than the prior case with one egg. Because in this case the F=ma has changed to F=7×m.a. thus, we need to have a stronger structure that can tolerate the bigger impulse forces.

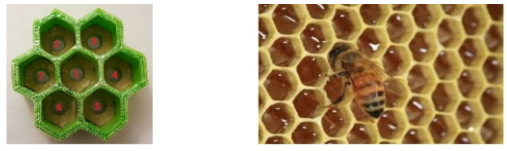

Fig. 5: Structural design according to the nest of bees

As seen in figure (6) when the egg hit the ground from the sides it will be cracked, however when it hits the ground on either of the ends, the impulsion effect would be much less. We would be able to save the egg, if we could protect the sides of the egg and try to distribute the forces evenly on both ends. We did this by placing a hexagonal paper with a hole in the center to fit the ends inside the hexagonal cell (Fig.7). The central hole caused the equal force distribution as the cell hit the ground and also protected the sides of the egg. Additionally, the walls of the cell will consume the impulsion effect and thus less pressure on the egg (Fig.8). Forces exerted on the entire structure is plotted in figure (9).

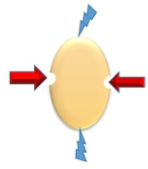

Fig. 6 : the effect of trauma to the body and head and bottom of the egg

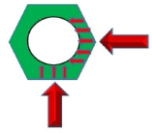

Fig. 7: bumpers hex

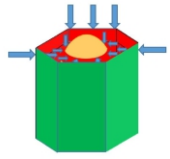

Fig. 8: forces exerted on the cell division

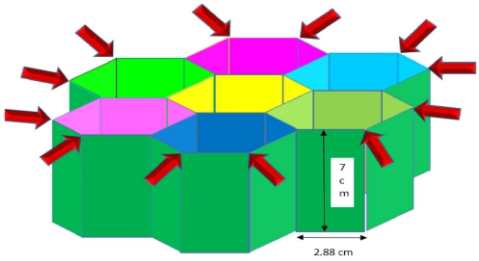

Fig. 9: The structure of the hexagonal single-cell

5. Experiment by First Structure

The purpose of this project is first to design a structure containing 20 to 30 eggs that not only can protect the eggs during falling from a height nearly 5.2 meters, but also economically feasible. The perimeter of a hexagonal cell is less than triangular and cubical cells. Therefore, hexagonal cell box is more efficient than the triangular or cubical cells in terms of strength and cost (Fig. 10).

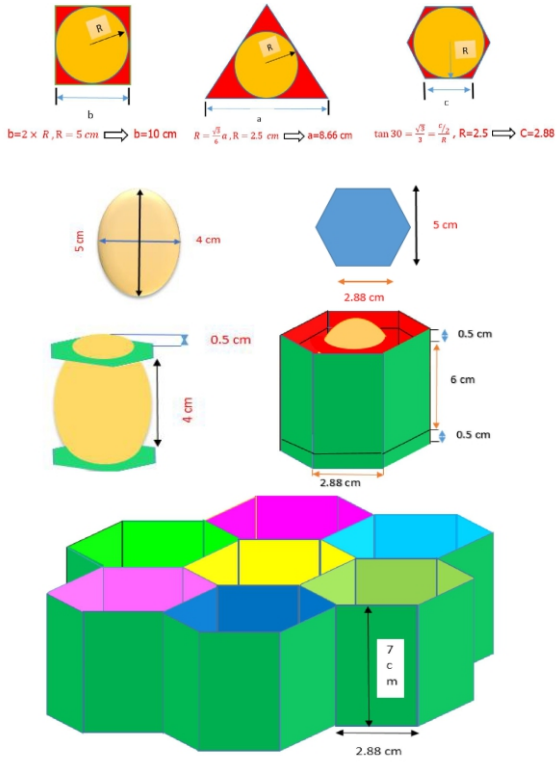

Fig. 10: Different shapes with 40 cm circumstance in square, 25.9 cm in triangular and 17.28 cm in hexagonal and the dimensions in hexagonal structure

The weight of the structure with and without the egg is calculated (Table 1).

Table 1: Weight of the structure

Structure weight without the egg	140 gr.
The weight of an egg	62 gr.
Structure weight with the egg	1000 gr.

6. The Second Structure

Materials were used in this structure are:

- cardboard
- a box of eggs
- rubber band
- Nylon bubble

This is one of the lowest cost structures because of using the cardboard in the most parts. We used the rubber band due to its elasticity. The circular instruction is used so when it hits the ground it is starting to roll and the potential energy convert to kinetic energy and the speed gradually reduced to zero. This will protect eggs against damage.

In the other hand, two poles of the eggs are stronger than the other side.This design can withstand more weight than the initial state (between 16kg -19kg) and the pressure doesn't concentrate at one point to harm eggs.

Rubber band are used in this structure creates resilience so they reduce the energy of impact. The rubber bands act as spring and can save energy . During this motion the potential energy is converting to kinetic energy.

Hooke's law, $F=k\,\Delta L$, for total possible deformation and the potential energy U (L) stored in a spring , $U= 1/2\ k\ x^2$, which comes from adding up the energy it takes to incrementally compress the spring. That is, the integral of the force over displacement so (Eq. 1):

$$k = \frac{2mgh}{L^2} \Rightarrow k = \frac{2\times 0.08\times 9.8\times 2.5}{(0.04)^2} = 2450\,{}^{N}/_{m}. \quad (1)$$

The maximum value of K is 17400 N/m and in our experiment it is about 2450 N/m. So if we let the rubber bands extended or compressed about 2~3 cm (0.02~0.03m) the constant factor will be about 9800 to 4355 N/m.
we repeated this experiment 19 times and it takes about 0.7 seconds to hit the land (Fig. 11) (Eq. 2).

Fig. 11: the second structure

$$h = \frac{1}{2}gt^2 \Rightarrow t = \sqrt{\frac{2h}{g}} = \sqrt{\frac{5}{9.8}} = 0.71\mathbf{s}. \quad (2)$$

Kinetic and rotational energy can be as (Eq. 3):

$$mgh = \frac{1}{2}mv^2 + \frac{1}{2}I\omega^2 + \alpha \quad (3)$$

Witch m is the mass, g is gravity acceleration, v is liniere speed, I is rotational momentum, ω is rotational speed and α is lost energy in hitting. So Rotational speed and energy is as (Eqs. 4-6):

$$\omega = 2\pi f = 2\times 5\times \pi = 10\pi \ \ rad/s. \quad (4)$$

$$gh = \frac{1}{2}v^2 + \frac{1}{5}r^2\omega^2 + \alpha \Rightarrow \frac{1}{2}v^2 = gh - \frac{1}{5}r^2\omega^2 - \alpha \quad (5)$$

$$\frac{1}{2}v^2 = 24.5 - 302.5\pi - \alpha \quad (6)$$

7. Results and Conclusions

In the first structure as corrugated plastic sheets are two outside flat plastic sheets made of high density polypropylene separated by small plastic beams placed

perpendicular to them. These sheets are strong against the pressure, durable in temperature between -15 to 60 degrees of centigrade, light, flexible, smell less, non-poisonous, reusable, electric and thermal proof.
The second design with cardboard and covering with nylon bubble makes it safe for landing.

References

[1] Halliday, Robert Resnick, 2012pp 10 to 29 and Rotational Dynamics topictranslator: Mahmommod Bahar, Nemat Allah Golestani)

[2] Day to Day Life: Egg-stremely Fun Egg Drop! http://carriesweetlife.blogspot.de/2010/09/egg-st…

[3] http://space.about.com/od/jupiter/tp/Facts-About-Jupiter.htm
http://www.physicsclassroom.com/Class/momentum/u4l1a.cfm

ARMED AUTONOMOUS HELICOPTER THAT CAN ATTACK USING IMAGE PROCESSING TECHNIQUES

Hüseyin Batuhan Oğuz,Göktuğ Koca,Arda Derici, Dumlupınar Bilim ve Sanat Merkezi ,Robilsa Technology Team,hboguz2005@gmail.com

ARTICLE INFO

Gold medalist in BUCA IMSEF 2022

Awarded by Ariaian Young Innovative

Minds Institute , AYIMI

http://www.ayimi.org ,info@ayimi.org

ABSTRACT

Alpin is an unmanned and autonomously controlled helicopter and there are areas of use for example transportation, agricultural spraying, camera shooting, fire extinguishing and military purposes such as surveillance and reconnaissance. TAI T-629 is an electric and unmanned heavy class attack helicopter and is under development. In the literature review, helicopters capable of autonomous flight were found, but no attack helicopters were found. The designed helicopter has 3 main autonomous missions: area scanning, target detection and attack.

Key Words : *Artificial Intelligence, Image Processing, Assault, Autonomous Helicopter*

1. Introduction

Today, the use of unmanned aerial vehicles has increased, so the areas of use of unmanned aerial vehicles have also varied. One of these areas is national defense. In the developed project, a helicopter was designed that can be used in military activities such as field scanning, target detection and target destruction by making helicopters normally controlled by a human autonomous. Türkiye's national and original vehicles Alpin and TUSAŞ T-629 can be given as examples of existing systems. Alpin is an autonomous helicopter capable of carrying payloads to target detection, surveillance and military areas. The T-629 is a remotely controlled heavy class attack helicopter. The feature that distinguishes the unmanned aerial vehicle designed in the project from these vehicles is that it can autonomously attack the determined target by performing area scanning and target detection. In addition, the project will be a project in the Presidential Eleventh Development Plan, which will serve the goal of meeting the needs of Türkiye's armed forces in national defense with national and domestic projects. In this context, within the scope of the national technology move, the software of a defense vehicle, whose flight capabilities and autonomous attack capabilities were determined by us, was developed.

National defense is to protect Türkiye against internal and external threats. One of the most important and supreme duties we will do for Türkiye is any action we will take for the defense of the homeland. With the developing technology, Türkiye's national defense remains strong largely based on Türkiye's defense industry.

The foundation of the Turkish defense industry goes back to the Ottoman Empire. For example, the production of cannons, which Mehmet the Conqueror named SHAHI during the conquest of Istanbul, which he drew and followed the castings, shows the importance given to the defense industry in the Ottoman Empire. Since then, Türkiye's national defense industry has developed more and more every day. Currently still developing and going strong. Among these developments, unmanned aerial vehicles, which have been studied and produced to a great extent in recent years, take their place.

In the Eleventh Development Plan of the Presidency, it is aimed to meet the needs of Türkiye's Armed Forces and security forces, with the understanding of continuous development, with national technologies and domestic opportunities to the maximum extent (TC Presidency Eleventh Development Plan, 2019). The project has been prepared in line with this goal. The use of domestic technologies in national defense is of great importance for Türkiye. Therefore, the production of domestic technologies will contribute to Türkiye's military power, inventory and, therefore, to the country's economy.

Unmanned vehicles are technological vehicles that do not contain human elements, can be managed remotely or autonomously, and are developed to perform predetermined tasks. Unmanned vehicles can be examined in four different groups depending on their application purposes: Unmanned Aerial Vehicles, Unmanned Land Vehicles, Unmanned Marine Vehicles, Unmanned Submarine Vehicles. Unmanned aerial vehicles are used in counter-terrorism, warfare, space, building security, and many scientific applications. For this reason, investments in this field are increasing day by day (Aksoy & Kurnaz, 2009).

UAVs, consisting of electronic and written systems, will strategically affect the defense technology of Türkiye negatively if they are not produced nationally and specifically, that is, imported. Since the software of the imported UAVs is not national and original, they have the potential to pose great threats to the national defense of Türkiye (BAKIR, 2019). If the UAVs used in military operations that must be carried out in secrecy are not national and original, it may lead to the leak of many important information that needs to be protected. Considering the geopolitical situation of Türkiye, it is very important to protect Türkiye's borders, ensure Türkiye's internal and external security, and especially successfully conduct the fight against terrorism (Kasapoğlu & Kırdemir , 2019). For these reasons, it is extremely important that the system and software used in the fight against terrorism and the protection of national borders are national and original.

There are some studies on autonomous helicopters in the world and in Türkiye. Black Hawk designed in the USA and Alpin and TUSAŞ T-629 designed in Türkiye can be given as examples. Black Hawk is an unmanned and autonomously controlled helicopter and performs military purposes such as surveillance and reconnaissance (Lockheed Martin, 2021). Alpin is an unmanned and

autonomously controlled helicopter and has uses for military purposes such as surveillance, reconnaissance, transportation, agricultural spraying, camera shooting, fireextinguishing (Titra , 2020). TAI T-629 is an electric and unmanned heavy class attack helicopter and is under development (TUSAŞ, 2022). The most important feature that distinguishes our project from other existing projects is that it attacks by scanning the target area. In the literature research on current projects, no attacking autonomous helicopter design was found.

Artificial intelligence technology, which is one of the technologies of the future, is a system that learns the relationships between events from examples and then makes decisions using the information they have learned about examples that they have never seen. Artificial intelligence is computer systems that perform the learning function, which is the most basic feature of the human brain. Artificial intelligence technology is developing more and more every day. New products emerge and show themselves more in daily life. Automation systems are also equipped with artificial intelligence technology and the decision-making power of the computer is utilized .

Image processing is a method developed to digitize the image and perform some operations, using artificial intelligence technology to obtain a special image or extract some useful information from it. (Türksan , 2018) Image processing; It is widely used in many applications, including areas such as medical imaging, industrial manufacturing, security systems, biometric recognition, human-computer interaction, and satellite imaging. It is also used for mapping in some UAV systems with image processing. In this project, field scanning and target detection were provided by using image processing techniques.

The developed autonomous helicopter performs the tasks of area scanning, target detection and destroying the target thanks to the ammunition on the helicopter, using image processing techniques. By using the developed unmanned aerial vehicle image processing techniques, it will obtain information about the target by performing Area Scanning, Enemy Detection or both according to the task given, and will be able to attack if desired. The image processing technique used in the project and the ability to attack autonomously are the most important points that make the project different from the existing systems.

1.1. Python

Python programming language; It is an open source free programming language that is object oriented, portable, easy to learn and software, and offers coders the opportunity to freely write code. Due to these features, it has become one of the popular languages in recent years. In 2017, it ranked first in the most popular programming languages according to IEEE (Wissen , 2018). While the project is being developed; Python language was preferred because of the rich image processing libraries it has and the easy and understandable writing language. Python programming language is used because it provides convenience in Raspberry 's programming. The developed algorithm is programmed in the python environment.

2. Method

Within the scope of the literature review, whether there are similar software to be developed and books, articles, papers and theses that can help the system to be developed have been scanned. Before the autonomous helicopter was designed and the software was developed, an interview was held with the military pilot working at the Gendarmerie General Command, and information was obtained about the differences between the system to be developed and the existing systems. (Information about these differences can be briefly mentioned.) In addition,information about the usability of the system to be developed was obtained. At the same time, meetings were held with relevant institutions and organizations that manufacture helicopters.

2.1. Project Construction Steps

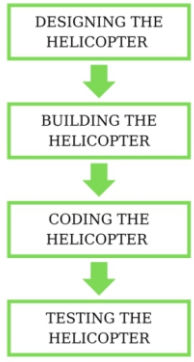

Fig. 1: Project Construction Steps

2.2. Materials

2.2.1. Raspberry Pi

The Raspberry Pi is a credit card sized computer made in the UK. Raspberry Pi is an inexpensive, small and multifunctional computer with simple programming. It provides ease of use thanks to the input and output units it contains. In addition, images can be taken by connecting to a monitor. Raspberry Pi, which uses a Linux-based operating system called Raspbian , also supports other Linux-based operating systems such as Ubuntu , OpenElec , RISC OS. (Dündar & Vural, 2018).

2.2.2. Pixhawk

Accelerometer, 3-axis gyroscope, barometer and compass modules , enabling flight with the engine control required for remote or autonomous flight. With the Raspberry interaction, it enables autonomous flight independently from the ground station.

Fig. 2: Pixhawk

2.2.3. ESC (Electronic Speed Control)

ESC stands for electronic speed controllers. It adapts the pilot's controls to the engine movements. It then sends this data to the engines as a precise instruction. ESCs are used to control the speed of the brushless motors used in the helicopters we design and to protect these motors against inrush currents.

2.2.4. Engines and Propellers

DC motors are the most widely used motor type in robotics. DC motors appear in a wide variety of shapes and sizes. For example: permanent magnet ferrous core motor, permanent magnet ferrous non-ferrous motor and permanent magnet brushless motor. The total weight of the helicopter designed in the project, including the fuselage and electronic components, is 795 gr. For this reason, 3400KV motors and 35A ESCs were preferred. Considering the engine power, 325D PRO Carbon Fiber blade set was preferred for propeller selection.

2.2.5. Servo Motor

Servo motors are a type of motor produced for parts that need to make rotation movement in fine tuning (specific acceleration, speed, angle). It was used to provide maneuverability to the helicopter.

2.2.6. Lipo Battery

containing Lithium and Polymer chemicals in their structure are called lipo batteries for short. In the project, a 2200mAh lipo battery was used as the power source of the helicopter.

2.2.7. Camera

The camera to be positioned on the helicopter will record every data in the field of view with Raspberry . By transferring it to the Pi, it will transmit the data that enables the detection of enemy elements to the station. In addition, the camera to be used, the Logitech C920, has a resolution of 1920 x 1080 px .

3. Project Work-Timeline

	MONTHS										
Job description	April 2021	May 2021	June 2021	July 2021	August 2021	September 2021	October 2021	November 2021	December 2021	January 2022	February 2022
Literature Review	x	x	x	x	x						
Arge work		x	x	x	x	x	x	x			
Data Collection and Analysis					x	x	x	x	x		
Project Report Writmg							x	x	x	x	x

4. Findings

4.1. Design of the Helicopter

Carbon fiber body was preferred in the design of the helicopter. 325D PRO Carbon Fiber blade set was used for 3400KV motors and propeller.

Fig. 3: Front View of the Helicopter

Fig. 4: Side View of the Helicopter

Fig. 5: Rear View of the Helicopter

4.2. Autonomous Operating System of the Helicopter

The designed helicopter has 3 main tasks: area scanning, target detection and attack. In the field scanning task, mapping is made using image processing techniques with the data coming from the camera. In the target detection task, target detection is made by using the data from the field scanning and image processing techniques in the first task. In the attack mission, the attack takes place by examining the data from the target detection and the existing ammunition data in the helicopter, or the data obtained from the military base is transmitted to the aid units and the target is destroyed.

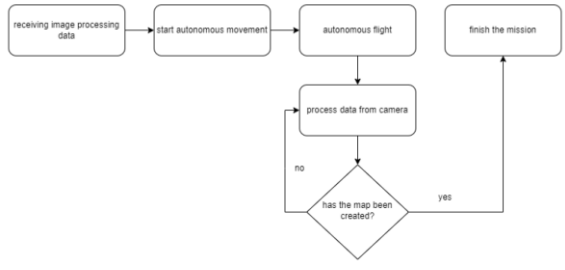

Fig. 6: Autonomous Operation Order of the Autonomous Attack Helicopter for Mission 1

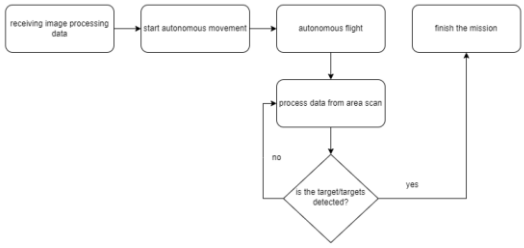

Fig. 7: Autonomous Operation Order of the Autonomous Attack Helicopter for Mission 2

Fig. 8: Autonomous Operation Order of the Autonomous Attack Helicopter for Mission 3

4.3. Coding of the Helicopter

By using the data coming from the camera and image processing techniques, the autonomous helicopter is provided with area scanning and target detection. The developed helicopter, after starting its autonomous flight, runs the image processing algorithm given in figures 14, 15, 16, 17 and 18 in the light of the data coming from the camera. In this way, the helicopter was ensured to be locked to the target.

The image processing algorithm of the helicopter consists of 4 main parts. First, image data is obtained with the fixed camera on the helicopter. Then, this image data is transmitted to the Raspberry Pi card for processing, and the image processed on the Raspberry Pi is sent to the ground station. With this image data, the process of locking to the enemy is performed. If the target escapes lockout by leaving the field of view, the lock-on-target algorithm is reset.

```
import cv2 as cv
import numpy as np

video = cv.VideoCapture(0)
whT = 320
confThreshold =0.5
nmsThreshold= 0.2

## Coco İsimleri
sınıf_dosyaları = "coco.names"
sınıf_isimleri = []
with open(sinif_dosyaları, 'rt') as f:
    sınıf_isimleri = f.read().rstrip('\n').split('\n')
print(sinif_isimleri)
## Model dosyaları
model_konfigürasyonu = "yolov3-320.cfg"
modelWeights = "yolov3-320.weights"
net = cv.dnn.readNetFromDarknet(model_konfigürasyonu, modelWeights)
net.setPreferableBackend(cv.dnn.DNN_BACKEND_OPENCV)
net.setPreferableTarget(cv.dnn.DNN_TARGET_CPU)

def obje_tanıma(çıktılar,img):
    hT, wT, cT = img.shape
    bbox = []
    classIds = []
```

Fig. 9: Image Processing Codes

In the working state of the above image processing codes, the output of detecting a person/target is as in Figures (10) and (11).

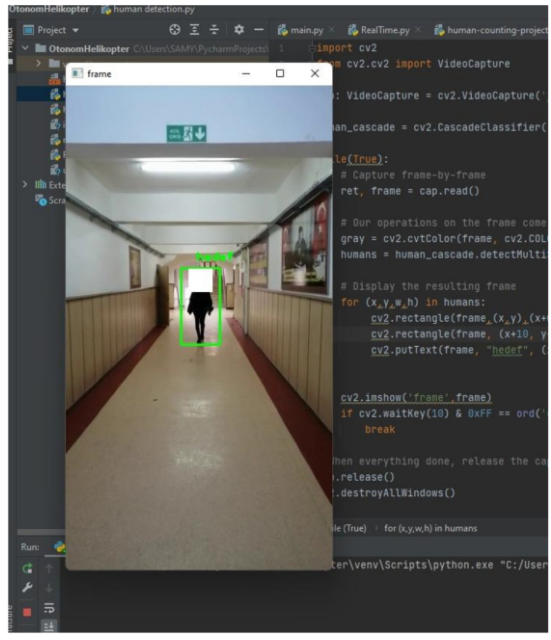

Fig. 10: Output of Image Processing Codes

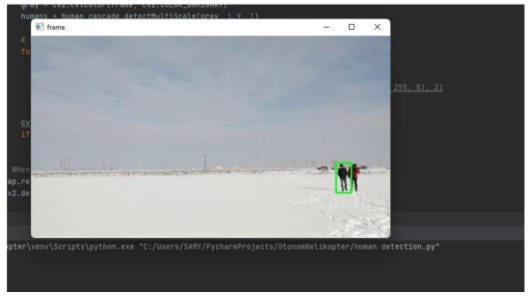

Fig. 11: Output of Image Processing Codes

5. Conclusion and Discussion

The developed system performs 3 different tasks with the data taken from the camera and image processing techniques: Area scanning, target detection and attack/destroying the target. The designed autonomous helicopter; It makes an attack on the target by scanning the area using image processing technique, target detection with the data from the area scanning, examining the data from the target detection and ammunition data. If the ammunition on the helicopter is insufficient to neutralize the target, it transmits data to the military base and ensures that the aid units head towards the target.

When the literature was searched, no helicopter was found with the ability to fly autonomously and the ability to detect and lock on the target and attack at the same time. Existing systems; attack in a remotely controlled manner. Helicopters operating autonomously are not used in the military field. In order to attack the autonomous helicopter designed in the project, unlike the existing systems, an autonomous armed attack helicopter using image processing technique for autonomous area scanning and target detection has been developed.

6. Suggestions

- Various additions to this developed autonomous helicopter can make the helicopter usable in fire and other natural disasters.
- integration with defense vehicles produced with

national technology in Turkey .

- An autonomous cargo helicopter can be built by placing a load instead of the ammunition equipment on the helicopter.
- The helicopter can use new engine and propeller to increase flight speed.
- It can be designed in different sizes for observation in extreme conditions and can also be used for civilian sectors.

References

[1] AKSOY, R. , & KURNAZ, S. (2009). Unmanned Ground Vehicles and Combat Requirements. Journal of Aerospace Technologies , 1-10.

[2] Eleventh Development Plan. (2019). sbb: Retrieved from: http://www.sbb.gov.tr/wpcontent/uploads/2019/07/OnbirinciKalkinmaPlani.pdf

[3] BAKIR, G. (2019). THE PLACE AND IMPORTANCE OF UNMANNED AERIAL VEHICLES IN DEFENSE INDUSTRY EXPENDITURE. (Journal of Eurasian Social and Economic Research , 6 (2), 127-134. www.asead.com

[4] Kasapoğlu, C. , & Kırdemir , B. (2019, February). THE NEW DIMENSION IN THE TERROR THREAT: RELATED TO DRONE ATTACKS AND TURKEY'S NATIONAL SECURITYDEVELOPMENTS . EDAM

[5] Foreign Policy & Security , 3 (2019). https:// edam.org.tr /wp content / uploads /2019/02/EDAM_Drone-Sald%C4%B1r%C4%B1lar%C4%B1-ve T%C3%BCrkiyenin-Milli-G%C3%BCvenli% C4%9Fi.pdf

[6] ÖZTEMEL, E. (2012). Artificial neural networks. Istanbul: Papatya Publishing .

[7] BAYKAR DEFENSE. (2017). Artificial Intelligence . Artificial Intelligence . https://www.baykarsavunma.com/page-Artificial Intelligence .html

[8] Turksan Corporation . (no date). Türksan Web Site: Retrieved from http://www.turksan.com/yuz-tanima.html

[9] TITRA. (2020). alpine . Alpine Unmanned Helicopter. https://titra.com.tr/products/alpin-insansiz-helicopter/

[10] Lockheed Martin. (2021). Black Hawk . Black Hawk helicopter https://www.lockheedmartin.com/en-us/products/sikorsky-black-hawk-helicopter.html

[11] Ozgul, F. (2016). python _ 5-4. Wissen _ (2018, February 27). Wissen Corporation. Retrieved from wissen Corporation .: https://www.wissenakademie.com/blog/ieee%E2%80%99yegore2017%E2%80%99nin-en populer -programming-languages

[12] Dundar, Y. , & Vural, RA (2018). Embedded System-Based Strategic Positioning with RFID ., (p. 408).

[13] TAI (2022). Heavy Class Attack Helicopter. Heavy Class Attack Helicopter. https://www.tusas.com/urunler/yeni-projeler/ozgun/agir-sinif-taaruz-helikopteri

SHORT LENGTH WIRE AS AN ELECTRICAL FUSE

[a] Maral Hasheminasab, [b] Mahan Fallahpour,
a) Farzanegan 7 High School , Tehran ; b) Alghadir High School, Kish, Iran

ARTICLE INFO

a) Participated in PYPT 2022 ,

b) participated in PYPT- IYPT 2022, Georgia

Accepted in country selection by Ariaian Young Innovative Minds Institute , AYIMI

http://www.ayimi.org ,info@ayimi.org

ABSTRACT

A short length of wire can act as an electrical fuse. A fuse is an electrical safety device that consists of a conductive wire or strip that is designed to melt and separate in the event of excessive current. We aim to determine and investigate the parameters that effect the time it takes for this fuse to blow. The two defining parameters are the current passing through the wire and the wire's melting point. The indirect parameter, resistance is also investigated as well as physical characteristics of the wire such as length and width also by assuming that a known current is passing through the wire and thus eliminating resistance as a direct defining parameter.

Key Words : *Fuse, Blow, Wire, Resistance*

1. Introduction

A fuse is an electrical safety device that operates to provide overcurrent protection of an electrical circuit. There are a myriad of different fuse designs which have specific current and voltage ratings, breaking capacity, and response times, depending on the application. The time and current operating characteristics of fuses are chosen to provide adequate protection without needless interruption. An important characteristic of a fuse in our work is the rated current, which is the maximum current that the fuse can continuously conduct without breaking and interrupting the circuit.

When the electric current passes from a short length of a wire, the wire produces heat. The heat is produced by ambience and crocodile clip by convection, conduction and a small part by radiation is wasted but in the special situation can be seen the wire blow.

2. Theory

Since in order for the fuse to blow the conducting part must melt this will happen if the heat generated in the wire because of the passage of the current is sufficient, making this current produced heat of paramount importance, with the reasonable assumption that the wire is an ohmic conductor, the heat generated in the wire while a current I is passing through it will be RI^2t, with t being the time has passed since the current was flowing through the wire.

The speed at which a fuse blows depends on how much current flows through it and the material of which the fuse is made, since wires made of different material have different melting points even if they have the same resistance. With this in mind that we are assuming a certain given current is flowing through the wire and thus resistance is no longer directly involved in the time it takes for the fuse to blow we will begin looking at the relevant parameters. Aside from this fuses usually have small resistance so as not to interfere with circuit.

2.1. Current

As seen in the generated heat relationship with current I passing through the wire, the current plays a crucial role in the heat generated and thus the time it takes for the fuse to blow. Moreover the current is squared so for instance if a fuse has the rated current of 1 A, it will blow much faster if a current of 10 A is passing through it than when a 2 A current is passing through it, since in the first case the heat produced is 25 times that of the second case (Fig. 1) (Eq. 1-2).

$$V = RI \tag{1}$$

$$P = \frac{W}{t} = \frac{q.\Delta V}{t} = I\Delta V = IV = \frac{V^2}{R} \tag{2}$$

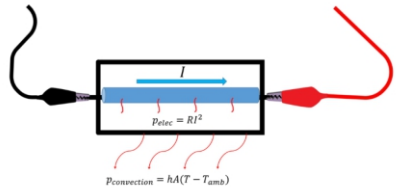

Fig. 1: When electrical current passes through a wire

It produces Heat (p_{elec})* Part of this heat is absorbed by the ambience (p_{conv})* Another part of the heat is lost by conduction, which will be shown in the fourth section of Theory.

2.2. Melting Point

Clearly this parameter dictates when the wire is going to melt. For instance imagine we have two fuses with wires made from aluminum and tin, the wires have the same resistance and the rated currents are the same. Since tin's melting point is less than aluminum's the tin wire is going to melt sooner.

2.3. Physical Characteristics of Wires: Length And Width

It is pretty clear that with the same current a thicker a wire takes longer to melt and fall of and vice versa, a thin wire will fall apart faster. This is the case regardless of other parameters.

It is known that a wire that is fixed in the two ends and suspended will form a catenary shape, the tension in different parts of the wire will vary. Again with the assumption that the passing current and the resistance are the same a longer wire will break faster since the bigger inner tension will aid gravity.

2.4. Other Parameters

Surface tension of the molten can have a minimal effect in the time it takes for the fuse to blow since it can cause the molten metal to form spheres and disconnect from the wire and thus cutting the current.

Orientation of the fuse can also play a role since it is ultimately the reason that the molten segment of the wire falls of.

3. Basic Theory

The temperature, heat transfer and its relation with blowing are as equations (3-11):

$$P_{elec} - P_{conv} = \mathbf{mc}.\frac{dT}{dt} \quad (3)$$

$$\int_0^Q dQ = \int_{T_i}^{T_f} mc \Longrightarrow Q\Big|_0^Q = mCT\Big|_{T_i}^{T_f} \Rightarrow Q = mc(T_f - T_i) \quad (4)$$

$$p_{elec} = p_{conv}$$

$$RI^2 = hA(T_F - T_{amb} \quad (5)$$

$$\boldsymbol{T_F = T_{Amb} + \frac{RI^2}{hA}} \quad (6)$$

$\boldsymbol{IF\ T_F < T_L}$ (dose't blow)

h=Convectional coefficient

e=2.71828, A=cross sectional area (7)

$\boldsymbol{IF(T_F > T_L}$:It blows $I = 0$

3.1. Instantaneous Temperature

Heat produced by current:

$$Q=RI^2t \quad (8)$$

Heat dissipated by the convection:

$$-hA(T - T_{amb}).dt \quad (9)$$

$$\boldsymbol{RI^2.dt - hA(T - T_{amb}).dt = mc.dT} \quad (10)$$

$$T = \frac{RI^2}{hA}.e^{-\frac{h}{m\times c}t} + \frac{RI^2}{hA} + \mathrm{T_{amb}} \quad (11)$$

3.2 Time of Blowing

It is supposed (T) in equation (11) is melting temperature so time of blowing is (Eq. 12):

$$t_{blow} = \frac{mc}{hA} \times \ln\left(\frac{RI^2}{RI^2 - hA(T_l - T_{amb})}\right) \quad (12)$$

3.3 Place of Melting

Because of conduction it seems that temperature of part 3 is higher than another part and it is the place of melting point, but it is not correct (Eq. 13)(Figs. 2 and 3).

$$R''I^2.t > R'I^2.t > RI^2.t$$
$$Q_{R''} > Q_{R'} > Q_R \quad (13)$$

Wire impurities is the reason of this phenomenon because the impurity of the wire in the R″ part produces more heat, although it is close to the crocodile wire, the conduction does not have much effect. That's why Low impact is considered as conduction in theory (Figs. 2-4).

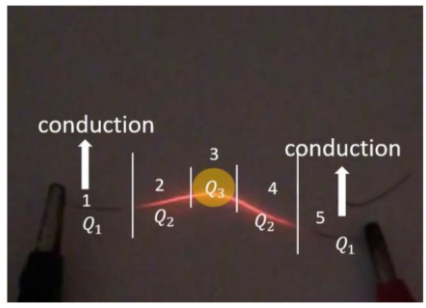

Fig 2:
Conductin 1 ≈ Conductin 5 > Conductin 2 ≈ Conductin 4 > Conductin 3

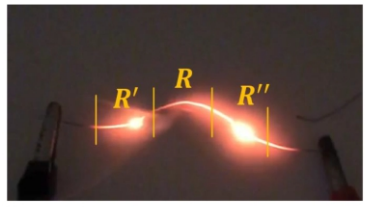

Fig. 3:

$R'' > R' > \mathrm{R}$

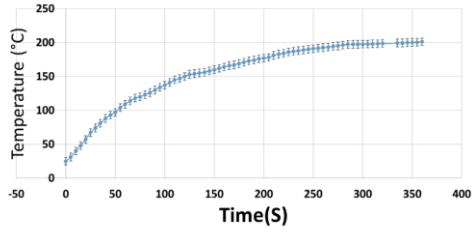

Fig. 4: Temperature vs time in the wire as Fuse

4. Experimental Setup

Experimental setup consists of (Fig. 5):

1. Multimeter
2. Short length wire as Fuse

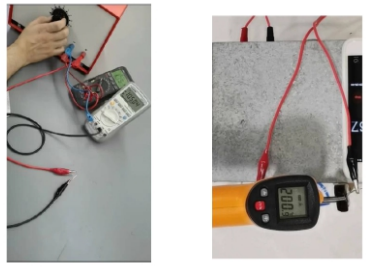

Fig.5: Experimental setup

5. Finding the Range of Current or Voltage Before Melting

The rang of (V),(I) for blowing are found (Eqs. 14- 21).

$$v < \sqrt{h_{(Laboratory)} A_{(WIRE)} R(T_L - T_{amb})} \longrightarrow \begin{cases} (T_L - T_{amb})_{cu} = 1060 \\ h_{(Lab)} = 28 \end{cases} \quad (14)$$

$$I < \sqrt{\frac{h_{(Laboratory)} A_{(WIRE)} (T_L - T_{amb})}{R}} \quad (15)$$

$$\begin{cases} v < \sqrt{AhR(T_L - T_{amb})} & (16) \\ I < \sqrt{\dfrac{Ah(T_L - T_{amb})}{R}} & (17) \end{cases}$$

$$h = \frac{\dfrac{V^2}{(T_{max} - T_{amb})R}}{A} \approx 28 \quad (18)$$

$$Ah = \frac{V^2}{(T_{max} - T_{amb})R} \approx 0.028, \quad A \approx 1 \times 10^{-3} \quad (19)$$

$$v < \sqrt{29680\, A_{(WIRE)}\, R} \quad (20)$$

$$I < \sqrt{\frac{29680\, A_{(WIRE)}}{R}} \quad (21)$$

6. Conclusions

By experiments the range of V(v) and I(A) are calculated. By increasing the length of the wire the time of blow is increased and also by increasing the voltage the time of blow for any length is increasing (Fig. 6).

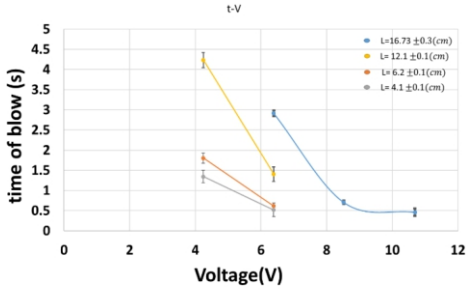

Fig. 6: Time of blowing vs voltage in Fuse

References

[1] Lessons in Electric Circuits by Tony R. Kuphaldt

[2] Arthur Wright, P. Gordon Newbery Electric fuses 3rd edition, Institution of Electrical Engineers (IET), 2004, ISBN 0-86341-379-X,

LAMIACEAE, MEDICINAL POTENTIAL & ANTI-ALLERGENIC DEVELOPMENTS

Sanika Datar, Marc Teitelbaum, Inglemoor High School Kenmore, Washington, United States, sanikadatar@gmail.com

ARTICLE INFO

National recipient for the NSTA Angela STEM award

Sanika high-school sophomore from Inglemoor High School in Kirkland, Washington has been working with a Senior PhD Candidate through a program called Polygence

Accepted by Ariaian Young Innovative Minds Institute , AYIMI

http://www.ayimi.org ,info@ayimi.org

ABSTRACT

Recently, allergic disorders have become a prevalent global epidemic affecting millions of people who experience asthma, allergies, and medication hypersensitivities. Medicinal plants such as Lamiaceae, commonly known as mint, are proving to be much more effective in treating the problem as they contain natural anti-allergenic compounds that act as anti-inflammatory agents to reduce and prevent cascading allergic reactions. This research paper will demonstrate how this plant's properties work, medicinal uses, and provide up-to-date research about the phytoconstituents from the Lamiaceae family and anti-allergenic activity.

Key Words : *Lamiaceae, Allergic reaction, IgE, anti-histamines, anti-allergenic compound*

1. Introduction

Allergies are the immune system's reaction to foreign substances in the body. These reactions can have a wide range of severity, from a runny nose and coughing, to anaphylaxis, a life-threatening reaction. The typically harmless foreign substances that cause these reactions are called allergens and can be found in dust, pets, pollen, food, and some medicines. Allergies can affect anyone and are generally more common in children. People whose family had allergies have a genetic tendency to develop allergies, and this is known as atopy [1]. When atopic people are exposed to the allergen, the immune system has a reaction, it over reacts by producing antibodies that attack the allergen, and this can cause allergic inflammation.

2. Significance of Allergies

The prevalence of allergies are increasing worldwide, and becoming more severe and complex. Allergies are the 6th leading cause of chronic illness in the U.S., costing an excess of $18 billion annually. More than 50 million people in the U.S. alone experience various types of allergies each year. In the U.S. asthma affects more than 24 million people, food allergies affect about 32 million people, and seasonal allergic rhinitis, or hay fever, affects about 24 million people [1]. In addition, data published from the 2014 National Health Interview Survey shows that 8.4% of US children under age 18 suffered from hay fever, 10% from respiratory allergies, 5.4% from food allergies, and 11.6% from skin allergies [2].

A major cause of allergies, other than genetics, is environmental conditions. Climate change and pollution contribute to people's health declining and increasing allergies. Health care costs are also high in many places, making it hard for people to get tested and the right medicines they need, making it harder to solve this worldwide issue. Allergies have many effects on individual people, including economic troubles, interruptions in quality of life, and possibly death. Allergies can prevent people from partaking in certain activities and can increase risks for other medical health problems.

3. Immunological Response

Common allergic reactions are linked to an antibody the body produces, called immunoglobulin E (IgE) [3]. The purpose of antibodies in our immune system is to help remove any foreign substances that invade our body. Everyone produces IgE antibodies but allergic people produce much larger quantities of it. Each IgE is very specific, which is the reason people can be allergic to one substance, yet not another. A person becomes sensitized when exposed to an allergen, causing B cells, a specific type of white blood cell, to produce IgE antibodies and release them in the blood. Some of the IgE attach themselves, using the high-affinity IgE receptor, FcεRI, to the surface of allergy-specific cells called mast cells and basophils, which are filled with grains containing allergic mediators [3].

All of these cells cause allergic symptoms by releasing the mediators stored in them. Repeated exposure to the allergen leads to an immediate reaction, triggered by cross-linking of the IgE, which is the binding to allergens, also called Activation, and results in rapid release of the allergic mediators, and this process is called degranulation [4].

Other white blood cells called T-cells drive a delayed and prolonged inflammatory reaction that can be seen hours later with itching, swelling, and other visible symptoms. These phases in the allergic reaction can be classified as immediate and late. The immediate responses are triggered by fast mast cell degranulation, and the late responses are caused by other inflammatory cells like eosinophils (also used in the immediate responses), neutrophils, and lymphocytes being attracted to the site because of chemotactic factors released by the mast cells, and producing more mediators [3].

4. Current Treatments, Downsides & Limitations

There are three main treatment options once it is known that a person has an allergy: avoiding the allergen, going through immunotherapy, or most commonly, taking medicine. Lastly, epinephrine is used during a severe reaction called anaphylactic shock and stimulates the adrenal glands and increases the rate and force of the heartbeat. [5] Despite all of the benefits that the three main treatment options provide, there are arguably many more downsides and limitations to them as well. In order to avoid the allergen, the allergy triggers need to be identified so they can be avoided. This is often not a viable option if the allergen is present in many places and in large amounts. It's

also unwise to avoid medications in the hopes that the allergen won't be encountered, which could cause a serious reaction.

Another treatment option is immunotherapy. The two types are allergy shots and sublingual immunotherapy (SLIT) [6]. Allergy shots are a series of injections of purified allergen extracts increasing in dose over time (usually a few years). The person gradually becomes less sensitive to that allergen because by gradually increasing the doses, the immune system is able to build up a tolerance to that allergen. Allergy shots slow down and reduce the production of the IgE antibody. Sublingual immunotherapy can be used for pollen allergies, and involves small doses of an allergen, in the form of a tablet, placed under the tongue, improving tolerance to the substance and reducing symptoms without using injections. This occurs because the allergen from the tablet crosses the mucous membranes in a matter of minutes and are captured by tolerogenic dendritic cells and are processed as small peptides. Through the lymphatic system, an immune response occurs and results in an early decrease in mast cell and basophil degranulation.

These immunotherapy methods can also have limitations. Allergy shots are generally limited to working for pollen, pets, dust, bees, and asthma allergies, but don't work well for allergies to food, medicines, feathers, or for hives or eczema. These shots can also cause redness, swelling, or irritation at the injection site, and there is also potential for a severe allergic reaction. Sublingual immunotherapy's most common side effects include itching and mild swelling inside the mouth, which can last up to an hour, and is experienced by one-quarter of people in SLIT therapy. Medications are used in allergy treatments are in table (1).

Table 1: Medications currently used in allergy treatments & limitations

Type of Allergy Med	Medication examples (brand name (active ingredient))	Mechanism of Action	Uses	Limitations
Anti-histamines	Benadryl (diphenhydramine) Clor-Trimeton (chlorpheniramine) Allegra (fexofenadine hydrochloride) Claritin (loratadine)	Block histamine, a chemical compound that triggers allergic symptoms such as inflammation when it binds to certain receptors in the body	Decrease the effects of histamine at certain cell receptors, and help with congestion, sneezing, itching, nasal swelling, rives, skin rashes, and itchy and watery eyes	Common: drowsiness, dry mouth, nose, and throat, and headaches Example: Allegra can cause common side effects and some more serious side effects include hives, rashes, itching, trouble breathing or swallowing, and inflammation
Mast-cell stabilizers [7]	Nasalcrom (sodium cromoglycate)	Inhibits release of histamines and allergic mediators (from mast cells); Blocks mast cell degradanulation -> also stabilizes mast cell membrane; A main mechanism: blocking the IgE-regulated calcium channels	Alleviates asthma & many allergic conditions (inhalers, oral solutions, and eye drops form)	Example: Commonly used sodium cromoglycate, can cause headaches, muscle aches, and diarrhea.
Corticosteroids [8]	Dexamethasone (tablet) Hydrocortisone (topical cream) Methylprednisolone (tablet) Prednisone (oral)	Suppress the inflammatory genes activated in chronic inflammatory diseases, by: 1) reversing "histone acetylation" of activated inflammatory genes through "binding of liganded glucocorticoid receptors (GR) to coactivators 2) recruitment of histone deacetylase-2 (HDAC2) to the activated transcription complex" [9]	Can be used in various forms: Nasal corticosteroids - nasal sprays that help with nasal allergies; corticosteroid creams or ointments - help topically with itchiness and rashes; oral corticosteroids- can be prescribed to prevent swelling or severe allergic reactions	Various forms of use enhances the potential for adverse effects for certain medications. Long term use of corticosteroids in general can cause: increased appetite and weight gain, acne, thinned skin (easy bruising), increased risk of infections, mood changes and swings, depression, diabetes, high blood pressure, osteoporosis, and withdrawal symptoms.
Leukotriene modifiers [3]	Leukotriene receptor antagonists: Zafirlukast (Accolate) Montelukast (Singulair) Leukotriene synthesis inhibitor: Zileuton (Zyflo)	Act by blocking 5-lipoxygenase activity and are either leukotriene receptor antagonists (block the effects of leukotrienes), or leukotriene synthesis inhibitors (prevents the body from making leukotrienes)	Asthma medication	Risks: Some leukotriene modifiers can cause liver damage

Medications are used as a treatment to help reduce immune system reaction and alleviate symptoms. This can include prescriptions as well as over-the-counter medicines. Some of the most widely used medicines include antihistamines, mast-cell stabilizers, corticosteroids, and leukotriene inhibitors [3]. Currently, allergy medicines are generally helpful for allergic reactions, however, they only help with short-term symptoms, and don't usually provide long-term effects or help cure the allergy. Due to this, an alternative should be explored for these medications. In addition, some medicines' effects only come into play days later, which can cause allergic discomfort until that time. Many medications are required to be taken multiple times a day and long-term use can cause many adverse effects, and may even worsen the condition. Most medications, if not all, have some sort of side effects and can be expressed differently in different people. As seen in Figure 1, the mechanism of action in current allergy medications create unnatural imbalances and lead to side effects in patients (Fig. 1).

Fig.1: Current Limitations and Downsides of Allergy Treatments (Created with BioRender.com)

Medicinal plants are being considered as a positive replacement to general medicines as it provides similar effects and benefits, but is often safer and healthier since it's natural. As many as 80% of people globally rely on herbal medicinal products for healthcare needs [10]. Herbal medicines include plant products that can be ingested as well as topical products that come from plants. Also, new drug discoveries and developments are being made as interest in herbal medicine increases. In fact, many drugs used nowadays include ingredients derived from medicinal plants. This is because plant-based chemicals are being seen as safe and more effective than synthesized chemicals. The versatility and effectiveness of natural treatments are causing herbal medications to become increasingly used worldwide, and one plant family that has been shown to have these potential benefits is Lamieaceae.

The plant family Lamiaceae has 236 genera and over 7,000 species, the largest family of the order, Lamiales [3]. Lamiaceae can be found nearly worldwide, and is known for its species' fragrant leaves and attractive flowers. Lamiaceae is usually found in dry, rock, woodland, or grassland habitats along forest margins and in fynbos. Some popular plants in this family include lavender, basil, mint, rosemary, sage, oregano, catnip, and thyme. Humans use these herb plants for flavor, fragrance, or its wide range of medicinal properties.

5. Uses of Lamiaceae

Lamiaceae has been known to be effective in alleviating conditions like exhaustion, weakness, depression, memory enhancement, circulation improvement, strengthening of fragile blood vessels, skin allergies, and asthma. Certain plants like Lamiaceae possess phytochemicals with anti-allergenic properties. These phytochemicals include flavonoids, terpenoids, and additional essential oils. The flavonoids within Lamiaceae plants are known for their antioxidant and anti-inflammatory properties, and have been shown to play a role in the treatment of various health conditions, including allergies and asthma. Terpenoids are responsible for the characteristic aromas of many plants in the Lamiaceae family. They also have anti-inflammatory and anti-allergenic properties, and they have been found to be effective in the treatment of various skin conditions. The other essential oils in the Lamiaceae plants have

phytochemicals that obtain similar properties to flavonoids and terpenoids.

These bioactive compounds have various mechanisms of action to combat the mediators or immune system involved in the inflammatory cascades or allergic reaction pathways, and these can be used as medicine for allergic symptoms [3]. For example, flavonoids have been shown to inhibit the release of histamine, a key mediator involved in the development of allergic symptoms. They also have been found to modulate the immune system and reduce the production of pro-inflammatory cytokines, which play a role in the development of allergies and other inflammatory conditions. Additionally, the essential oils present in Lamiaceae plants have been found to have a relaxing effect on the airways, which can help to relieve symptoms of asthma and other respiratory conditions.

6. Lamiaceae Studies

Prior research has been conducted to look into the potential benefits of Lamiaceae in allergic responses. These studies encompass the different mechanisms of actions that alter the immune response. Some of these studies have investigated the mechanisms of action of Lamiaceae species in modulating immune responses, particularly in suppressing IgE levels and IgE-mast cell cross-linking. The in-vivo studies highlighted in table 2 elucidate the therapeutic effect of Lamiaceae species in treating allergies by reducing passive cutaneous anaphylaxis and decreasing mortality due to anaphylactic shock-induced bronchospasm. In these studies, different Lamiaceae species, including Mentha arvensis, Mosla dianthera, and Perilla frutescens, have been shown to have a suppressive effect on IgE levels and the reaction to allergens. The usage of Lamiaceae plant is in table (2).

Table 2: Lamiaceae Plants Used in In-Vivo Studies

Specimen	Assay Extract	Application & Concentration	Observation & Results
OVA-sensitized mice [11]	N/A	N/A	• Essential oil of Mentha arvensis significantly decreased the serum IgE level • Identification of three compounds in the essential oil: menthol, menthone, and 1,8-cineole, with particularly large percentage contents of menthol
Mice sensitized with compound 48/80 and anti-DNP IgE [12]	Aqueous extract of Mosla dianthera	Intraperitoneal pretreatment of 1-1,000 mg/kg	• Reduction in passive cutaneous anaphylaxis (PCA) reaction • Effectively reduced mortality (41%) due to anaphylactic shock-induced bronchospasm in tested subjects with a significant drop in IgE level
Mice injected with anti-ovalbumin serum [13]	Isolated rosmarinic acid from leaves of Perilla frutescens	N/A	• Perilla extract significantly suppressed the PCA-reaction, which was brought about by rosmarinic acid ○ anti-allergic titer of rosmarinic acid was 8 folds higher than the conventional anti-allergic drug tranilast, where 19 mg/kg of rosmarinic acid was sufficient to achieve an equivalent PCA reaction suppression as 150 mg/kg of tranilast (an anti-allergenic drug)
BALB/c mice sensitized intraperitoneally and challenged with ovalbumin (OVA) [14]	Water & ethanol extracts of Perilla frutescent leaves	Each group of mice was tube-feeding with 0 (control), 80 μg (PfWL), or 320 μg (PfWH) water extracts or 80 μg (PfEL) or 320 μg (PfEH) ethanol extracts of perilla leaves daily for 3 weeks	• OVA-specific IL-5 and IL-13 secretions from OVA-stimulated splenocytes were significantly suppressed in the ethanol extract groups PfEL and PfEH • Serum level of anti-OVA IgE tended to be lower in the PfEH group • Inflammatory mediators, such as eotaxin and histamine, and total cells, particularly eosinophils in bronchoalveolar lavage fluid (BALF), were also decreased in the PfEL and the PfEH groups • PfEL and the PfEH groups had significantly lower methacholine-induced hyperresponsiveness (AHR) • Conclusion: Ethanol extracts, rather than water extract, of perilla leaves could significantly suppress Th2 responses and airway inflammation in allergic murine model of asthma

These studies show the progress the scientific community has made towards research towards Lamiaceae, but there are next steps needing to be taken and future directions that can be explored. In studies where multiple compounds were shown to cause anti-allergenic activity, it's important to isolate the primary compound that contributed to this, and perform experiments that show its potential as herbal medicine. Some experimental studies could also focus on the prospective of including compounds from multiple plant species in a medication. It is also essential to obtain research related to toxicology studies for Lamiaceae. Lamiaceae used as a medication would clearly be plant-based, therefore providing a more sustainable option.

7. Additional Benefits of Manufactured Lamiaceae

Currently, large-scale drug production is known to have negative impacts on the environment due to the large number of medications being produced. A research project by Laximnarayan, Duse, Wattal et al published in The Lancet in November 2013 shows that "contamination of water sources with antimicrobial drugs (combined with mass misuse of antibiotics and poor sanitation) has had grave consequences in India, where an estimated 58,000 new-borns die from multidrug-resistant infections every year". Pharma pollution affects people and animals who live near production plants because water and food sources can be contaminated with waste products from the pharma. [15] Plant-based medications could reduce environmental effects such as pollution and would be more sustainable for the environment in the long-term. Further analysis will be needed to determine positive outcomes of plant-based manufacturing.

Specifically, green manufacturing with Lamiaceae is a much more ethical and sustainable option for mass producing allergy medication, and would be a better alternative for the wellbeing of the planet as well as the benefits it offers to individual people, as an allergy medication. The use of plant-based products can be more beneficial because they have fewer toxic byproducts that often find themselves polluting streams, rivers, and communities nearby during the drug's manufacturing. Plant-based drug manufacturing has been shown to produce much lower levels of greenhouse gas emissions as demonstrated in US biotech Amgen's biomanufacturing plant where 69% less carbon emissions are produced compared to a traditional manufacturing facility. [16] As described in this paper, current allergy medications have many limitations as well as downsides related to their sustainability. Lamiaceae is an important alternative to consider and further research will be able to prove its effectiveness.

8. Conclusion

In conclusion, allergic disorders have become a major global health concern, with millions of people suffering from asthma, food allergies, allergic rhinitis, and medication hypersensitivities. While traditional medicines may not be as effective, natural products derived from medicinal plants, such as the Lamiaceae family, have been found to contain anti-allergenic compounds. The research provided in this paper has shown that Lamiaceae plants have been proven to target IgE responses in the allergy cascade and act as anti-inflammatory agents, reducing allergic reactions. This paper has highlighted the properties, medicinal uses, and up-to-date research on the phytoconstituents and anti-allergenic activity of the Lamiaceae family, and their potential use as a natural alternative in the treatment of allergies. However, additional research needs to be done in a clinical setting in order to explore Lamiaceae's use as a viable option to replace current allergy medications.

References

1] "Facts and Stats - 50 Million Americans Have Allergies:

Acaai Patient." ACAAI Public Website, American College of Allergy, Asthma & Immunology, 16 Sept. 2022.

[2] Clements, Julie. "Spring Time Ailments and Their ICD-10 Codes." Outsource Strategies International, 10 Nov. 2022.

[3] Sim, Lee Yen, et al. "Lamiaceae: An Insight on Their Anti-Allergic Potential and Its Mechanisms of Action." Frontiers, Frontiers, 24 May 2019, doi:10.3389/fphar.2019.00677

[4] Bax, Heather J et al. "Cytokinergic IgE Action in Mast Cell Activation." Frontiers in immunology vol. 3 229. 6 Aug. 2012, doi:10.3389/fimmu.2012.00229

[5] "Allergies and the Immune System." Allergies and the Immune System | Johns Hopkins Medicine, 8 Aug. 2021.

[6] "Slit: Allergy Treatment." ACAAI Public Website, 15 Apr. 2022.

[7] "Mast Cell Stabilizer." Wikipedia, Wikimedia Foundation, 23 Nov. 2022.

[8] Rahim, Nur Amira et al. "Anti-Allergic Rhinitis Effects of Medicinal Plants and Their Bioactive Metabolites via Suppression of the Immune System: A Mechanistic Review." Frontiers in pharmacology vol. 12 660083. 13 Apr. 2021, doi:10.3389/fphar.2021.660083

[9] Barnes, Peter J. "How corticosteroids control inflammation: Quintiles Prize Lecture 2005." British journal of pharmacology vol. 148,3 (2006): 245-54. doi:10.1038/sj.bjp.0706736

[10] Ekor, Martins. "The growing use of herbal medicines: issues relating to adverse reactions and challenges in monitoring safety." Frontiers in pharmacology vol. 4 177. 10 Jan. 2014, doi:10.3389/fphar.2013.00177

[11] Sharma, S., Rasal, V. P., Patil, P. A., Joshi, R. K. (2018). Mentha arvensis essential oil suppressed airway changes induced by histamine and ovalbumin in experimental animals. Nat. Prod. Res. 32, 468–472. doi: 10.1080/14786419.2017.1311891

[12] Lee, D. H., Kim, S. H., Eun, J. S., Shin, T. Y. (2006). Mosla dianthera inhibits mast cell-mediated allergic reactions through the inhibition of histamine release and inflammatory cytokine production. Toxicol. Appl. Pharmacol. 216, 479–484. doi: 10.1016/j.taap.2006.06.007

[13] Makino, T., Furuta, Y., Wakushima, H., Fujii, H., Saito, K., Kano, Y. (2003). Anti-allergic effect of Perilla frutescens and its active constituents. Phytother. Res. 17, 240–243. doi: 10.1002/ptr.1115

[14] Miaw-Ling Chen, Chi-Heng Wu, Li-Shiuan Hung, Bi-Fong Lin, "Ethanol Extract of Perilla frutescens Suppresses Allergen-Specific Th2 Responses and Alleviates Airway Inflammation and Hyperreactivity in Ovalbumin-Sensitized Murine Model of Asthma", Evidence-Based Complementary and Alternative Medicine, vol. 2015, Article ID 324265, 8 pages, 2015. https://doi.org/10.1155/2015/324265

[15] Nawrat, Allie. "Pharma and the Environment: Pollution Continues despite Public Pressure." Pharmaceutical Technology, 14 Feb. 2022

[16] "Green Buildings." Amgen, Inc.

Ariaian Young Innovative Minds Institute, AYIMI
Unit 14, No. 32, Malek Ave., Shariati St.
Post Code: 1565843537
Tel - Fax: +9821-77522395, 77507013
Tehran/ Iran
URL: http://www.ayimi.org
http://journal.ayimi.org
Email: info@ayimi.org